

The Organometallic Chemistry of Carbon Dioxide

Dorothy H. Gibson

Department of Chemistry and Center for Chemical Catalysis, University of Louisville, Louisville, Kentucky 40292

Received January 31, 1996 (Revised Manuscript Received July 22, 1996)

Contents

I. Abbreviations	2063
II. Introduction and Scope	2063
III. Synthetic Methods	2064
A. η^1 - and η^2 -CO ₂ Complexes	2064
B. Complexes with Bridging CO ₂ Ligands	2066
1. μ_2 - η^2 Complexes	2066
2. μ_2 - η^3 Complexes	2067
3. μ_3 - η^3 Complexes	2070
4. μ_3 - η^4 Complexes	2071
5. μ_4 - η^4 Complexes	2071
6. μ_4 - η^5 Complexes	2071
C. Metallo-carboxylate Anions	2071
IV. Structures of Metal–CO ₂ Complexes	2072
A. η^1 Complexes	2073
B. η^2 Complexes	2073
C. μ_2 - η^2 Complexes	2073
D. μ_2 - η^3 Complexes	2075
1. Class I Compounds	2075
2. Class II Compounds	2076
E. μ_3 - η^3 Complexes	2077
F. μ_3 - η^4 Complexes	2077
G. μ_4 - η^4 Complexes	2077
H. μ_4 - η^5 Complexes	2078
V. Bonding	2078
VI. Spectral Characterization	2079
A. Infrared Spectral Data	2079
1. η^1 Complexes	2080
2. η^2 Complexes	2080
3. μ_2 - η^2 Complexes	2081
4. μ_2 - η^3 Complexes	2082
5. μ_3 - η^3 Complexes	2084
6. μ_4 - η^4 Complexes	2084
7. μ_4 - η^5 Complexes	2084
8. Metallo-carboxylate Anions	2085
B. ¹³ C NMR Spectral Data	2085
C. Electronic Spectra	2086
VII. Characteristic Reactions	2086
A. Thermolysis Reactions	2086
1. Dissociation of CO ₂	2086
2. Cleavage of a Carboxyl C–O Bond	2087
3. Thermolysis with Loss of an Ancillary Ligand and/or with Rearrangement	2088
B. Photolysis Reactions	2088
C. Reactions with Electrophiles	2088
D. Intra- or Intermolecular Oxygen Transfer Reactions	2091
E. Reactions with Nucleophiles	2092
F. Fluxional Behavior	2093
VIII. Concluding Remarks	2093

IX. Acknowledgments	2094
X. References	2094

I. Abbreviations

bpy	2,2'-bipyridyl
COD	1,5-cyclooctadiene
COT	cyclooctatriene
Cp	η^5 -cyclopentadienyl
Cp'	η^5 -methylcyclopentadienyl
Cp''	η^5 -trimethylsilylcyclopentadienyl
Cp*	η^5 -pentamethylcyclopentadienyl
Cy	cyclohexyl
depe	1,2-bis(diethylphosphino)ethane
diars	<i>o</i> -phenylenebis(dimethylarsine)
diphoe	1,2-bis(diphenylphosphino)ethylene
dmpe	1,2-bis(dimethylphosphino)ethane
dmpm	1,2-bis(dimethylphosphino)methane
dpe	1,2-bis(diphenylphosphino)ethane
dppm	1,2-bis(diphenylphosphino)methane
dppp	1,3-bis(diphenylphosphino)propane
en	ethylenediamine
Ind	η^5 -indenyl
OT _f	trifluoromethanesulfonate
PPN	bis(triphenylphosphiniminium)
salen	<i>N,N</i> -ethylenebis(salicylideneiminato)
<i>t</i> -Bupy	4- <i>tert</i> -butylpyridine
<i>t</i> -BuNC	<i>tert</i> -butylisocyanide
tmtaa	dianion of 7,16-dihydro-6,8,15,17-tetramethylidibenzo[<i>b, i</i>][1,4,8]tetraazacyclotetradecine

II. Introduction and Scope

Compounds having one or more carbon dioxide ligands bound to a metal center through carbon are of interest for several reasons. The possibility of recycling CO₂ from industrial emissions and of removing some of this greenhouse gas, an environmental pollutant, is receiving increased attention.¹ Also, the possibility of using CO₂ as the starting material for the synthesis of fine chemicals provides an attractive alternative to compounds presently derived from petroleum.² Efforts to convert CO₂ to useful chemicals will inevitably center on transition metal catalysts.³ Furthermore, efforts to enhance the yield of hydrogen in water gas shift reactions are also centered on carbon dioxide interactions with transition metal catalysts.⁴ For all these reasons, a broader understanding of the organometallic chemistry of CO₂ is being sought.

Transition metal carbon dioxide complexes may provide both structural and functional models for surface-bound intermediates in catalytic conversion processes. Particularly in the past decade, many such compounds have been identified. Although



Dorothy Gibson grew up in Waxahachie, TX. After receiving B.A. and M.A. degrees in chemistry from Texas Christian University, she served as an Instructor there for several years before beginning doctoral work at the University of Texas (Austin). She received the Ph.D. in 1965 (with Rowland Pettit). After postdoctoral stints at Texas (Pettit) and the University of Colorado (with Charles H. DePuy), she moved to the University of Louisville in 1969. She has been Professor of Chemistry there since 1975 and at present is Director of the newly formed Center for Chemical Catalysis at the University of Louisville. She has also served on the Editorial Advisory Board of *Organometallics*. Recent research activities have concentrated on transition metal C_1 chemistry that is related to small molecule activation.

initially thought to be a poor ligand,^{3b} carbon dioxide has demonstrated surprising versatility by exhibiting a great variety of coordination modes in its metal complexes.

In this article, only those compounds that can be clearly identified as having carbon dioxide bound to metal centers through carbon will be considered. Thus the discussions will not include metal formate complexes whose chemistry has been reviewed recently.⁵ Also, the discussions will not include metalcarboxylic acids or metalcarboxylate esters except where these compounds have been used as reagents for the synthesis of CO_2 complexes or result from reactions of these compounds.

III. Synthetic Methods

The synthetic procedures for carbon dioxide complexes are described in the sections below according to the structural types that have been characterized. The nomenclature for these compounds includes a simple descriptor which indicates the bonding type. Thus, the number of bonds between each coordinated CO_2 and the metal atom, or atoms, in the complex is indicated by η^n whereas the number of metal atoms involved in bonding to each CO_2 ligand is indicated by μ_n . The structural types are illustrated in Figure 1 (see discussion in section IV). A further section is focused on the synthesis of metalcarboxylate anions and includes a $\mu_3-\eta^4$ complex which remains the only structurally characterized compound in this group. The discussions are limited to those compounds which can be isolated or at least studied by IR and NMR spectral techniques to establish the presence of a metal-bound CO_2 ligand. Complexes formed under electrochemical, flash photolysis, or pulse radiolysis conditions have been reviewed recently⁶ and will not be covered here.

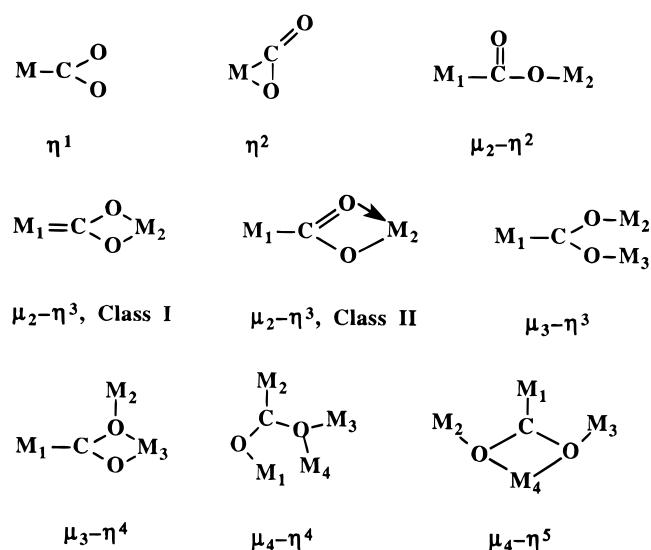
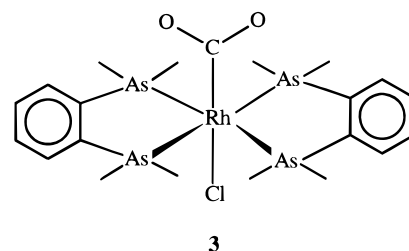


Figure 1. Structural types of metal- CO_2 complexes.

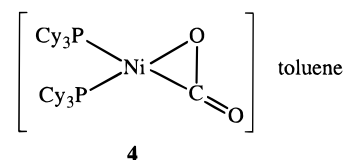
A. η^1 - and η^2 - CO_2 Complexes

Complexes of these types have usually been generated by direct reaction of a metal complex with carbon dioxide. Thus metal centers that have a coordination vacancy (or an easily displaced ligand) and are highly nucleophilic because of the presence of electron-donating ligands can bind the weakly electrophilic CO_2 molecule through carbon directly. The η^1 - CO_2 complexes are far from being robust; conditions for their isolation usually include glovebox or Schlenk techniques, low temperatures, and strict exclusion of oxygen and water. The compounds that have been prepared by direct reaction with CO_2 are shown in Table 1. As might be expected, many of these compounds dissociate the CO_2 ligand readily (see discussion in section VII).

With the η^1 complexes reported by Herskovitz,^{7,8} it was necessary to pressurize the system with CO_2 in order to form iridium and rhodium complexes **1–3**; displacement of an ancillary ligand does not occur in forming these compounds. Both compounds have octahedral metal centers as shown for $Rh(\text{diars})_2(\text{Cl})(CO_2)$ (**3**). Once formed, however, the compounds were



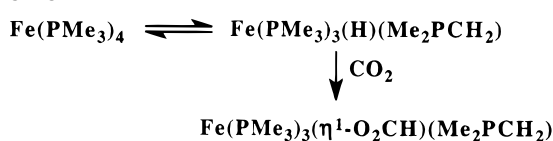
relatively stable toward CO_2 loss. The η^2 complex $Ni(CO_2)(PCy_3)_2$ (**4**) studied by Aresta⁹ was made by



reaction of $Ni(PCy_3)_3$ or $[Ni(PCy_3)_3]N_2$, in toluene,

Table 1. Summary of η^1 - and η^2 -CO₂ Complexes Prepared by Direct Carbonation

compound	precursors	ref
η^1 Complexes		
Ir(diars) ₂ (Cl)(CO ₂) (1)	Ir(diars) ₂ (Cl)	7
Ir(dmpe) ₂ (Cl)(CO ₂) (2)	Ir(dmpe) ₂ (Cl)	7
Rh(diars) ₂ (Cl)(CO ₂) (3)	Rh(diars) ₂ (Cl)	8
η^2 Complexes		
Ni(PCy ₃) ₂ (CO ₂) (4)	Ni(PCy ₃) ₃ or [Ni(PCy ₃) ₃] ₂ N ₂	9–11
Ni(PR ₃) ₂ (CO ₂) (5 , 6) R = <i>n</i> -Bu, Et	Ni(PR ₃) ₄	12
Rh[P(<i>n</i> -Bu) ₃] ₂ (Cl)(CO ₂) (7)	[Rh(Cl)(C ₂ H ₄) ₂] ₂ , P(<i>n</i> -Bu) ₃	13
Fe(PMe ₃) ₄ (CO ₂) (8)	Fe(PMe ₃) ₄	14
Fe(depe) ₂ (CO ₂) (9)	Fe(depe) ₂ (N ₂)	15
Pd(PMePh ₂) ₂ (CO ₂) (10)	Pd(PMePh ₂) ₂ (CH ₂ =CHCO ₂ Me)	16
Cp ₂ Nb(CO ₂)(CH ₂ SiMe ₃) (11)	Cp ₂ Nb(Cl)(CH ₂ SiMe ₃)	17
Cp ₂ Mo(CO ₂) (12)	Cp ₂ Mo(PhC≡CPh)	18
Cp ₂ Ti(PMe ₃)(CO ₂) (13)	Cp ₂ Ti(PMe ₃) ₂	19
<i>trans</i> -W(dppe) ₂ (CO)(CO ₂) (19)	W(H)[η^2 -O ₂ CN(CH ₂) ₄](CO)(η^1 -dppe)(η^2 -dppe)	23
<i>trans</i> -Mo(PMe ₃) ₄ (CO ₂) ₂ (20)	<i>cis</i> -Mo(PMe ₃) ₄ (N ₂) ₂	25b
<i>trans</i> -Mo(PMe ₃) ₃ (CNR)(CO ₂) ₂ , R = Me, <i>i</i> -Pr, <i>t</i> -Bu, Cy, CH ₂ Ph (21–25)	<i>trans</i> -Mo(PMe ₃) ₄ (CO ₂) ₂ , RNC	25a,c
<i>trans</i> -Mo(CO ₂) ₂ (PMe ₃) ₂ (P–P), P–P = dmpm, depe, dmpe, dppe (26–29)	<i>trans</i> -Mo(PMe ₃) ₄ (CO ₂) ₂ , P–P	25d
<i>trans</i> -Mo(dmpe) ₂ (CO ₂) ₂ (30)	<i>trans</i> -Mo(PMe ₃) ₄ (CO ₂) ₂ , dmpe	25e
<i>trans</i> -Mo(depe)(PMe ₃)(CNR)(CO ₂) ₂ , R = <i>t</i> -Bu, Cy (31,32)	<i>trans</i> -Mo(depe)(PMe ₃) ₂ (CO ₂) ₂ , RNC	25f

Scheme 1

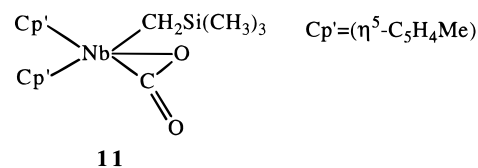
with CO₂ at atmospheric pressure and was obtained as the toluene solvate **4**. The solvent-free complex was later obtained by Jolly *et al.*¹⁰ Mason and Ibers¹¹ prepared the same complex by direct reaction of the dinitrogen complex with liquid CO₂. Also, Aresta¹² reported the related complexes Ni(CO₂)(PR₃)₂ (**5**, **6**; R = *n*-Bu, Et) prepared from reactions involving gaseous CO₂. Aresta¹³ reported rhodium complexes Rh(Cl)(CO₂)(PEt₂Ph)₃ and Rh(Cl)(CO₂)(PEt₂Ph)₂ from reactions of CO₂ with [Rh(Cl)(C₂H₄)₂]₂; the compounds were not fully characterized. However, Rh(Cl)(CO₂)[P(*n*-Bu)₃]₂ (**7**) was prepared from the ethylene complex and spectrally characterized.

Synthesis of an η^2 -CO₂ complex (**8**) was reported by Karsch¹⁴ from reaction of Fe(PMe₃)₄ with CO₂ in pentane; a second product, Fe(PMe₃)₃(CO)(CO₃) was also obtained. However, the structural assignment of the CO₂ complex was somewhat clouded by the fact that the starting iron complex exists in equilibrium with a hydrido isomer as shown in Scheme 1. An alternate product was obtained from reactions of Fe(PMe₃)₄ with CO₂ conducted in THF; it was identified as the insertion derivative Fe(H)(PMe₃)₃(O₂CCH₂PMe₂). Thus, it seems possible that the "CO₂ complex" may be the formate complex Fe(PMe₃)₃(O₂CH)(CH₂PMe₂) instead since CO₂ insertion into metal hydride bonds occurs readily.⁵ Indeed, the IR spectral properties of the "CO₂ complex" are not in agreement with other η^2 -CO₂ complexes, as discussed in section IV. However, properties of the complex Fe(CO₂)(depe)₂ (**9**), fully characterized recently by Komiya *et al.*,¹⁵ lend support to the formulation by Karsch; structural characteristics (which result in a coordinated CO₂ that is intermediate between η^1 and η^2) appear to be responsible for the unusual IR spectral properties of the compound (see discussion

in section VI). Compound **9** was prepared by CO₂ displacement of nitrogen from the corresponding dinitrogen complex.

The first palladium complex of CO₂ was reported only recently by Yamamoto *et al.*¹⁶ The compound, Pd(CO₂)(PMePh₂)₂ (**10**), was prepared by allowing the corresponding methyl acrylate complex (generated *in situ* from *trans*-PtEt₂(PMePh₂)₂) to stand under 18–20 atm of CO₂ for 12 h.

Lappert *et al.*¹⁷ found that reduction of Cp₂Nb(Cl)-CH₂SiMe₃ with Na(Hg) followed by reaction with CO₂ afforded the first η^2 -CO₂ complex involving a metallocene fragment (**11**). Other such compounds involv-

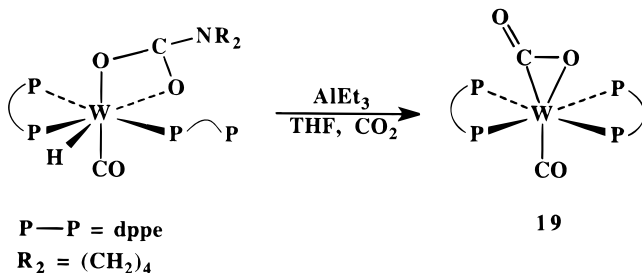


ing molybdenum¹⁸ (**12**) and titanium¹⁹ (**13**) have been prepared by simple ligand substitution reactions.

In a few instances, an η^2 -CO₂ complex has resulted from aerobic oxidation of a metal carbonyl complex. Iwashita and Hayata²⁰ first reported that a CO₂ complex was formed from reaction of molecular oxygen with a rhodium cluster complex, but the compound was not fully identified. More recently, Nicholas *et al.*²¹ prepared Cp₂Nb(R)(CO₂) [**14–17**; R = CH₂Si(CH₃)₃, CH₂C(CH₃)₃, CH₂Ph, CH₃] in high yields by aerobic oxidation of the corresponding carbonyl complexes. Oxidation of Cp₂Mo(CO) afforded a small amount of the CO₂ complex together with Cp₂Mo(η^2 -CO₃) and Cp₂Mo=O. It was found that oxidation of Cp₂Ta(CO)H also afforded the carbon dioxide complex Cp₂Ta(CO₂)H (**18**).²¹

The synthesis of *trans*-W(CO)(dppe)₂(CO₂) (**19**) reported by Hidai *et al.*²³ is unique. As shown in Scheme 2, the CO₂ complex results from the reaction of AlEt₃ with W(H)[η^2 -O₂CN(CH₂)₄](CO)(η^1 -dppe)(η^2 -dppe) under an atmosphere of CO₂. The reaction was conducted at 50 °C; a 49% yield of the product was obtained.

Scheme 2



In 1974 Chatt *et al.*²⁴ reported that the reaction of *cis*-Mo(N₂)₂(PMe₂Ph)₄ with CO₂ afforded an unstable compound "Mo(CO₂)₂(PMe₂Ph)₄", which rearranged to a dimer with a terminal carbonyl group on each Mo atom and with two bridging carbonate ligands. The CO₂ adduct could not be fully characterized, but structural data were obtained for its decomposition product, (PMe₂Ph)₃(CO)Mo(CO₃)₂Mo(CO)(PMe₂Ph). Carmona *et al.*^{25b} later used the dinitrogen complex to prepare the more stable *trans*-Mo(CO₂)₂(PMe₃)₄ (**20**) and has used this product to prepare a number of other stable complexes in which one or more PMe₃ ligands were replaced by other ligands (**21**–**32**; see Table 1).²⁵

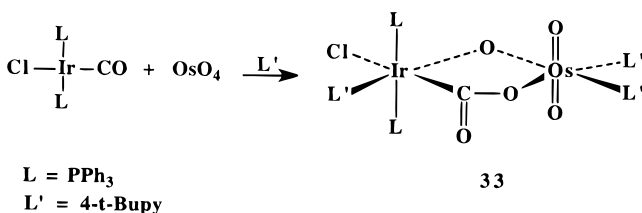
B. Complexes with Bridging CO₂ Ligands

More numerous strategies have been developed for these compounds than have been employed for the compounds described in section A. Because of the variety of bridged complexes that have been prepared, this section has been subdivided according to the structural type of the bridged CO₂ ligand.

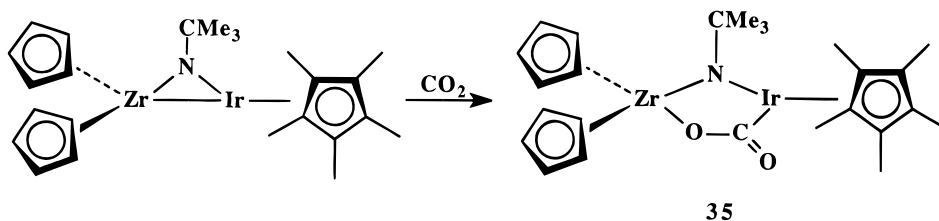
1. $\mu_2\text{-}\eta^2$ Complexes

Addition of an oxo complex to a CO ligand in a 16e compound was used by Collins *et al.*²⁶ to generate metallacyclic complexes **33** and **34** containing a bridging CO₂ ligand as shown in the example in Scheme 3. More recently Bergman *et al.*²⁷ used direct CO₂ insertion to generate the related bridged iridium–zirconium complex **35** shown in Scheme 4. The reaction of [Rh₂(CO)₂(dppm)₂] with CO₂ was reported by Eisenberg *et al.*²⁸ to give a product thought to be an A-frame complex (**36**), having CO₂ bridged be-

Scheme 3



Scheme 4



tween the two rhodium atoms in a seven-membered ring. A four-membered metallacyclic complex (**37**) was synthesized by Haines *et al.*²⁹ by converting the bridging CO ligand in Ru₂(μ -CO)(CO)₄[μ -(PrO)₂PN-(Et)P(OPr)₂]₂ to COOH and then deprotonating the acid.

Bennett³⁰ prepared a CO₂-bridged platinum complex **38** through a coupling reaction as shown in Scheme 5. The same bridged compound was also prepared by thermolysis of the related metallocarboxylic acid at 60–100 °C. Strukul³¹ used a similar strategy to prepare additional platinum complexes of the same type (**39**, **40**).

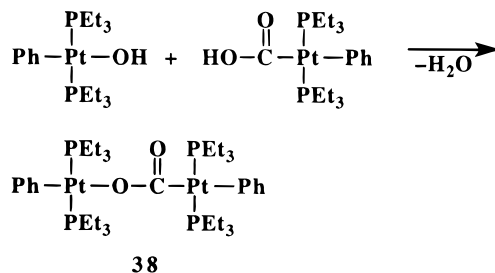
Displacement of a weakly coordinated ligand (BF₄[−] or ethylene) from a transition metal by a metallocarboxylate anion (or, in some cases, the acid) has been used by Gibson *et al.*^{32–34} to generate several $\mu_2\text{-}\eta^2$ -type complexes (**41**–**47**). The reactions are illustrated in Schemes 6–8. The hydrolysis of a carbamoyl complex resulted in a small yield of *cis*,*fac*-Re(CO)₄(L)(CO₂)Re(CO)₃(L)₂ (**48**; L = NH₂CH₂CH=CH₂).³⁵

An unusual method has been used by Szalda, Creutz, *et al.*³⁶ for the synthesis of a polymeric compound with CO₂ bridges between cobalt centers (**49**) as shown in Scheme 9. Replacement of coordinated hydroxyl by perchlorate ion provides the coordination vacancies necessary for development of CO₂-bridged dicobalt monomer units.

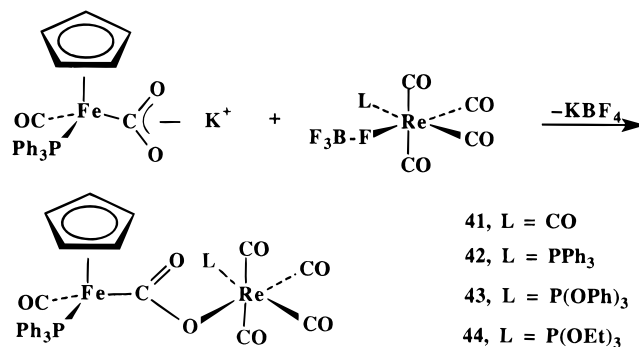
Perhaps the most unusual synthesis of a $\mu_2\text{-}\eta^2$ CO₂-bridged complex is the recently observed³⁷ conversion of *cis*-Ru(bpy)₂(CO)(CHO)⁺PF₆[−] (bpy = 2,2'-bipyridyl) to *cis*,*cis*-Ru(bpy)₂(CO)(CO₂)Ru(bpy)₂(CO)²⁺2PF₆[−] (**50**) by the action of water and oxygen. The reaction was complete after 3 h; with photoassistance, it was complete after 5 min. A proposed path for the reaction is shown in Scheme 10.

Whether a $\mu_2\text{-}\eta^2$ or $\mu_2\text{-}\eta^3$ complex (see Figure 1) results from the reaction of a metallocarboxylate with a main group complex depends upon the nature of the metallocarboxylate, the substituents on the main group atom (M₂) and the metal (M₁) itself. The $\mu_2\text{-}\eta^3$ form is favored when strongly nucleophilic metallocarboxylates are used, but electron donor groups on M₂ can reverse this to a $\mu_2\text{-}\eta^2$ complex. The two types of compounds (none characterized so far are metallacyclic) are easily distinguished by their IR spectral characteristics (see section VI). Syntheses of the $\mu_2\text{-}\eta^2$ CO₂-bridged compounds are summarized at the bottom of Table 2; the reactions usually employ a main group halide in combination with a metallocarboxylate. The use of a germanium halide together with a rhenium metallocarboxylate anion to give a CO₂-bridged compound (**51**) was done by Gladysz *et al.*³⁸ as shown in Scheme 11. Cutler³⁹ (**52**) and Gibson⁴⁰ (**52**–**57**) used related techniques to generate

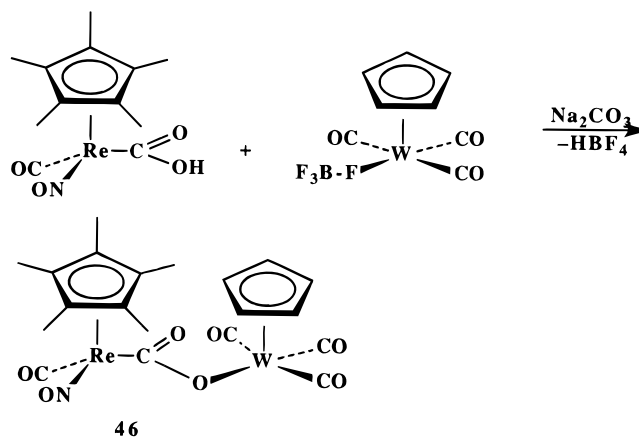
Scheme 5



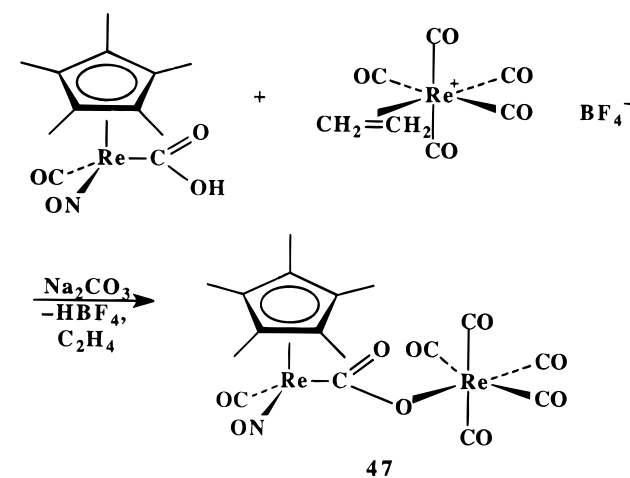
Scheme 6



Scheme 7

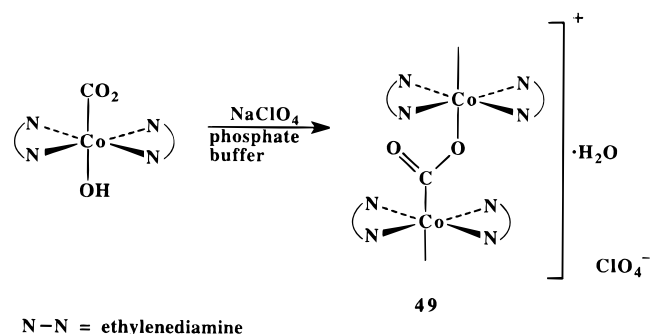


Scheme 8



$\mu_2\text{-}\eta^2$ CO₂-bridged complexes in which a single carboxylate oxygen is bound to a tin atom. In several instances the labile metalcarboxylate anions were generated by Gibson *et al.* *in situ*,⁴⁰ in aqueous media, and the tin halide was then added; the CO₂-bridged tin complexes are stable under these conditions and

Scheme 9



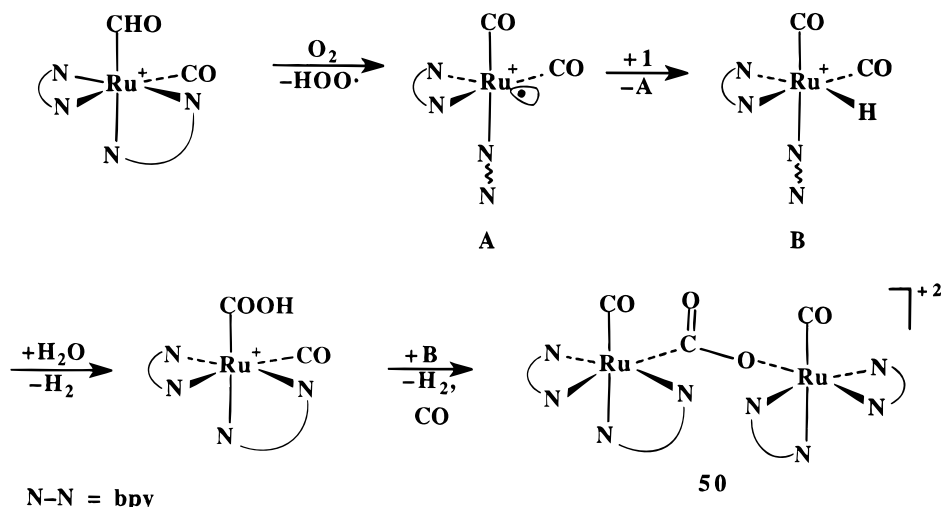
are generally more robust than their transition metal analogs (see discussion below in section C.2b). This method is effective for the preparation of CpFe(CO)₂(CO₂)SnPh₃ (**55**) whereas direct reaction³⁹ of CpFe(CO)₂CO₂-K⁺ with the tin halide yields only CpFe(CO)₂SnPh₃. The failure of the direct reaction appears to be solvent-related. In cases where the metalcarboxylate anion has been generated from CO₂ and the metal anion, the reactions are usually conducted in THF; some of the CO₂-bridged compounds are unstable in this solvent. The acid Cp*Re(CO)(NO)COOH is sufficiently nucleophilic that it can be used in reactions with tin halides directly without conversion to the anion.⁴⁰

2. $\mu_2\text{-}\eta^3$ Complexes

There are two structurally distinct types of these complexes now known as discussed in section IV. Those in class I have the CO₂ ligand symmetrically bonded (O-M₂ bonds) to a transition metal while those in class II have unequal O-M₂ bond lengths (where, in most cases, M = Sn); both types have the carboxyl carbon bound to a late transition metal. The syntheses of these are discussed separately below.

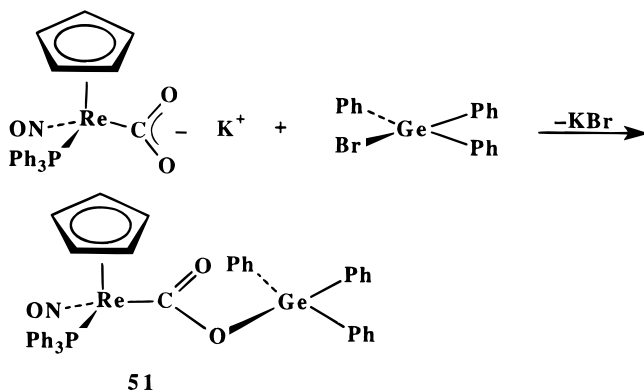
(a) *Class I Compounds.* Bridged compounds having both carboxyl oxygens bound to a single transition metal (early or late) have been prepared during the past decade. The first such compound (**58**) was prepared by Tso and Cutler⁴¹ and involved zirconium, an early transition metal, as the anchoring atom for the carboxylate oxygens. Initially the bridging group was created by taking advantage of the sensitivity of a zirconium alkyl complex toward acid as shown in Scheme 12. Later,⁴² this group prepared additional complexes **59**–**62** by reactions of iron and ruthenium metalcarboxylates CpM(CO)₂CO₂⁻Na⁺ (M = Fe, Ru) with zirconocene or titanocene dichlorides. This group of complexes is particularly labile in solution and only the Ru/Zr complex could be fully characterized. More recently, Cutler *et al.*⁴³ have prepared Fe/Zr and Ru/Zr complexes by direct insertion of CO₂ into the metal-metal bonds. Additional zirconocene derivatives **63**–**68** have recently been synthesized by Gibson *et al.*⁴⁴ Some of the compounds were prepared by removal of an acid-sensitive functional group from zirconium; however, others were prepared by transmetalation reactions from $\mu_2\text{-}\eta^3$ CO₂-bridged tin complexes as shown in Scheme 13. These are also highly moisture-sensitive and must be handled in a glovebox. A further early transition metal complex was reported by Geoffroy *et al.*,⁴⁵ the compound was prepared as shown in

Scheme 10

Table 2. Summary of Preparative Routes to $\mu_2\text{-}\eta^2$ CO₂-Bridged Complexes

compound	precursors	ref
(PPh ₃) ₂ (Cl)(<i>t</i> -Bupy)Ir(μ -O)(CO ₂)Os(O) ₂ (<i>t</i> -Bupy) ₂ (33)	Ir(Cl)(CO)(PPh ₃) ₂ , OsO ₄ , <i>t</i> -Bupy	26
(PPh ₃) ₂ (<i>t</i> -BuNC)(<i>t</i> -Bupy)Ir(μ -O)(CO ₂)Os(O) ₂ (<i>t</i> -Bupy) ₂ ⁺ Cl ⁻ (34)	33 , <i>t</i> -BuNC	26
Cp*Ir(μ - <i>t</i> -BuN)(CO ₂)ZrCp ₂ (35)	Cp*Ir(μ - <i>t</i> -BuN)ZrCp ₂ , CO ₂	27
[Rh ₂ (CO ₂)(CO) ₂ (dppm) ₂] (36)	Rh ₂ (CO) ₂ (dppm) ₂	28
Ru ₂ (CO) ₄ [μ -(RO) ₂ PN(Et)P(OR) ₂] ₂ (CO) ₂ , R = <i>i</i> -Pr (37)	Ru ₂ (CO) ₅ (R'OH)[μ -(RO) ₂ PN(Et)P(OR) ₂] ₂ , pyridine	29
Pt(Ph)(PEt ₃) ₂ (CO ₂)Pt(Ph)(PEt ₃) ₂ (38)	Pt(COOH)(Ph)(PEt ₃), Pt(OH)(Ph)(PEt ₃) ₂	30
Pt(CF ₃)(diphoe)(CO ₂)(Pt(CF ₃)(diphoe) (39)	Pt(COOH)(CF ₃)(diphoe), Pt(OH)(CF ₃)(diphoe)	31
Pt(CF ₃)(dppe)(CO ₂)Pt(CF ₃)(dppe) (40)	Pt(COOH)(CF ₃)(dppe), Pt(OH)(CF ₃)(dppe)	31
<i>cis</i> -CpFe(CO)(PPh ₃)(CO ₂)Re(CO) ₄ (L), L = CO, PPh ₃ , P(OPh) ₃ , P(OEt) ₃ (41–44)	CpFe(CO)(PPh ₃)CO ₂ ⁻ K ⁺ , <i>cis</i> -Re(CO) ₄ (L)(F-BF ₃)	32, 33
<i>fac</i> -CpFe(CO)(PPh ₃)(CO ₂)Re(CO) ₃ [P(OEt) ₃] ₂ (45)	<i>fac</i> -CpFe(CO)(PPh ₃)(CO ₂)Re(CO) ₃ [P(OEt) ₃], P(OEt) ₃	33
Cp*Re(CO)(NO)(CO ₂)Re(CO) ₅ (46)	Cp*Re(CO)(NO)COOH, Re(CO) ₅ (C ₂ H ₄) ⁺ BF ₄ ⁻	34
Cp*Re(CO)(NO)(CO ₂)W(CO) ₃ Cp (47)	Cp*Re(CO)(NO)COOH, CpW(CO) ₃ (F-BF ₃)	34
<i>fac</i> , <i>cis</i> -Re(CO) ₃ (L) ₂ (CO ₂)Re(CO) ₄ (L), L = NH ₂ CH ₂ CH=CH ₂ (48)	<i>cis</i> -Re(CO) ₄ (L)(CONHCHMe ₂), H ₂ O	35
[Co(en) ₂ (CO ₂)(ClO ₄)·H ₂ O] _n (49)	Co(en) ₂ (OH)(CO ₂), NaClO ₄ , phosphate buffer	36
<i>cis</i> , <i>cis</i> -Ru(bpy) ₂ (CO)(CO ₂)Ru(bpy) ₂ (CO) ²⁺ 2PF ₆ ⁻ (50)	<i>cis</i> -Ru(bpy) ₂ (CO)(CHO) ⁺ PF ₆ ⁻ , H ₂ O, O ₂	37
CpRe(NO)(PPh ₃)(CO ₂)GePh ₃ (51)	CpRe(NO)(PPh ₃)CO ₂ ⁻ K ⁺ , BrGePh ₃	38
Cp*Fe(CO) ₂ (CO ₂)SnMe ₃ (52)	Cp*Fe(CO) ₂ CO ₂ ⁻ K ⁺ , ClSnMe ₃	39, 40
Cp*Fe(CO) ₂ (CO ₂)SnR ₃ , R = Me, <i>n</i> -Bu (52 , 53)	Cp*Fe(CO) ₃ ⁺ BF ₄ ⁻ , KOH, ClSnR ₃	40
Cp*Re(CO)(NO)(CO ₂)SnMe ₃ (54)	Cp*Re(CO)(NO)COOH, ClSnMe ₃	40
CpFe(CO) ₂ (CO ₂)SnPh ₃ (55)	CpFe(CO) ₃ ⁺ BF ₄ ⁻ , KOH, ClSnPh ₃	40
CpFe(CO)(PPh ₃)(CO ₂)SnR ₃ , R = Me, <i>n</i> -Bu (56 , 57)	CpFe(CO)(PPh ₃)CO ₂ ⁻ , K ⁺ , ClSnR ₃	40

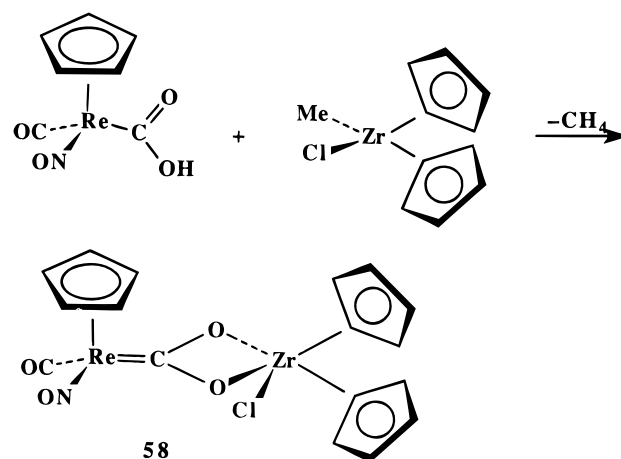
Scheme 11



Scheme 14. A summary of the complexes involving early transition metals is shown in Table 3 together with their precursors.

Symmetrical (class I) $\mu_2\text{-}\eta^3$ complexes involving two late transition metals are also well known, and several have been fully characterized. Geoffroy *et al.*⁴⁶ reported the first compounds of this type by net [2 + 2] cycloaddition reactions such as the one shown

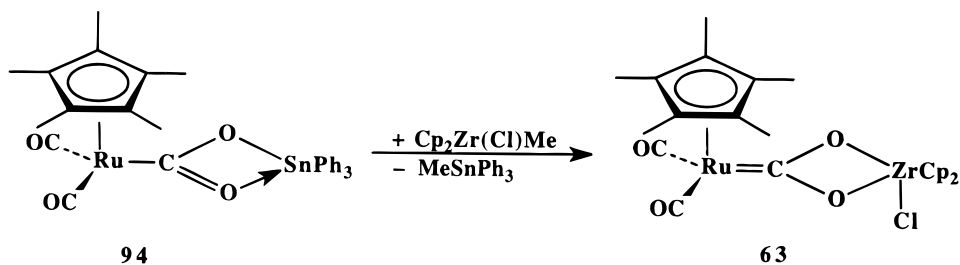
Scheme 12



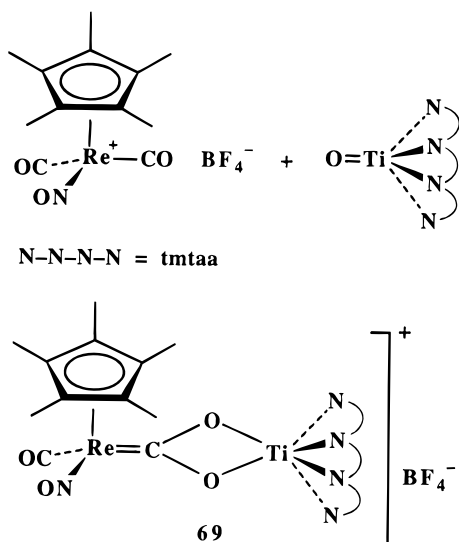
in Scheme 15 for the Re/W complex (**70**), which has been structurally characterized. This and several related compounds (**71–76**) prepared in this way are identified in Table 4.

Thermolysis, with CO displacement, has been used by Gibson *et al.*^{32,33} to prepare other late transition

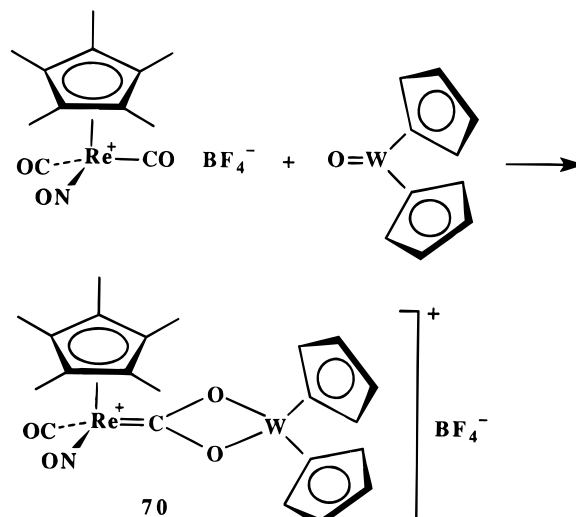
Scheme 13



Scheme 14



Scheme 15



metal complexes of this type (**77–83**); the method is illustrated in Scheme 16. However, in several instances, $\mu_2\text{-}\eta^3$ complexes **81–83** can be obtained directly from reactions that would be expected to yield the $\mu_2\text{-}\eta^2$ complexes instead, apparently by facile

conversion of the intermediate $\mu_2\text{-}\eta^2$ complex.^{34,47} An example of this reaction is shown in Scheme 17; the conversion to the $\mu_2\text{-}\eta^3$ complex **81** takes place at room temperature and is thought to be facilitated by the strongly electron donating Cp* ligand, which enhances the nucleophilicity of the metallocarboxy-

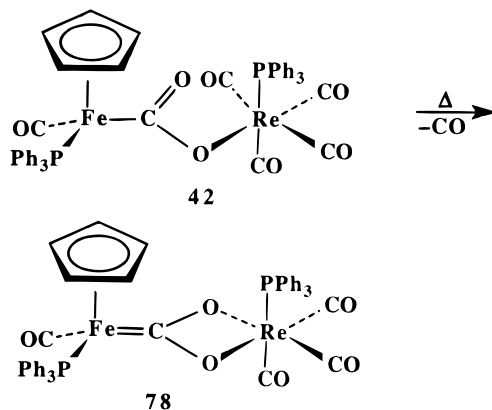
Table 3. Summary of Preparative Routes to Class I $\mu_2\text{-}\eta^3$ CO₂-Bridged Compounds Involving Late and Early Transition Metals

compound	precursors	ref
CpRe(CO)(NO)(CO ₂)Zr(Cl)Cp ₂ (58)	CpRe(CO)(NO)COOH, Cp ₂ Zr(Cl)(CH ₃)	41
CpRu(CO) ₂ (CO ₂)Zr(Cl)Cp ₂ (59)	CpRu(CO) ₂ CO ₂ ⁻ Na ⁺ , Cp ₂ ZrCl ₂ or CpRu(CO) ₂ Zr(Cl)Cp ₂ , CO ₂	42, 43
CpRu(CO) ₂ (CO ₂)Ti(Cl)Cp ₂ (60)	CpRu(CO) ₂ ⁻ Na ⁺ , Cp ₂ TiCl ₂ or CpRu(CO) ₂ Ti(Cl)Cp ₂ , CO ₂	42
CpFe(CO) ₂ (CO ₂)Zr(Cl)Cp ₂ (61)	CpFe(CO) ₂ CO ₂ CO ₂ ⁻ Na ⁺ , Cp ₂ ZrCl ₂	42
CpFe(CO) ₂ (CO ₂)Ti(Cl)Cp ₂ (62)	CpFe(CO) ₂ CO ₂ ⁻ Na ⁺ , Cp ₂ TiCl ₂	42
Cp*Ru(CO) ₂ (CO ₂)Zr(Cl)Cp ₂ (63)	Cp*Ru(CO) ₂ COOH, Cp ₂ Zr(H)(Cl) or Cp*Ru(CO) ₂ (CO ₂)SnPh ₃ , Cp ₂ Zr(Me)(Cl)	44
Cp*Re(CO)(NO)(CO ₂)Zr(Cl)Cp ₂ (64)	Cp*Re(CO)(NO)COOH, Cp ₂ Zr(H)(Cl)	44
Cp*Ru(CO) ₂ (CO ₂)Zr(Me)Cp ₂ (65)	Cp*Ru(CO) ₂ COOH, Cp ₂ Zr(Me)(OCH ₃)	44
Cp*Re(CO)(NO)(CO ₂)Zr(Me)Cp ₂ (66)	Cp*Re(CO)(NO)COOH, Cp ₂ ZrMe ₂	44
Cp*Ru(CO) ₂ (CO ₂)Zr(SnPh ₃)Cp ₂ (67)	Cp*Ru(CO) ₂ (CO ₂)SnPh ₃ , Cp ₂ Zr(H)(Me)	44
Cp*Re(CO)(NO)(CO ₂)Zr(SnPh ₃)Cp ₂ (68)	Cp*Re(CO)(NO)(CO ₂)SnPh ₃ , Cp ₂ Zr(H)(Me)	44
Cp*Re(CO)(NO)(CO ₂)Ti(tmtaa) ⁺ BF ₄ ⁻ (69)	Cp*Re(CO) ₂ (NO) ⁺ BF ₄ ⁻ , (tmtaa)Ti=O	45

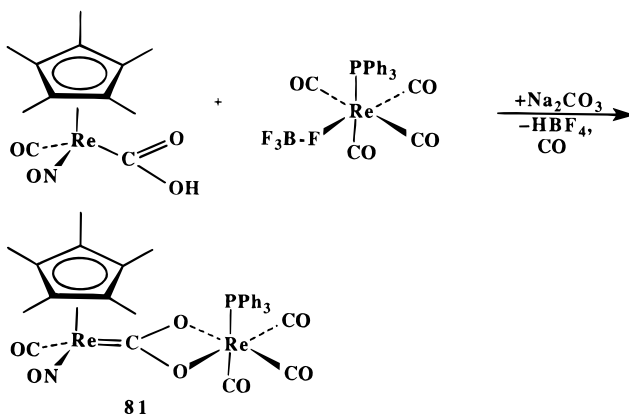
Table 4. Summary of Preparative Routes to Class I $\mu_2\text{-}\eta^3$ CO₂-Bridged Compounds Involving Two Late Transition Metals

compound	precursors	ref
Cp*Re(CO)(NO)(CO ₂)MCp ₂ ⁺ BF ₄ ⁻ , M = W or Mo (70, 71)	Cp*Re(CO) ₂ (NO) ⁺ BF ₄ ⁻ , Cp ₂ M = O, M = W or Mo	46
Cp*Mn(CO)(NO)(CO ₂)MCp ₂ ⁺ BF ₄ ⁻ , M = W or Mo (72, 73)	Cp*Mn(CO) ₂ (NO) ⁺ BF ₄ ⁻ , Cp ₂ M = O, M = W or Mo	46
CpM(CO) ₂ (CO ₂)WCp ₂ ⁺ BF ₄ ⁻ , M = Fe or Ru (74, 75)	CpM(CO) ₃ ⁺ BF ₄ ⁻ , Cp ₂ W = O, M = Fe or Ru	46
Pt(Cl)(PEt ₃)(CO ₂)WCp ₂ ⁺ BF ₄ ⁻ (76)	Pt(Cl)(PEt ₃)(CO) ₃ ⁺ BF ₄ ⁻ , Cp ₂ W = O	46
<i>fac</i> -CpFe(CO)(PPh ₃)(CO ₂)Re(CO) ₃ (L), L = CO, PPh ₃ , P(OPh) ₃ , P(OEt) ₃ (77–80)	<i>cis</i> -CpFe(CO)(PPh ₃)(CO ₂)Re(CO) ₄ (L)	32, 33
<i>fac</i> -Cp*Re(CO)(NO)(CO ₂)Re(CO) ₃ (PPh ₃) (81)	Cp*Re(CO)(NO)COOH, <i>cis</i> -Re(CO) ₄ (PPh ₃)(F-BF ₃)	47
Cp*Re(CO)(NO)(CO ₂)Mo(CO) ₂ Cp (82)	Cp*Re(CO)(NO)COOH, CpMo(CO) ₃ (F-BF ₃)	34, 48
Cp*Re(CO)(NO)(CO ₂)W(CO) ₂ Cp (83)	Cp*Re(CO)(NO)COOH, CpW(CO) ₃ (F-BF ₃)	34
<i>fac, cis</i> -Re(CO) ₃ (dppp)(CO ₂)Re(CO) ₂ (dppp) (84)	<i>fac</i> -Re(CO) ₃ (dppp)COOH, KOH	49

Scheme 16



Scheme 17



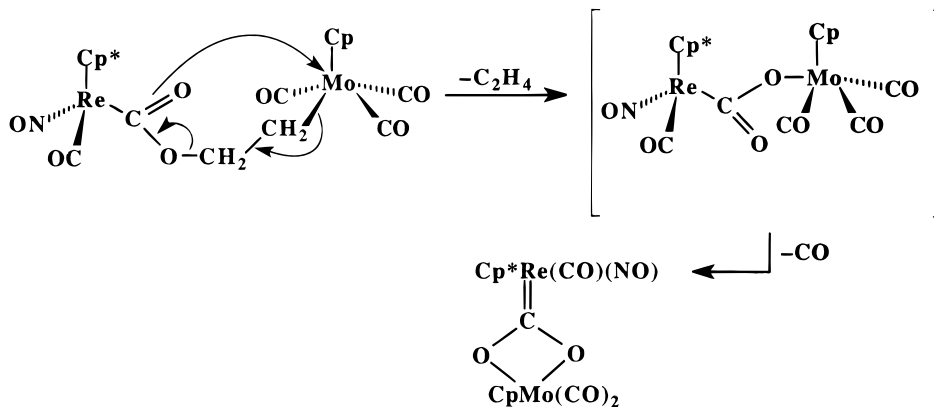
late. A summary of the compounds prepared in this way is also in Table 4.

Quite recently⁴⁸ it was found that thermolysis of a carboxyethylene-bridged bimetallic complex can lead to a $\mu_2\text{-}\eta^3$ CO_2 -bridged complex as shown in Scheme 18. This method is less effective than the alternative one, involving displacement of BF_4 , indicated for the same compound in Table 4.

Finally, a dirhenium complex **84** has been prepared⁴⁹ by treating *fac*- $\text{Re}(\text{CO})_3(\text{dppp})\text{COOH}$ with solid KOH . This may be an instance in which some of the acid decomposes to the corresponding hydride, $\text{Re}(\text{CO})_3(\text{dppp})(\text{H})$, which then reacts with additional acid yielding an intermediate $\mu_2\text{-}\eta^2$ complex followed by loss of CO to yield the observed product.

Compounds of these late transition metals are also air-sensitive and labile in solution; most have been

Scheme 18



prepared under N_2 either in a glovebox or in Schlenk-ware. The compounds containing zirconium are especially air- and moisture-sensitive.

(b) *Class II Compounds.* The first compounds of this type (**85–87**) were reported by Gladysz *et al.*³⁸ by reactions of $\text{CpRe}(\text{NO})(\text{PPh}_3)\text{CO}_2\text{-K}^+$ with main group halides; the reactions are illustrated in Scheme 19. Initially, the compounds were made to support the formulation of the metalcarboxylate anion since the triphenyltin complex is a nicely crystalline compound. However, the compounds undergo some interesting reactions and also show promise as relatively stable shelf reagents for the synthesis of other CO_2 -bridged compounds (see section VII.C.2).

The next systems to be prepared were the iron complexes (**88, 89**) reported by Gibson *et al.*⁵⁰ these also were prepared from metalcarboxylate anions and ClSnPh_3 . Compounds **91** and **92** were prepared similarly. This group also developed an alternative method for the synthesis of CO_2 -bridged tin complexes derived from highly labile metalcarboxylates. In this procedure, the metalcarboxylate was formed *in situ* in aqueous media from a metal carbonyl cation and in the presence of the tin halide.^{40,51} Good to excellent yields (54–90%) of the CO_2 -bridged compounds (**90, 93, 94**) can be obtained in this way since the products are not moisture-sensitive. This method was used first with the highly labile indenyliron system, $\text{IndFe}(\text{CO})(\text{PPh}_3)\text{COO}^-\text{K}^+$, and has been used effectively with complexes derived from $\text{Cp}^*\text{Fe}(\text{CO})_2\text{-CO}_2\text{-K}^+$ and $\text{Cp}^*\text{Ru}(\text{CO})_2\text{CO}_2\text{-K}^+$ (see Table 5).

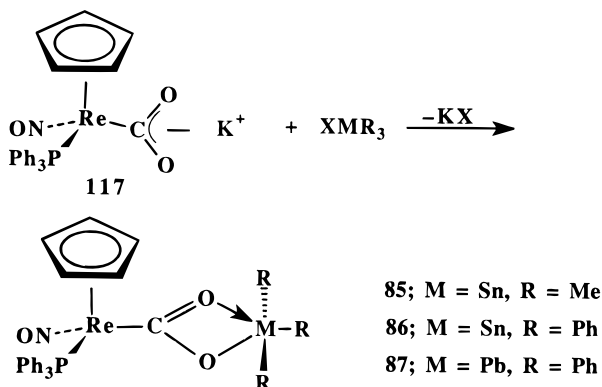
In some cases, it has been possible to use a metalcarboxylic acid directly with the tin halide to generate a CO_2 -bridged complex. Thus $\text{Cp}^*\text{Re}(\text{CO})(\text{NO})\text{COOH}$ reacts with ClSnPh_3 to provide the $\mu_2\text{-}\eta^3$ CO_2 -bridged complex **95**;⁴⁴ higher yields are obtained when Na_2CO_3 is added to take up liberated HCl (the metalcarboxylic acid is not deprotonated by this base). Also, the first compound (**96**) containing two bridging carboxylate ligands to tin has been prepared from this rhenium acid in combination with Me_2SnCl_2 .⁵²

3. $\mu_3\text{-}\eta^3$ Complexes

The first compound of this type was reported by Lewis and Johnson and their co-workers. Initially it was reported⁵³ that the reaction of $\text{Os}_6(\text{CO})_{18}$ with $\text{Os}_3(\text{CO})_{11}\text{H}^-$ afforded the cluster anion $\text{HOs}_3\text{-}$

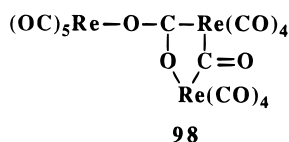
Table 5. Summary of Class II $\mu_2\text{-}\eta^3$ CO₂-Bridged Compounds Involving Late and Main Group Metals

compound	precursors	ref
CpRe(NO)(PPh ₃)(CO ₂)SnMe ₃ (85)	CpRe(NO)CO ₂ ⁻ K ⁺ , ClSnMe ₃	38
CpRe(NO)(PPh ₃)(CO ₂)SnPh ₃ (86)	CpRe(NO)(PPh ₃)CO ₂ ⁻ K ⁺ , ClSnPh ₃	38
CpRe(NO)(PPh ₃)(CO ₂)PbPh ₃ (87)	CpRe(NO)(PPh ₃)CO ₂ ⁻ K ⁺ , ClPbPh ₃	38
CpFe(CO)(PPh ₃)(CO ₂)SnPh ₃ (88)	CpFe(CO)(PPh ₃)CO ₂ ⁻ K ⁺ , ClSnPh ₃	50
Cp*Fe(CO)(PPh ₃)(CO ₂)SnPh ₃ (89)	Cp*Fe(CO)(PPh ₃)CO ₂ ⁻ K ⁺ , ClSnPh ₃	50
IndFe(CO)(PPh ₃)(CO ₂)SnPh ₃ (90)	IndFe(CO) ₂ (PPh ₃) ⁺ BF ₄ ⁻ , KOH, ClSnPh ₃	51
CpFe(CO)(PPh ₃)(CO ₂)SnR ₃ , R = Me, <i>n</i> -Bu (91, 92)	CpFe(CO)(PPh ₃)CO ₂ ⁻ K ⁺ , ClSnR ₃	40
Cp*Fe(CO) ₂ (CO ₂)SnPh ₃ (93)	Cp*Fe(CO) ₂ ⁺ BF ₄ ⁻ , KOH, ClSnPh ₃	40
same	Cp*Fe(CO) ₂ CO ₂ ⁻ K ⁺ , ClSnPh ₃	39
Cp*Ru(CO) ₂ (CO ₂)SnPh ₃ (94)	Cp*Ru(CO) ₂ ⁺ BF ₄ ⁻ , KOH, ClSnPh ₃	40
Cp*Re(CO)(NO)(CO ₂)SnPh ₃ (95)	Cp*Re(CO)(NO)COOH, ClSnPh ₃	47
[Cp*Re(CO)(NO)(CO ₂) ₂ SnMe ₂ (96)	Cp*Re(CO)(NO)COOH, Me ₂ SnCl ₂	52

Scheme 19

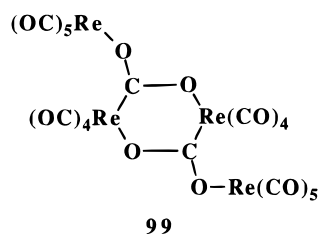
(CO)₁₀(O₂C)Os₆(CO)₁₇⁻ (**97**); the PPN⁺ salt of the anion was structurally characterized. However, in preparing additional related compounds,⁵⁴ it became apparent that oxygen was a necessary co-reagent. Only the first compound was structurally characterized; the others are formulated as $\mu_3\text{-}\eta^3$ complexes on the basis of IR and elemental analysis data.

The rhenium cluster complex **98** was generated in low yield from the photolysis of Re₂(CO)₁₀ in the



presence of NO and COT by Ziegler *et al.*⁵⁵ The compound was formulated as a metalcarboxylic acid on the basis of the presence of ν_{OH} in IR data, but the carboxyl C–O and O–Re bond distances do not show the differences which would be expected from such a compound. The proton could not be located.

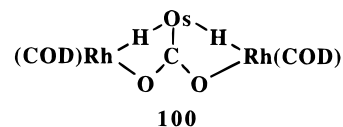
The related tetranuclear rhenium cluster **99** was reported by Beck *et al.*⁵⁶ in 1982. It was prepared



by dehydration of “Re(CO)₅(OH)” in acetone solution. The compound has been structurally characterized and shows carboxyl C–O and O–Re bond distances

that are quite similar to those reported by Ziegler for the other rhenium cluster with a single bridging CO₂.

Caulton *et al.*⁵⁷ reported and structurally characterized the cluster compound **100** by the direct



reaction of CO₂ with two equivalents of (COD)RhH₃-Os(PMe₂Ph)₃. The reaction also yields H₃Os(CO)-(PMe₂Ph)₃ and water as reaction products.

4. $\mu_3\text{-}\eta^4$ Complexes

The only examples of this type of complex are the metalcarboxylate salts characterized by Floriani.⁵⁸ The preparation of these compounds are discussed together with other metalcarboxylate salts in section II.C.

5. $\mu_4\text{-}\eta^4$ Complexes

Reaction of *cis*-Ru(bpy)₂(CO)₂²⁺, 2PF₆⁻ with 2 equiv of *n*-Bu₄NOH yields a hydrated CO₂ complex (**101**) which was initially formulated as an “ η^1 complex”.⁵⁹ However, the analytical and structural work showed that the carboxyl group was hydrated. Further analysis of the structural data⁶⁰ (see discussion in section IV.G) has revealed a structural unit consisting of two *cis*-Ru(bpy)₂(CO)(CO₂) molecules held together by six water molecules. Although other CO₂ complexes have been generated by deprotonation of a metalcarboxylic acid, the type of complex studied by Tanaka *et al.* is, so far, unique. This group also reported the preparation of the “anhydrous” analog by conducting the reaction of *n*-Bu₄NOH with the cation in dry CH₃CN.^{55b}

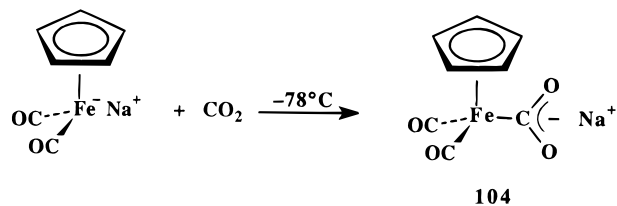
6. $\mu_4\text{-}\eta^5$ Complexes

Only one compound of this type has been reported. Caulton *et al.*^{57b} showed that the $\mu_3\text{-}\eta^3$ complex **100** would react with ZnBr₂ to afford a compound in which both carboxyl oxygens were bound to zinc; the compound (**102**) was structurally characterized (see section IV.H).

C. Metalcarboxylate Anions

Direct reaction between a simple metal anion complex and CO₂ has been used with several systems to generate the corresponding carbon dioxide complex

Scheme 20

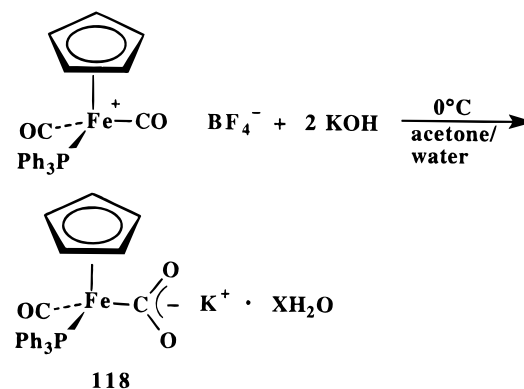


as illustrated in Scheme 20. The reactions usually require extremely low reaction temperatures because of the reversible nature of many of the reactions. Anionic complexes which have been formed in this way are indicated in Table 6. Several groups have worked with the metalcarboxylates derived from $\text{CpFe}(\text{CO})_2\text{-Na}^+$, but the early observations of Evans *et al.*⁶¹ prompted much of the subsequent work between this or other metal carbonyl anions and CO_2 . Among the carbon dioxide complexes, metalcarboxylate anions are typically the most difficult compounds to handle since they are highly labile in solution and very air-sensitive. As the work of Cutler^{62,63} and Cooper⁶⁴ showed, it is necessary to generate the metalcarboxylate salts at -78°C in an inert atmosphere in order to observe them directly. Cooper had also generated the metalcarboxylate dianion from $\text{Li}_2\text{W}(\text{CO})_5$ in a similar way.^{65,66}

By contrast, cobalt(salen)- M^+ ($\text{M} = \text{Li}, \text{Na}, \text{K}, \text{Cs}$) complexes **110–113** were carbonated rapidly at room temperature, and the metalcarboxylate salts precipitated from the THF solution.⁵⁸ The potassium salt required 5 days at room temperature for complete reaction with CO_2 . The sodium and potassium salts lost CO_2 under vacuum, but the lithium salt did not. Related metalcarboxylate complexes having Et-salen (**114, 115**) and *n*-Pr-salen (**116**) ligands on cobalt were also prepared by direct reaction with CO_2 .

Other metalcarboxylate anions have been generated by deprotonation of a metalcarboxylic acid.^{38,67,68,50} Some have been generated as a result of addition of 2 equiv of hydroxide ion to a metal carbonyl cation as shown in Scheme 21. Others have been generated *in situ* in this way.^{51,40} This method is sometimes effective for synthetic purposes even when the metalcarboxylate anion cannot be isolated. Also, it is the only route to metalcarboxylate anions for which the corresponding metal anion cannot be prepared. Note, however, that metalcarboxylate anions do not result from metal carbonyl

Scheme 21



cations bearing aryl phosphite ligands. Reactions of these iron cations with hydroxide ion result in good preparations for phosphonate complexes instead.⁶⁹ Synthetic routes from the acids are also summarized in Table 6.

IV. Structures of Metal-CO₂ Complexes

Although carbon dioxide is a linear molecule with equivalent C–O bond distances of 1.155(1) Å,⁷⁰ all structurally characterized CO_2 complexes contain transition metal–carbon bonds and possess a bent carbon dioxide ligand. Thus, with regard to geometry, the coordinated CO_2 groups bear a formal resemblance to the formate radical anion, $\cdot\text{CO}_2^-$, produced by one-electron reduction of CO_2 , as discussed in section VI. Several types of complexes are possible, depending upon the mode of coordination of the ligated CO_2 and the number of metal centers that interact with the ligand.

In the discussion below, division has been made simply according to the number of bonds between each ligated CO_2 and the metal centers or hydrogen atoms from water molecules in the complex (designated in terms of η^n) and according to the number of metal centers (including hydrogen) binding each CO_2 (designated in terms of μ_n). All types have the carboxylate carbon bound to a metal center; no compounds have yet been isolated in which the CO_2 is bound solely through one or both oxygen atoms, although such species may exist on metal surfaces (see discussion in section VI). The compounds constitute structural models for complexes in cata-

Table 6. Summary of Preparations for Metalcarboxylate Anion Complexes

compound	precursors	ref
By Direct Carbonation		
$\text{CpFe}(\text{CO})_2\text{CO}_2\text{-M}^+$, $\text{M} = \text{Li}, \text{Na}, \text{K}, 1/2 \text{Mg}$ (103–106)	$\text{CpFe}(\text{CO})_2\text{-M}^+$	62–64
$\text{CpRu}(\text{CO})_2\text{CO}_2\text{-Na}^+$ (107)	$\text{CpRu}(\text{CO})_2\text{-Na}^+$	43
$\text{W}(\text{CO})_5\text{CO}_2^{2-}2\text{Li}^+$ (108)	$\text{W}(\text{CO})_5^{2-}2\text{Li}^+$	65, 66
$\text{Cp}^*\text{Fe}(\text{CO})_2\text{CO}_2\text{-K}^+$ (109)	$\text{Cp}^*\text{Fe}(\text{CO})_2\text{-K}^+$	39
$\text{Co}(\text{salen})\text{CO}_2\text{-M}^+$ (110–113)	$\text{Co}(\text{salen})\text{-M}^+$	58
$\text{Co}(\text{Et-salen})\text{CO}_2\text{-M}^+$, $\text{M} = \text{Li}, \text{Na}$ (114, 115)	$\text{Co}(\text{Et-salen})\text{-M}^+$	58
$\text{Co}(\textit{n}\text{-Pr-salen})\text{CO}_2\text{-K}^+$ (116)	$\text{Co}(\textit{n}\text{-Pr-salen})\text{-K}^+$	58
By Deprotonation of MCOOH		
$\text{CpRe}(\text{NO})(\text{PPh}_3)\text{CO}_2\text{-K}^+$ (117)	$\text{CpRe}(\text{NO})(\text{PPh}_3)\text{COOH}, \text{KH}$	38
$\text{CpFe}(\text{CO})(\text{PPh}_3)\text{CO}_2\text{-K}^+$ (118)	$\text{CpFe}(\text{CO})_2(\text{PPh}_3)^+\text{BF}_4^-, \text{KOH}$	50, 67
$\text{Cp}^*\text{Fe}(\text{CO})(\text{PPh}_3)\text{CO}_2\text{-K}^+$ (119)	$\text{Cp}^*\text{Fe}(\text{CO})_2(\text{PPh}_3)^+\text{BF}_4^-, \text{KOH}$	50
$\text{Cp}^*\text{Ru}(\text{CO})_2\text{CO}_2\text{-K}^+$ (120)	$\text{Cp}^*\text{Ru}(\text{CO})_3^+\text{BF}_4^-, \text{KOH}$	40
$\text{Ind Fe}(\text{CO})_2\text{CO}_2\text{-K}^+$ (122)	$\text{Ind Fe}(\text{CO})_3^+\text{BF}_4^-, \text{KOH}$	51

lytic processes leading to conversion of CO₂ to other carbon compounds.

A. η^1 Complexes

The only complex of this type to be structurally characterized is the rhodium complex **3** reported by Herskovitz *et al.*⁸ X-ray structural analysis showed a Rh–C(1) bond distance of 2.05(2) Å and C–O bond distances of 1.20(2) and 1.25(2) Å. The O–C–O angle was 126(2)°. Earlier, structural analysis of the methylated derivative of Ir(dmpe)₂(Cl)(CO₂) had also supported the designation of this compound as an η^1 complex.⁷²

B. η^2 Complexes

The first compound of this type to be structurally characterized (and the first CO₂ complex to be so characterized), **4**, was reported by Aresta and Nobile⁹ and involved an almost planar coordination environment about the nickel atom with two bulky phosphine ligands in addition to the CO₂. As illustrated in the diagram for **4**, the carbon dioxide ligand is bound through carbon and one oxygen and thus has one short C–O bond (1.17 Å) and one longer one of 1.22 Å. The compound also showed a very large O–C–O angle of 133°. Later, Jolly, Romao, and their co-workers¹⁰ were able to structurally characterize the solvent-free complex. Detailed analysis of the compound showed C–O bond lengths of 1.211(4) and 1.257(5) Å and an O–C–O bond angle of 136.2°.

The structural report by Aresta was followed by crystallographic characterization of the niobium complex Cp'₂Nb(CO₂)(CH₂SiMe₃) (**11**) by Lappert *et al.*,¹⁷ which also showed dissimilar C–O bond distances (1.216(8) and 1.283(8) Å) and a large O–C–O angle (132.4(7)°). Again, the data showed bonding between the metal and only one carboxyl oxygen. Nicholas *et al.*²¹ characterized the related Cp'₂Nb(CO₂)(CH₂Ph) (**16**), which shows similar structural parameters. Soon after Lappert's report, Floriani and co-workers¹⁸ reported the characterization of Cp₂Mo(CO₂), which showed an even larger difference in the carboxyl C–O bond lengths (1.201(14) and 1.288(14) Å) and showed bonding between molybdenum and only one carboxyl oxygen.

The iron complex, Fe(CO₂)(depe)₂ (**9**), characterized by Komiya *et al.*¹⁵ has trigonal-bipyramidal geometry about the iron atom with the CO₂ ligand in the equatorial plane. It is unique among η^2 -CO₂ complexes with two relatively long C–O bonds, 1.25(3) and 1.28(2) Å, and a relatively small O–C–O angle of 124(2)°. On the basis of these data and IR spectral characteristics (see section VI.A.2), the CO₂ ligand was described as being intermediate between η^1 - and η^2 -coordinated.

Preliminary structural data has been reported recently by Hidai *et al.*²³ on a tungsten complex, *trans*-[W(CO)(CO₂)(dppe)₂], which appears to be of the η^2 type also. However, detailed bond distances and bond angles are not yet available for the compound.

Carmona and co-workers have reported structural data on two bis(carbon dioxide) complexes of molybdenum. The first compound, *trans*-[Mo(CO₂)₂(PMe₃)₃-

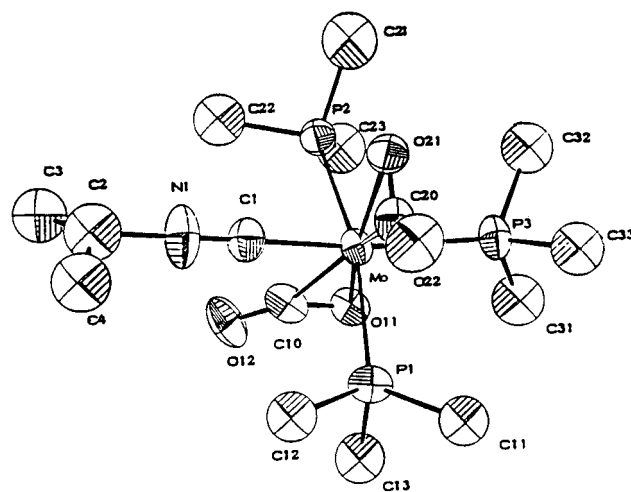


Figure 2. Molecular structure of *mer,trans*-Mo(CO₂)₂(PMe₃)₃(CN-*i*-Pr) (**22**).

(CN-*i*-Pr)]^{25a} whose structure is shown in Figure 2, showed equivalently ligated CO₂ molecules (1.22(2) and 1.26(2) Å in the first and 1.22(1) and 1.26(1) Å in the second). As expected for an η^2 complex, the O–C–O angles are large (133(1)° and 134(1)°) and bonding to molybdenum involves a single carboxyl oxygen in each case. The planes of the two metallalactone rings are orthogonal. The second compound is the closely related *trans*-[Mo(CO₂)₂(PMe₃)₃(CNCH₂-Ph)].^{25c} In this compound, however, there are greater differences in C–O bond lengths between each ligated CO₂ molecule (1.25(2) and 1.28(3) Å in one and 1.20(2) and 1.28(3) Å in the other) and smaller O–C–O bond angles (128(2)° for both) than are seen for most η^2 -type complexes. Again the two metallalactone rings are orthogonal.

C. μ_2 - η^2 Complexes

The simplest type of CO₂-bridged bimetallic complex involves coordination of the carboxyl carbon to one metal and bonding of one carboxyl oxygen to a second metal center. However, interesting variations result depending upon whether the two metal centers are bound together, bridged by other groups, totally independent or, alternatively, have the bridging CO₂ as a repeating unit of a polymer chain.

The first compounds of the μ_2 - η^2 type (**33**, **34**) were reported by Collins *et al.*²⁶ Although neither were structurally characterized directly, the O-alkylated derivative of **34** was characterized by X-ray analysis, thus providing unequivocal support for the formulation of the precursor and its relatives. The molecular structure of the cation indicated that the bridging CO₂ of the precursor was actually part of a five-membered metallacyclic ring because of the presence of a bridging oxo ligand between iridium and osmium. More recently, Bergman *et al.*²⁷ structurally characterized a related metallacyclic complex (**35**) with CO₂ bridged between iridium and zirconium as shown in Scheme 4 and in Figure 3. One C–O bond was much shorter than the other, 1.229(12) and 1.306(12) Å, and the O–C–O angle was 122.2(9)°.

Haines *et al.*²⁹ first reported the preliminary structural characterization of a CO₂-bridged diruthenium

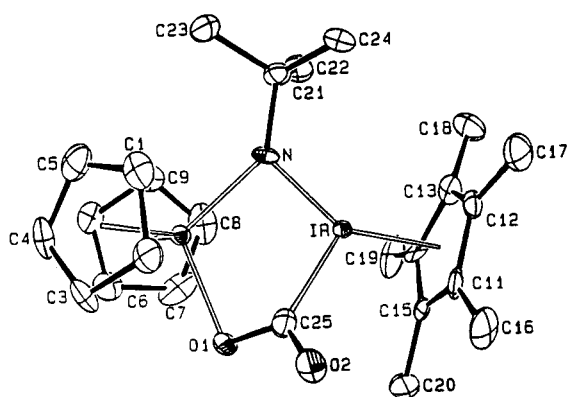
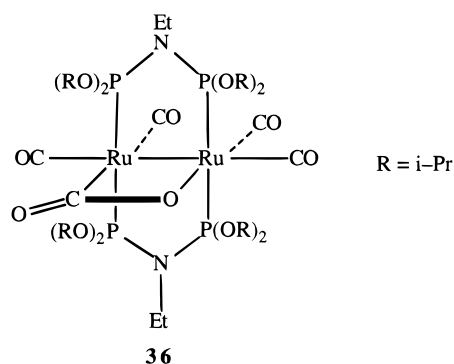


Figure 3. Molecular structure of $\text{Cp}^*\text{Ir}(\mu\text{-}t\text{BuN})(\text{CO}_2)\text{-ZrCp}_2$ (**35**).

complex (**36**) in 1990 and later refined the data more



completely. The compound has a CO_2 ligand bridged between bonded ruthenium atoms, thus generating a four-membered metallacyclic ring. The compound exhibits a C–O distance of only 1.06(3) Å for the noncoordinated carboxyl oxygen, the shortest for any CO_2 complex yet known; the other C–O bond distance is normal at 1.29(3) Å. The compound showed an internal O–C–O angle of 101(2)°, the smallest such angle known for any CO_2 complex.

Carbon dioxide complexes of cobalt have been studied by Creutz *et al.*³⁶ The structure of a polymeric complex, $[\text{Co}^{\text{III}}(\text{en})_2(\text{CO}_2)(\text{ClO}_4)\cdot\text{H}_2\text{O}]_n$ (**49**), was reported in 1992. The polymer has repeating units with CO_2 bridged in $\mu_2\text{-}\eta^2$ fashion between cobalt atoms and showing one short carboxylate C–O bond (1.214(19) Å) and one longer C–O bond (1.285(18) Å) and an internal O–C–O angle of 124(2)°. The polymeric structure was proposed to be stabilized by hydrogen-bonding interactions involving, in each case, six amine hydrogens and the carboxylate oxygens as well as further H-bonding between remaining amine hydrogens and those of H_2O with the perchlorate anion.

At about the same time, Gibson *et al.*³³ reported the characterization of the iron–rhenium compound, $\text{CpFe}(\text{CO})(\text{PPh}_3)(\text{CO}_2)\text{Re}(\text{CO})_4(\text{PPh}_3)$ (**42**), shown in Figure 4, which has the CO_2 ligand bound through carbon to the iron atom and through one oxygen to the rhenium atom. This complex also showed one short carboxyl C–O bond (1.226(3) Å) and one longer bond (1.298(3) Å) and had an O–C–O angle of 121.9(3)°. More recently, structural data on a $\mu_2\text{-}\eta^2$ CO_2 -bridged dirhenium complex (**48**) has been reported by Lin *et al.*³⁵ Again, one short C–O bond (1.24(1) Å)

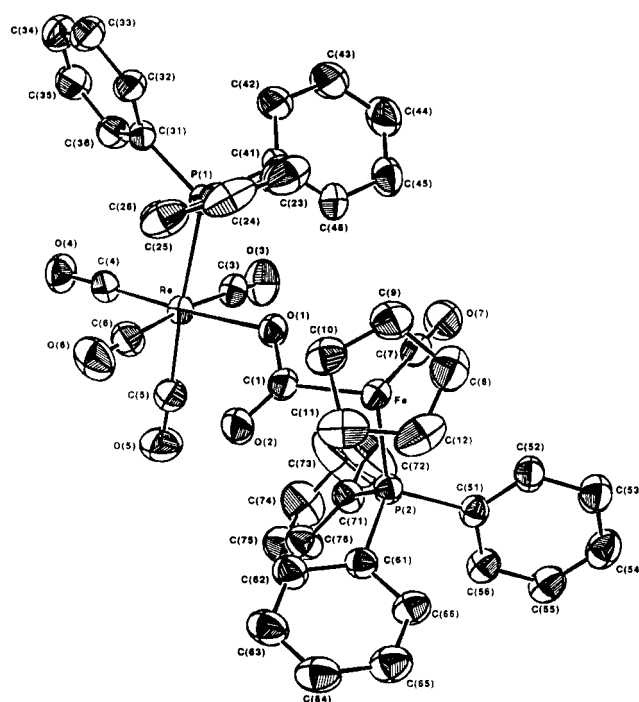


Figure 4. Molecular structure of $\text{CpFe}(\text{CO})(\text{PPh}_3)(\text{CO}_2)\text{-Re}(\text{CO})_4(\text{PPh}_3)$ (**42**).

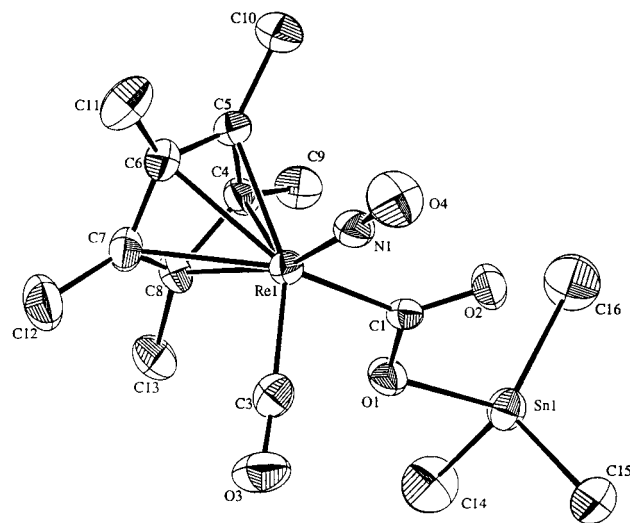


Figure 5. Molecular structure of $\text{Cp}^*\text{Re}(\text{CO})(\text{NO})(\text{CO}_2)\text{-SnMe}_3$ (**54**).

and one longer C–O bond (1.30(1) Å) were found in the CO_2 ligand. The O–C–O angle in this complex is somewhat smaller (119.0(8)°) than those in the others of this structural type.

Also, Gibson *et al.*⁴⁰ reported the structural characterization of $\text{Cp}^*\text{Re}(\text{CO})(\text{NO})(\text{CO}_2)\text{SnMe}_3$ (**54**) in which only one carboxylate oxygen is coordinated to tin. Again, the C–O bond lengths are unequal: 1.237(6) and 1.311(6) Å. The O–C–O bond angle is 117.0(5)°, but it is clearly the O–Sn distances (2.054(4) Å and 2.806(4) Å) which confirm that the compound is of the $\mu_2\text{-}\eta^2$ type. The Re–carboxyl carbon bond length is 2.103(5) Å; an ORTEP diagram for this compound is shown in Figure 5.

As a group, all of the $\mu_2\text{-}\eta^2$ complexes show one short and one long C–O bond; the nonmetallacyclic complexes show a relatively large O–C–O angle, varying from 117 to 124° in the compounds charac-

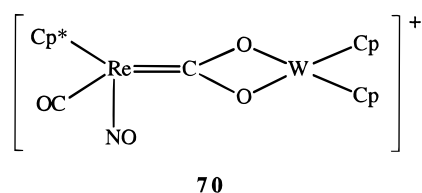
terized to the present time. Clearly, ring size in the metallacyclic compounds can have a large impact on these parameters.

D. $\mu_2\text{-}\eta^3$ Complexes

There are two structurally distinct types of compounds having the carboxylate carbon bound to one metal center and both oxygens bound to a second metal. The characteristics of the two types are discussed below.

1. Class I Compounds

The compounds in this class at present all have the CO_2 ligand bridged between two transition metals. The first to be reported⁴⁶ was the rhenium/tungsten cationic complex **70**. The rhenium-carboxylate car-



bon bond is short at 2.04(4) Å, supporting the dimetalated dioxycarbene formulation shown. The C–O bond distances, 1.34(4) and 1.32(4) Å, are both longer than in the tin complex shown in Figure 5. The O–W bond distances, also, are highly symmetrical at 2.09(2) and 2.08(2) Å and the O–C–O angle is 106(3)°. The Geoffroy group also reported the characterization of a related CO_2 -bridged cation, $\text{Cp}^*\text{Re}(\text{CO})(\text{NO})(\text{CO}_2)\text{Ti}(\text{tmtaa})^+$ (**69**) soon afterward.⁴⁵ This system has a slightly less symmetrically bonded CO_2 ligand: C–O bond distances are 1.281(11) and 1.309(11) Å and the O–Ti distances are 2.023(7) and 2.066(6) Å. The O–C–O angle is 111.9(8)°. Also, the rhenium-carboxyl carbon bond is somewhat longer at 2.081(9) Å.

Several related, but neutral, symmetrical complexes derived from the same rhenium metallocarboxylate have been characterized by Gibson *et al.*^{34,44,47,71} Data for all compounds derived from this rhenium system are summarized in Table 7; ORTEP diagrams for two of these compounds are shown in Figures 6 and 7. Gibson *et al.* also characterized two related compounds derived from other metallocarboxylates. Thus, $\text{CpFe}(\text{CO})(\text{PPh}_3)(\text{CO}_2)\text{Re}(\text{CO})_3\text{-}[\text{P}(\text{OEt})_3]$ (**80**)³³ also shows symmetrical bonding about the bridging CO_2 ligand with C–O bond lengths of 1.322(8) and 1.274(8) Å and O–Re bond lengths of 2.163(5) and 2.143(5) Å. The internal O–C–O angle is 111.3(6)°; the ORTEP diagram is shown in Figure 8. $\text{Cp}^*\text{Ru}(\text{CO})_2(\text{CO}_2)\text{Zr}(\text{Cl})\text{Cp}_2$ (**63**)⁴⁴

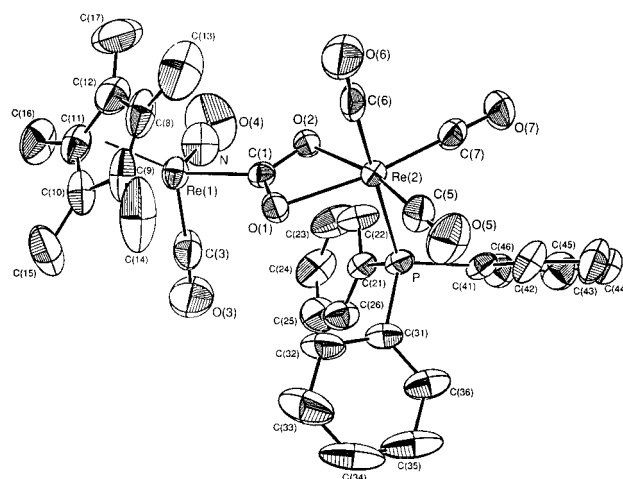


Figure 6. Molecular structure of *fac*- $\text{Cp}^*\text{Re}(\text{CO})(\text{NO})(\text{CO}_2)\text{Re}(\text{CO})_3(\text{PPh}_3)$ (**81**).

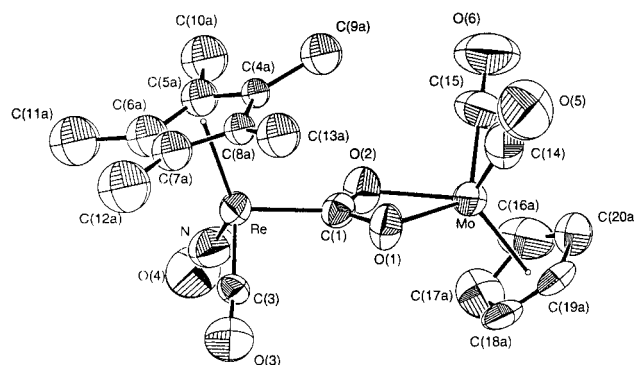


Figure 7. Molecular structure of $\text{Cp}^*\text{Re}(\text{CO})(\text{NO})(\text{CO}_2)\text{Mo}(\text{CO})_2\text{Cp}$ (**82**).

shows C–O bond lengths of 1.285(5) and 1.281(5) Å and O–Zr bond lengths of 2.221(3) and 2.236(3) Å. Here the O–C–O bond angle is 113.4(3)°. The ORTEP diagram for this compound is shown in Figure 9. The two complexes with zirconocene fragments have similar structures with regard to the bonding around this fragment. Considering the centroids to each cyclopentadienyl ring as bonds, the geometry about the Zr atom can be described as edge-capped tetrahedral with the two carboxyl oxygens and the chlorine atom lying in a plane.

Recently, also, Mandal *et al.*⁴⁹ characterized a CO_2 -bridged dirhenium compound in this class, $(\text{dppp})(\text{CO})_3\text{Re}(\text{CO}_2)\text{Re}(\text{CO})_2(\text{dppp})\cdot\text{C}_6\text{H}_6$ (**84**). The compound showed C–O bond distances of 1.260(15) and 1.289(14) Å and O–Re bond distances of 2.198(8) and 2.208(8) Å. The rhenium-carboxylate carbon bond length is 2.191(13) Å; thus it is somewhat longer than in those compounds with a $\text{Cp}^*\text{Re}(\text{CO})(\text{NO})$ fragment.

Table 7. Structural Parameters for Symmetrical $\mu_2\text{-}\eta^3$ CO_2 -Bridged Complexes, $\text{Cp}^*\text{Re}(\text{CO})(\text{NO})(\text{CO}_2)\text{ML}_n$

ML _n	bond lengths (Å)			O–C–O angle (deg)	ref
	C–O	O–M			
WCp ₂ ⁺ (70)	1.32(4), 1.34(4)	2.08(2), 2.09(2)		106(3)	46
Ti(tmtaa) (69)	1.281(11), 1.309(11)	2.023(7), 2.066(6)		111.9(8)	45
Re(CO) ₃ (PPh ₃) (81)	1.289(8), 1.296(6)	2.165(4), 2.175(3)		113.2(5)	47
Re(CO) ₂ (PPh ₃) ₂	1.285(8), 1.303(8)	2.178(5), 2.215(5)		112.7(7)	71
Zr(Cl)Cp ₂ (58)	1.271(7), 1.296(8)	2.201(3), 2.245(4)		113.9(4)	44
Mo(CO) ₂ Cp (82)	1.26(1), 1.29(1)	2.149(7), 2.158(7)		112.8(10)	34

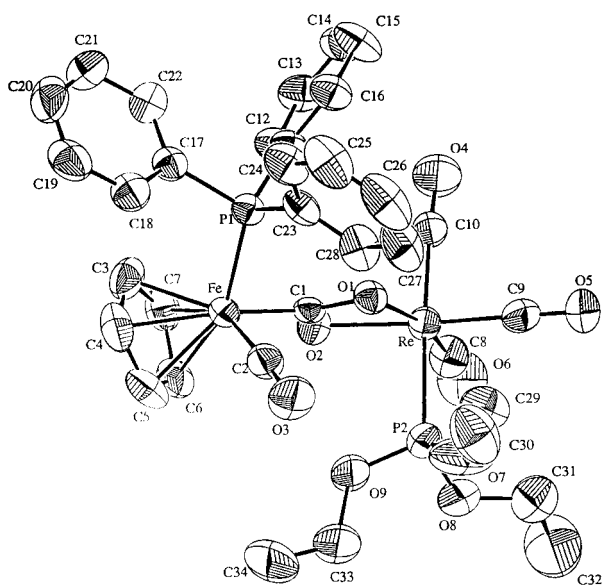


Figure 8. Molecular structure of *fac*-CpFe(CO)(PPh₃)(CO₂)Re(CO)₃[P(OEt)₃] (**80**).

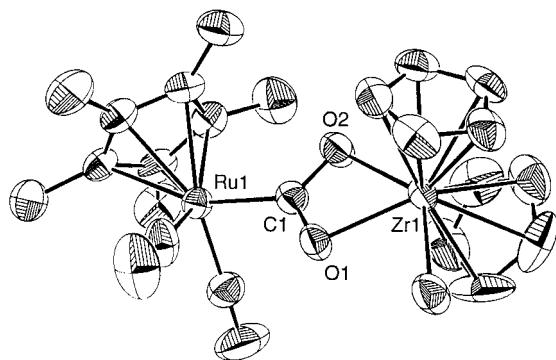


Figure 9. Molecular structure of Cp^{*}Ru(CO)₂(CO₂)Zr(Cl)-Cp₂ (**63**).

Thus, the class I compounds are characterized by nearly equal C–O bond lengths as well as nearly equal O–M₂ bond lengths and a small O–C–O bond angle (in the range 106–114° in the compounds characterized to date). Except for **70**, which has an unusually small O–C–O angle, variations in coordination geometry at M₂ do not have a large impact on these characteristics.

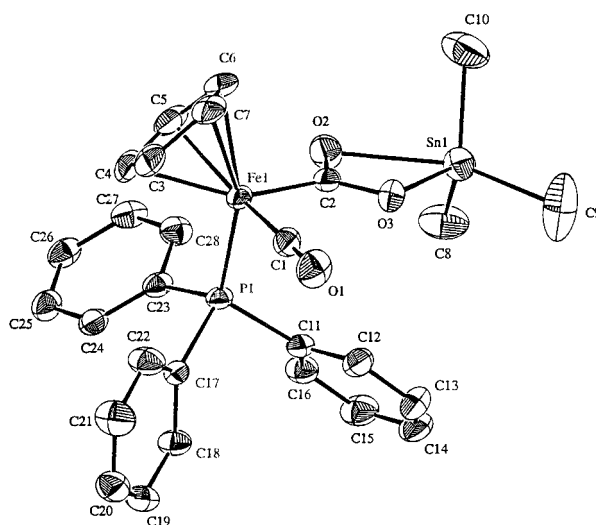


Figure 10. Molecular structure of CpFe(CO)(PPh₃)(CO₂)-SnMe₃ (**91**).

2. Class II Compounds

The compounds in this class that have been structurally characterized, so far, are ones in which the two carboxylate oxygens are bound, unequally, to a tin atom. Structural data relating to bonding of the carboxyl group in these compounds are summarized in Table 8. All except the final entry in the table have distorted trigonal-bipyramidal geometry at the tin atom and the carboxyl oxygens occupy one axial and one equatorial site. The most symmetrical of the compounds is the first one in Table 8, and the most unsymmetrical is the indenyl complex (**90**). The large difference in O–Sn bond lengths and the relatively large O–C–O angle (115.9(3)°) in this compound appear to represent the limits for compounds in this class. Note that the $\mu_2\text{-}\eta^2$ CO₂-bridged rhenium–trimethyltin complex **54** in Figure 5 shows an only slightly greater O–C–O angle but has one significantly longer O–Sn distance and is, by IR spectral characterization also, of the $\mu_2\text{-}\eta^2$ type. ORTEP diagrams for two representative compounds in class II are shown in Figures 10 and 11. The trimethyltin derivative **91** in Figure 10 is clearly of the $\mu_2\text{-}\eta^3$ type, but it was necessary to obtain the structural data at

Table 8. Summary of Carboxylate Bonding Parameters for $\mu_2\text{-}\eta^3$ Complexes Involving Tin

compound	bond lengths (Å)		O–C–O angle (deg)	ref
	C–O	O–Sn		
CpRe(NO)(PPh ₃)(CO ₂)SnPh ₃ (86)	1.269(11) 1.313(11)	2.257(7) 2.175(7)	112.2(8)	38
CpFe(CO)(PPh ₃)(CO ₂)SnPh ₃ (88)	1.270(6) 1.305(6)	2.342(4) 2.123(4)	113.4(4)	50b
CpFe(CO)(PPh ₃)(CO ₂)SnMe ₃ (91)	1.260(6) 1.321(5)	2.476(3) 2.089(3)	114.3(3)	40
CpFe(CO)(PPh ₃)(CO ₂)Sn(<i>n</i> -Bu) ₃ (92)	1.266(7) 1.316(7)	2.432(4) 2.105(4)	114.2(5)	40
IndFe(CO)(PPh ₃)(CO ₂)SnPh ₃ (90)	1.236(3) 1.336(3)	2.536(2) 2.069(2)	115.9(3)	51
Cp [*] Fe(CO) ₂ (CO ₂)SnPh ₃ (93)	1.252(3) 1.312(3)	2.394(2) 2.102(2)	114.5(2)	40
Cp [*] Re(CO)(NO)(CO ₂)SnPh ₃ (95)	1.24(1) 1.322(9)	2.399(1) 2.092(3)	114.6(7)	47
Cp [*] Ru(CO) ₂ (CO ₂)SnPh ₃ (94)	1.245(5) 1.306(5)	2.425(3) 2.100(3)	115.7(4)	44
[Cp [*] Re(CO)(NO)(CO ₂) ₂ SnMe ₂ (96)	1.26(1) 1.31(1)	2.524(8) 2.078(6)	116.8(9)	52

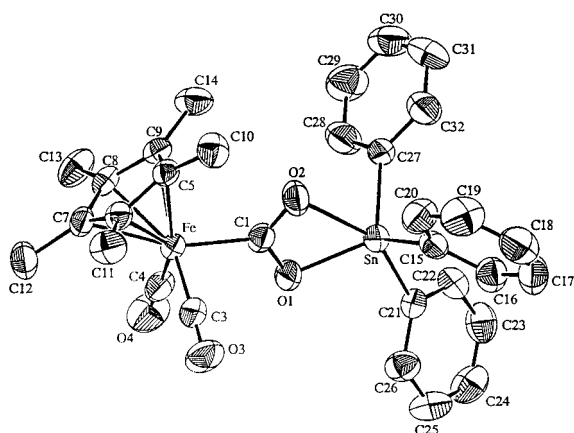


Figure 11. Molecular structure of $\text{Cp}^*\text{Fe}(\text{CO})_2(\text{CO}_2)\text{SnPh}_3$ (**93**).

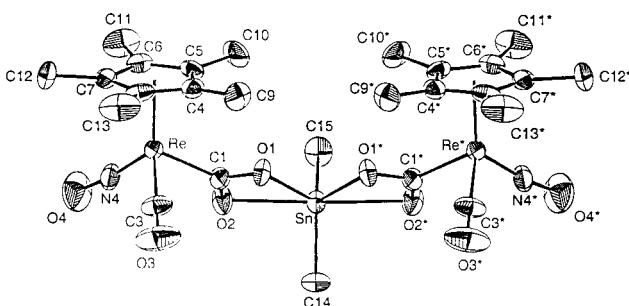


Figure 12. Molecular structure of $[\text{Cp}^*\text{Re}(\text{CO})(\text{NO})(\text{CO}_2)]_2\text{-SnMe}_2$ (**96**).

very low temperature, which enhances this form of the compound. Structural data on rhenium complex **54** were obtained at room temperature.

Quite recently,⁵² structural data have been obtained for a compound with two bridging carbon dioxide ligands to a single tin atom. The ORTEP diagram for the compound, $[\text{Cp}^*\text{Re}(\text{CO})(\text{NO})(\text{CO}_2)]_2\text{-SnMe}_2$ (**96**), is shown in Figure 12. This is the only tin complex in class II that has an octahedrally coordinated tin atom; still, the O–Sn bond lengths, 2.078(6) and 2.524(8) Å, are highly unequal. The O–C–O bond angle for **96** is large at 116.8(9)°.

The main feature distinguishing the class II compounds from those in class I is the highly unequal nature of the O–M₂ bond lengths in class II compounds. Also, the shorter C–O bond is always paired with the longer O–M₂ bond. Additionally, the O–C–O bond angles of class II compounds are slightly larger than those in class I.

E. $\mu_3\text{-}\eta^3$ Complexes

The first CO₂-bridged compound of this type to be structurally characterized was an osmium cluster anion with a fully chelated carbon dioxide ligand. The compound, $[(\text{Ph}_3\text{P})_2\text{N}]^+[\text{HO}_3(\text{CO})_{10}(\text{CO}_2)\text{Os}_6(\text{CO})_{17}]$ (**97**), was characterized by Lewis, Johnson, and their co-workers.⁵³ Later, Guy and Sheldrick reported⁷³ the complete structural analysis of the compound, which showed C–O bond distances of 1.276(5) and 1.322(5) Å and O–Os bond distances of 2.115(40) and 2.192(42) Å. The O–C–O angle is 112.4(48)°.

The next compound of this general type to be characterized was the trinuclear rhenium complex **98** characterized by Ziegler⁵⁵ and showing a sym-

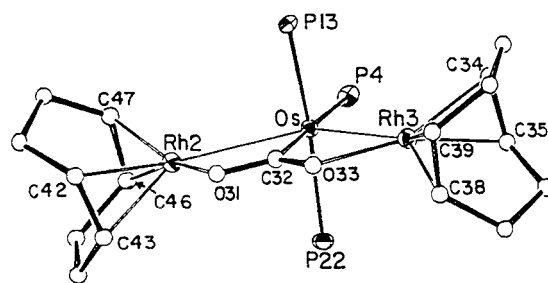


Figure 13. Molecular structure of $[(\text{COD})\text{Rh}]_2\text{OsH}_2(\text{CO}_2)(\text{PMe}_2\text{Ph})_3$ (**100**).

metrically bridged carboxyl group. Analytical and IR data suggested a bridging COOH group, but this has not been confirmed. Shortly thereafter, a tetranuclear rhenium complex (**99**) was reported by Beck *et al.*⁵⁶ that showed two bridging CO₂ ligands, each bound in $\mu_3\text{-}\eta^3$ fashion. This brief report gives averages for the C–O bond distances which are either internal to the six-membered metallacyclic ring or external to it with oxygen bonding to an $\text{Re}(\text{CO})_5$ moiety. Internal C–O bond lengths average 1.28 Å and the external ones average 1.25 Å while O–Re bond distances average 2.16 Å (internal) and 2.13 Å (external); thus the binding of the CO₂ ligands appears to be highly symmetrical. The O–C–O angles were not reported.

Caulton *et al.*⁵⁷ reported the characterization of $[(\text{COD})\text{Rh}]_2\text{OsH}_2(\text{CO}_2)(\text{PMe}_2\text{Ph})_3$ (**100**), which has the carboxylate carbon bound to the osmium center. The bonding of the CO₂ ligand is highly symmetrical, with C–O bond lengths slightly greater (1.300(21) and 1.309(22) Å) than in the previous examples and with essentially equal O–Rh bond lengths (2.062(13) and 2.065(12) Å). The O–C–O angle is 116.3(16)°; the structure is shown in Figure 13.

F. $\mu_3\text{-}\eta^4$ Complexes

The only compound of this type to be characterized is $\text{Co}(n\text{-Pr-salen})(\text{CO}_2)\text{K}(\text{THF})$ (**116**), studied by Floriani *et al.*^{58b,c} The crystals of the polymeric compound were dimorphous, and X-ray analysis was carried out on both forms. The structural data for the two forms are closely similar, and only those for form B will be described here. The carboxyl C–O bond lengths are 1.20(2) and 1.24(2) Å and the analogous O–K bond lengths are 2.74(1) and 2.66(1) Å. However, as Figure 14 shows, one of the carboxyl oxygens (O3) is also bound to a second potassium ion. The O–C–O bond angle in this compound is unusually large at 134.9(26)°, possibly because of the interaction with the second K⁺. This is also the only metalcarboxylate anion complex to have been structurally characterized.

G. $\mu_4\text{-}\eta^4$ Complexes

Although previously described⁵⁹ as an $\eta^1\text{-CO}_2$ complex with the molecular formula $\text{cis-}[\text{Ru}(\text{bpy})_2(\text{CO})(\text{CO}_2)]\cdot 3\text{H}_2\text{O}$, each structural unit in the complex (**101**) actually consists of two such assemblies held together with the aid of hydrogen bonding involving six water molecules as shown in Figure 15.⁶⁰ Each CO₂ ligand shows hydrogen bonding of one oxygen to a single water molecule while the second oxygen

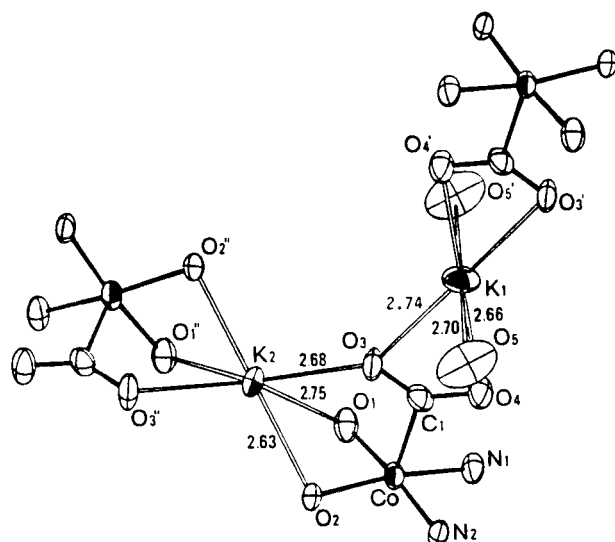


Figure 14. Molecular structure of $\text{Co}(n\text{-Pr-salen})(\text{CO}_2)\text{K}(\text{THF})$ (**116**).

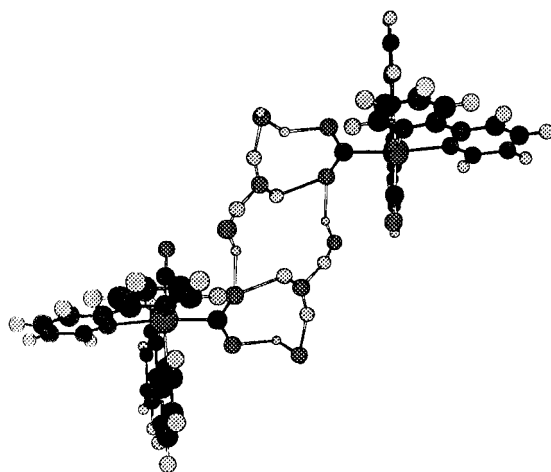


Figure 15. Representation of the dimeric structure of $\text{cis-}[\text{Ru}(\text{bpy})_2(\text{CO})(\text{CO}_2)\cdot 3\text{H}_2\text{O}]_2$ (**101**).

is bound to two other water molecules. The bonding can be described as $\mu_4\text{-}\eta^4$ with hydrogen bonds assuming three of the coordination sites. As might be expected, the O–C bond is slightly longer (1.283(15) Å as compared to 1.245(16) Å) where the carboxylate oxygen is bound to two water molecules. The O–C–O angle was reported as 120.9(12)°.

H. $\mu_4\text{-}\eta^5$ Complexes

Caulton and co-workers^{57b} characterized the ZnBr_2 derivative of the $\mu_3\text{-}\eta^3$ rhodium–osmium complex discussed above. The derivative (**102**) shows both carboxylate oxygens bound to the zinc atom. The C–O bond lengths are slightly unequal at 1.29(14) and 1.322(14) Å and the O–Rh bonds are lengthened slightly to 2.080(8) and 2.097(7) Å in comparison to the present complex. The O–Zn bond lengths are slightly unequal at 2.081(7) and 2.124(8) Å. The major structural change is compression of the O–C–O angle from 116.3(16)° in the parent to 112.2(10)° in the derivative.

V. Bonding

A number of theoretical treatments of the bonding of a carbon dioxide molecule to a single metal center

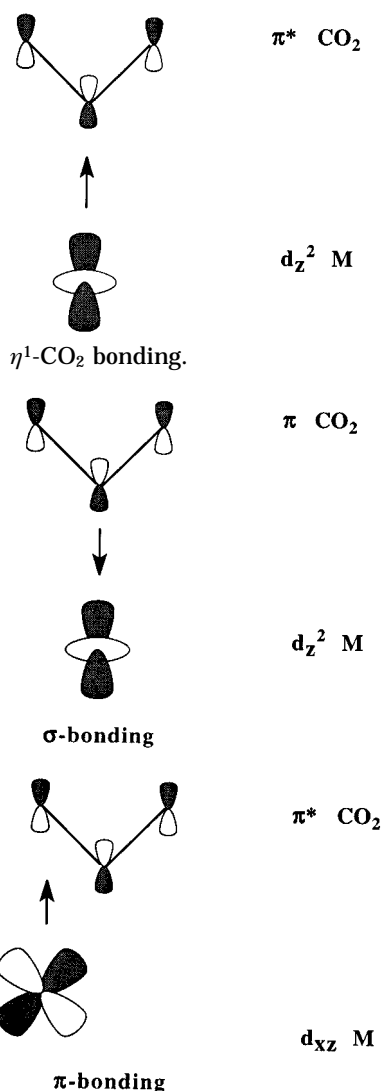


Figure 16. $\eta^1\text{-CO}_2$ bonding.

Figure 17. $\eta^2\text{-CO}_2$ bonding.

have appeared. The calculations have focused on four basic modes of CO_2 coordination: (a) $\eta^1\text{-C}$, (b) $\eta^2\text{-C,O}$ (side-on), (c) $\eta^1\text{-O}$ (end-on), and (d) $\eta^2\text{-O,O}$. A review of the results of calculations on the organometallic complexes (modes a and b) appeared in 1992.⁷⁴ Therefore, only a summary of these results and comments on more recent results will be provided. Many other treatments have dealt with modes c and d, but these are not included here (except in one recent study which yields similar energies for modes b and c for one system) since metal–carbon bonds are not involved.

As a heterocumulene, CO_2 has two sets of π molecular orbitals which are orthogonal. For η^1 and η^2 bonding to a metal, these are in two sets: (a) the π , $n\pi$, and π^* molecular orbitals, which lie in the plane of the metal and CO_2 (parallel), and (b) an equivalent set, which is in a plane perpendicular to the first set (perpendicular). The “parallel” molecular orbitals play the most significant role in bonding to transition metals. In qualitative terms, for the $\eta^1\text{-C}$ mode there is a strong charge transfer interaction between a d_z metal orbital and the π^* orbital of CO_2 (see Figure 16). In contrast, the η^2 mode has been compared to olefin–metal binding, and a model with similarities to this for CO_2 is shown in Figure 17. This model shows σ bonding involving the π orbital

of CO₂ and an empty d_{z²} metal orbital together with π bonding involving a filled d_{xz} metal orbital and the empty π^* orbital of CO₂.

The η^1 mode is most favored when the transition metal fragment has a doubly occupied d σ -type orbital that is relatively high in energy; this is best achieved when the metal is in a relatively low oxidation state. This mode is predicted for CO₂ adducts of d⁸ square-planar, square-pyramidal, or trigonal-bipyramidal metal complexes. The η^2 mode is favored by a high-lying d π -type orbital (e.g., in trigonal-bipyramidal iron complexes) which stabilizes the interaction with the π^* CO₂ orbital; stronger stabilization is achieved if the d σ orbital pointing toward the CO₂ ligand is empty (e.g., in Cp₂Mo(CO₂) (**12**), and related complexes).

Because of the importance of defining the characteristics of CO₂ adsorbed on metal surfaces (see section VI), Salahub *et al.*⁷⁵ recently completed a density functional study of the interaction of CO₂ with a single palladium atom. With this system also, the η^2 -coordination mode was found to be lowest in energy. IR spectral bands for the CO₂ ligand were calculated as 2018, 1212, and 689 cm⁻¹ for the asymmetric, symmetric, and bending vibrational modes in this model.

Using ab initio treatments that included electron correlation and methods based on the density functional approach, Sodupe *et al.*⁷⁶ recently studied the bonding of CO₂ to the early transition metal scandium and found that the η^2 -C,O mode and the η^2 -O,O mode are nearly degenerate in energy by these calculations. Vibrational modes for the CO₂ ligand in these models were calculated also. The SCF method gave band positions of 1968, 1020, and 779 cm⁻¹ for the η^2 -C,O mode and the DF method gave 1754, 832, and 615 cm⁻¹ for the vibrational bands. For the η^2 -O,O mode, the SCF method gave 1256, 1174, and 902 cm⁻¹ for the CO₂ vibrational bands while the DF method gave 983, 927, and 745 cm⁻¹ for these bands.

Sanchez-Marcos *et al.*⁷⁷ performed ab initio calculations on *trans*-Mo(CO₂)₂(PH₃)₄ and *mer,trans*-Mo(CO₂)₂(CNH)(PH₃)₃ in efforts to establish conformational preferences of the CO₂ ligands as well as the main metal-carbon dioxide interactions. The most stable conformation for the first has the CO₂ ligands mutually perpendicular and eclipsing the Mo-P bonds. Substitution of the CNH group for one PH₃ ligand introduces back donation through d- π^* interactions involving the CNH group, increasing the net charge on molybdenum from +1.3 to +1.68 and decreasing the charge on the CO₂ from -0.57 to -0.42. However, the most stable conformation for this molecule is also the staggered-eclipsed one, and this was found by Carmona^{25a} in the solid state structure for *trans*-Mo(CO₂)₂(PMe₃)₃(CN-i-Pr).

VI. Spectral Characterization

A. Infrared Spectral Data

It is apparent from a review of the data presented above that all transition metal complexes which have been structurally characterized possess bent CO₂ ligands with the internal O-C-O angle varying from

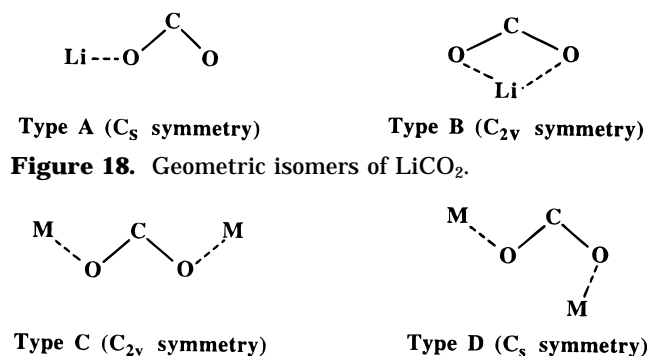


Figure 18. Geometric isomers of LiCO₂.

Figure 19. Geometric isomers of M₂CO₂ (M = K, Cs).

Table 9. Calculated and Observed IR bands for Li and Cs Adducts Formed in Ar Matrices (cm⁻¹)^{81,82}

adduct (symmetry)	IR band	obsd	calcd
LiCO ₂ (C _{2v})	ν_{asym}	1569.9, 1568.6	1570.9
	ν_{sym}	1329.9	1326.6
	δ	798.7	798.9
LiCO ₂ (C _s)	ν_{asym}	1755.7, 1750.9	1751.5
	ν_{sym}	1221.4, 1208.7	1219.4
	δ	739.5	739.3
Li ₂ CO ₂ (C _s)	ν_{asym}	1447.9	
	ν_{sym}	984.2	
CsCO ₂ (C _{2v})	ν_{asym}	1595.3	
	ν_{sym}	1352.8	
Cs ₂ CO ₂ (C _{2v})	ν_{asym}	1341.0	
	ν_{sym}	1174.0	
	δ	744.5	
Cs ₂ CO ₂ (C _s)	ν_{asym}	1334.8	
	ν_{sym}	1017.6	

101 to 136°. Certainly, the IR spectral bands for coordinated CO₂ should not resemble those of the free linear molecule (ν_{asym} 2349, ν_{sym} 1388 or 1285, (one of these is due to Fermi resonance) and δ 667 cm⁻¹),⁷⁸ but can be expected to be more closely related to certain types of metal-bound ⁻CO₂ or, possibly, to the radical anion itself. IR spectral bands for the free radical anion have been calculated⁷⁹ as 1677, 1405, and 607 cm⁻¹; the first two are stretching vibrations and the last is an O-C-O bending vibration. From calculations, Yoshioka and Jordan⁸⁰ predicted the possible existence of two geometric isomers for LiCO₂: one in which the Li⁺ would interact equally with both oxygens of CO₂⁻ (C_{2v} symmetry and an O-C-O angle of 132.4°) and one in which the Li⁺ would interact with only one of the oxygens of the radical anion (C_s symmetry and an O-C-O angle of 124.5°); these structures are illustrated in Figure 18. Margrave *et al.*⁸¹ studied the reactions of Li atoms with CO₂ in Ar matrices and obtained IR spectral data for two species (including their labeled analogs). Normal coordinate analyses were performed using the two geometries calculated previously; the stretching and bending frequencies that were observed and calculated for the two isomers were in good agreement as shown in Table 9. In experiments involving a high concentration of the alkali metal, an additional species was observed: Li₂CO₂. Furthermore, labeling studies indicated that the two oxygens in this species were inequivalent. The structure suggested for this species is similar to type D shown in Figure 19 and the IR bands for it are also shown in Table 9. Margrave,⁸² *et al.* later studied the reactions of Na, K, and Cs with CO₂ in argon, nitrogen, and neat

matrices. The $M^+CO_2^-$ species found for all three metals was the one with C_{2v} symmetry. At high metal concentrations, only K and Cs formed M_2CO_2 species, and in both cases, two geometric forms were observed. After labeling studies, it appeared that one isomer had C_{2v} symmetry but the other one had inequivalent oxygen atoms and C_s symmetry as observed from the Li reactions; the structures suggested for these species are shown in Figure 19. The IR bands for the products formed from reactions of Cs with CO_2 in Ar matrices are shown in Table 9. Both bands for $CsCO_2$ are shifted to slightly higher frequencies than those observed for the Li analog. The two bands observed for the Cs_2CO_2 species with C_s symmetry, however, differ greatly from those of the corresponding Li analog; the reasons for these differences are not understood. Also, it was found that the species with C_{2v} symmetry isomerized thermally to the ones with C_s symmetry; thus, only the more stable Li compound of type Li_2CO_2 was observed.

Mascetti and Tranquille⁸³ studied the interaction of a series of metal atoms with CO_2 in neat matrices at 15 K by FTIR. The metals used were titanium, chromium, vanadium, iron, cobalt, nickel, and copper; all formed complexes in which the CO_2 ligand was highly bent. The oxophilic metals (Ti, Cr, V) were observed to be oxidized and then coordinated to CO_2 in η^2 fashion. The ν_{OCO} bands in these compounds were found at 1750–1690 and 1180–1090 cm^{-1} . The iron and cobalt adducts were thought to be C-coordinated with ν_{OCO} bands at 1630–1565 and 1210–1190 cm^{-1} ; the cobalt adduct showed the greater $\Delta\nu$ in agreement with an expected greater O–C–O angle. These band positions are very similar to ones observed by Herskovitz^{7,8} for η^1 complexes (see below). Normal coordinate analysis was performed on the Fe– CO_2 adduct, and the observed (1565 and 1210 cm^{-1}) and calculated (1559 and 1238 cm^{-1}) ν_{OCO} band positions were in good agreement. For the copper adduct, ν_{OCO} bands were observed at 1716 and 1215 cm^{-1} . The band positions and the values of the observed isotopic shifts suggested end-on coordination of a bent CO_2 in agreement with calculations by Sanchez-Marcos *et al.*⁷⁰ Several adducts were formed with nickel; the complexity in the bands did not allow the types of adducts to be identified.

Manceron *et al.*⁸⁴ deposited Al and CO_2 together in argon matrices. The adduct formed was found to reversibly interconvert between two geometric isomers. The low-temperature form had C_s symmetry with inequivalence of the two C–O bonds; at higher temperatures, the chelated form (with C_{2v} symmetry) was preferred. Normal coordinate analysis was performed after data were obtained from isotopically labeled species; the isomer with C_s symmetry showed the ν_{OCO} bands at 1780 and 1146.5 cm^{-1} while the one with C_{2v} symmetry showed bands at 1443.5 (corrected) and 1265.5 cm^{-1} .

Recently, surface-bound and negatively charged (CO_2^-) species have been identified on several transition metals. The vibrational bands of these species, some obtained from HREELS data, are shown in Table 10 and are attributed to a bent form of the

Table 10. Vibrational Frequencies of CO_2^- Adducts on Transition Metal Surfaces (in cm^{-1})

metal	ν_{asym}	ν_{sym}	δ	ref
Ni(110)	1620	1130	750	85
Re(0001)	1650–1600	1230	650	86
Pd(110)		1200	770	87
Mo(110)		1155	855	88

CO_2^- with both oxygens thought to be bound to the metal surface. Again, the band positions are closely related to those of η^1 complexes as can be seen from the discussions below.

In the sections below, only the C–O stretching vibrations will be identified for each carbon dioxide complex. As with the structural data, the compounds are separated by class. The higher frequency band, in all cases, is assigned to the asymmetric stretching mode and the lower one is assigned to the symmetric vibration.

1. η^1 Complexes

The rhodium complex $Rh(diars)_2(Cl)(CO_2)$ (**3**) structurally characterized by Herskovitz *et al.*⁸ showed IR stretching bands at 1610 and 1210 cm^{-1} . Earlier Herskovitz had prepared iridium⁷ complexes with CO_2 ligands. Thus, $Ir(dmpe)_2(Cl)(CO_2)$ (**1**) showed IR bands at 1550 and 1230 cm^{-1} which were confirmed as CO_2 bands by isotopic labeling. Similarly, $Ir(diars)_2(Cl)(CO_2)$ (**2**) showed bands for the CO_2 ligand at 1550 and 1220 cm^{-1} ; these compounds appear to be η^1 complexes also. The band positions are quite similar to those observed by Mascetti and Tranquille⁸³ for matrix-isolated adducts of CO_2 with cobalt and iron, which were thought to be C-coordinated.

2. η^2 Complexes

The structurally characterized complex $Ni(PCy_3)_2(CO_2)$ (**4**) reportedly⁹ showed ν_{OCO} bands at 1740, 1150, and 1094 cm^{-1} . The compound has been re-examined recently by Mascetti *et al.*⁸⁹ with FTIR; isotopic labeling has been used to help in identifying the bands. In a Nujol mull, the compound showed ν_{OCO} bands at 1741, 1150, and 1093 cm^{-1} , with the lowest frequency band being much weaker than the band at 1150 cm^{-1} ; in solution the bands shifted to 1750, 1154, and 1095 cm^{-1} . The presence of two low-frequency bands was not expected but could be ascribed to Fermi resonance or to the presence of both η^2 and end-on forms of the compound. The ν_{OCO} bands for $Ni(PR_3)_2(CO_2)$ (**5**, **6**; R = *n*-Bu, Et) appear at approximately 1660, 1200, and 1110 cm^{-1} and are obviously quite different from those in the complex containing PCy_3 ligands. Structural data on the compounds with alkyl phosphine ligands are not available, and the differences in the IR spectral data between these and the cyclohexyl phosphine complex are not well understood. Aresta and Nobile¹³ reported IR bands at 1668, 1630, 1165, and 1130 cm^{-1} for the complex $Rh[P(n-Bu)_3]_2(Cl)(CO_2)$ (**7**). The doubling of bands suggests the presence of isomers, but further work with this system has not been reported.

Soon after the work of Aresta, Karsch¹⁴ reported an iron complex, $Fe(CO_2)(PMe_3)_4$ (**8**), which was also formulated as an η^2 complex; it showed ν_{OCO} bands

Table 11. IR ν_{OCO} Bands (cm^{-1}) for $\mu_2\text{-}\eta^2$ Complexes

compound	ν_{asym}	ν_{sym}	ref
[Pt(PEt ₃) ₂ (Ph)] ₂ (CO) ₂ (38)	1495	1290, 1190	30
[Pt(diphoe)(CF ₃) ₂](CO) ₂ (39)	1535	1205	31
[Pt(dppe)(CF ₃) ₂](CO) ₂ (40)	1545	1200	31
[Co(en) ₂ (CO) ₂](ClO ₄)·H ₂ O (49)	1512		36
CpRe(NO)(PPh ₃)(CO) ₂ GePh ₃ (51)	1545	1048	38
CpFe(CO)(PPh ₃)(CO) ₂ Re(CO) ₄ (PPh ₃) (42)	1505	1135	32
CpFe(CO)(PPh ₃)(CO) ₂ Re(CO) ₄ [P(OPh) ₃] (43)	1485		32
CpFe(CO)(PPh ₃)(CO) ₂ Re(CO) ₅ (41)	1477	1142	32
CpFe(CO)(PPh ₃)(CO) ₂ Re(CO) ₄ [P(OEt) ₃] (44)	1497	1144	33
CpFe(CO)(PPh ₃)(CO) ₂ Re(CO) ₃ [P(OEt) ₃] ₂ (45)	1510	1140	33
Cp*Re(CO)(NO)(CO) ₂ W(CO) ₃ Cp (47)	1541	1100	34
Cp*Re(CO)(NO)(CO) ₂ Re(CO) ₅ (46)	1514	1182	34
CpFe(CO) ₂ (CO) ₂ SnPh ₃ (55)	1499	1159	40
<i>cis, cis</i> -Ru(bpy) ₂ (CO)(CO) ₂ Ru(bpy) ₂ (CO) ²⁺ 2PF ₆ ⁻ (50)	1507	1176	37
Cp*Re(CO)(NO)(CO) ₂ SnMe ₃ (54)	1510	1179	40
Cp*Fe(CO) ₂ (CO) ₂ SnMe ₃ (52)	1516	1150 or 1122	40
Cp*Fe(CO) ₂ (CO) ₂ Sn(<i>n</i> -Bu) ₃ (53)	1534	1118	40
CpFe(CO)(PPh ₃)(CO) ₂ SnMe ₃ (56)	1491	1134	40
CpFe(CO)(PPh ₃)(CO) ₂ Sn(<i>n</i> -Bu) ₃ (57)	1491	1113	40
[(PPh ₃) ₂ (<i>t</i> -BuNC)(<i>t</i> -Bupy)Ir(μ -O)(μ -CO) ₂ Os(O) ₂ (<i>t</i> -Bupy) ₂] ⁺ Cl ⁻ (34)	1583		26
[(PPh ₃) ₂ (Cl)(<i>t</i> -Bupy)Ir(μ -O)(μ -CO) ₂ Os(O) ₂ (<i>t</i> -Bupy) ₂] (33)	1593	1022	26
Cp*Ir(μ - <i>n</i> -Bu)(μ -CO) ₂ ZrCp ₂ (35)	1569	1015	27
Ru ₂ (CO) ₂ (CO) ₄ [(μ -OPr) ₂ PNEtP(OPr) ₂] ₂ (37)	1710		29
Rh ₂ (CO) ₂ (dpmm) ₂ (CO) ₂ (36)	1645 or 1590		28

at 1620 and 1108 cm^{-1} . Mascetti *et al.*⁹⁰ have also re-examined this system with the help of isotopic labeling and normal coordinate analysis and confirmed these band positions at 1623 and 1106 cm^{-1} . In the absence of structural data, as discussed in section III.A, a formato complex cannot be completely ruled out as the product rather than the CO₂ complex. This alternative is particularly appealing in view of the very low position of the ν_{asym} band (1623 cm^{-1}) as compared to most of the structurally characterized η^2 complexes and the fact that it is closely similar to the ν_{asym} band in η^1 -formato complexes.⁹¹ However, the closely related, and structurally characterized¹⁵ Fe(CO)₂(depe)₂ (**9**) has IR ν_{OCO} bands at 1630 and 1096 cm^{-1} and has been described (see discussion in section IV.B) as intermediate between η^1 and η^2 types. The positions of the ν_{asym} bands for these two compounds and the rhodium complex **3**, of the η^1 type, are quite similar; however, the positions of the lower frequency bands differ.

Alt *et al.*¹⁹ reported the titanium complex Cp₂Ti(CO)₂(PMe₃) (**13**) and indicated a ν_{OCO} band at 1673 cm^{-1} ; the lower band was not reported. Mascetti *et al.*⁹² assigned the bands for this compound at 1671 and 1187 cm^{-1} after isotopic labeling studies.

Floriani *et al.*¹⁸ reported bands at 1705 (Nujol) or 1745 (THF) cm^{-1} for the structurally characterized Cp₂Mo(CO)₂ (**12**); the lower frequency band was not reported. The niobium complex Cp'₂Nb(CO)₂CH₂-SiMe₃ (**11**), obtained by Lappert *et al.*,¹⁷ showed a ν_{OCO} band at 1695 cm^{-1} . Nicholas *et al.*²¹ reported that the related Cp'₂Nb(CO)₂CH₂Ph (**16**) showed the ν_{asym} band at 1732 cm^{-1} in toluene (1704 cm^{-1} in KBr); the ¹⁸O-labeled analog showed this band at 1713 cm^{-1} (and 1675 cm^{-1} in KBr).

Recently Yamamoto *et al.*¹⁶ reported the first palladium-CO₂ complex Pd(CO)₂(PMePh₂)₂ (**10**) and indicated two high-frequency bands, 1658 and 1634 cm^{-1} , presumably due to ν_{OCO} . This group did not identify any low-frequency ν_{OCO} band for the compound. Hidai *et al.*²³ reported bands at 1677, 1187,

and 1120 cm^{-1} for the CO₂ ligand in *trans*-W(dppe)₂(CO)(CO)₂ (**19**).

Carmona *et al.*²⁵ reported ν_{OCO} bands for the structurally characterized bis CO₂ complex, *trans*-Mo(CO)₂(PMe₃)₃(CNR)(R=CN-*i*Pr) (**22**), as 1675, 1160, and 1100 cm^{-1} . The structure of the benzyl isonitrile analog **25** was obtained later, and its IR spectrum showed ν_{OCO} bands at 1670, 1150, and 1100 cm^{-1} . Complexes having R = Me (**21**), *t*-Bu (**23**), and Cy (**24**) had closely similar bands. Also, *trans*-Mo(CO)₂(PMe₃)₄ (**20**) showed bands at 1670, 1155, and 1100 cm^{-1} for the CO₂ ligands. Mascetti⁹⁰ has also examined this latter compound by isotopic labeling techniques and identified bands at 1690 (sh), 1668, 1153, and 1103 (sh) cm^{-1} for the CO₂ ligands. The related complex *trans*-Mo(CO)₂(PMe₃)₃(dmpm) (**26**) showed ν_{OCO} bands at 1670, 1155, and 1100 cm^{-1} also, and the bands for the dmpe, depe, and dppe analogs are closely similar. The ν_{OCO} bands for *trans*-Mo(CO)₂(dmpe)₂ (**30**) are closely similar to the ones for this group. The ν_{OCO} bands for the less symmetrical complexes *trans*-Mo(CO)₂(depe)(PMe₃)(CNR) (**31**, **32**; R = *t*-Bu, Cy) are moved to slightly higher frequencies, and both show four bands: 1710, 1690 (1680), 1160, and 1105 cm^{-1} .

As indicated in section IV, very few η^2 complexes have been structurally characterized. Even with those, IR spectral data for the ν_{OCO} bands in the compounds are sometimes incomplete. Thus, the precise relationships between structural parameters and ν_{OCO} bands for the compounds and the effects of ancillary ligands are not clear at present.

3. $\mu_2\text{-}\eta^2$ Complexes

Although few compounds of this type have been structurally characterized, there are examples of both acyclic and metallacyclic complexes with CO₂ bound in this way that are well characterized. Table 11 summarizes the IR data on the compounds of this type that have been reported. The first acyclic compound of this type (**38**) to be characterized was

Table 12. IR ν_{OCO} Bands (cm^{-1}) for $\mu_2\text{-}\eta^3$ CO_2 -Bridged Complexes Involving Transition Metals (Class I Compounds)

compound	ν_{asym}	ν_{sym}	ref
$\text{Cp}^*\text{Re}(\text{CO})(\text{NO})(\text{CO}_2)\text{Re}(\text{CO})_3(\text{PPh}_3)$ (81)	1437	1282	47
$\text{CpFe}(\text{CO})(\text{PPh}_3)(\text{CO}_2)\text{Re}(\text{CO})_3[\text{P}(\text{OEt})_3]$ (80)	1435	1252	33
$\text{CpFe}(\text{CO})(\text{PPh}_3)(\text{CO}_2)\text{Re}(\text{CO})_3(\text{PPh}_3)$ (78)	1435	1247	32
$\text{Cp}^*\text{Re}(\text{CO})(\text{NO})(\text{CO}_2)\text{Re}(\text{CO})_2(\text{PPh}_3)_2$	1435	1278	71
$\text{CpRe}(\text{CO})(\text{NO})(\text{CO}_2)\text{Zr}(\text{Cl})\text{Cp}_2$ (58)	1352	1265	41
$\text{CpRu}(\text{CO})_2(\text{CO}_2)\text{Zr}(\text{Cl})\text{Cp}_2$ (59)	1348	1290	42, 43
$\text{CpFe}(\text{CO})_2(\text{CO}_2)\text{Zr}(\text{Cl})\text{Cp}_2$ (61)	1363	1268	42
$\text{CpRu}(\text{CO})_2(\text{CO}_2)\text{Ti}(\text{Cl})\text{Cp}_2$ (60)	1349	1284	42
$\text{CpFe}(\text{CO})_2(\text{CO}_2)\text{Ti}(\text{Cl})\text{Cp}_2$ (62)	1379	1273	42
$\text{Cp}^*\text{Re}(\text{CO})(\text{NO})(\text{CO}_2)\text{Zr}(\text{Cl})\text{Cp}_2$ (64)	1348	1288	44
$\text{Cp}^*\text{Re}(\text{CO})(\text{NO})(\text{CO}_2)\text{Zr}(\text{Me})\text{Cp}_2$ (66)	1340	1288	44
$\text{Cp}^*\text{Re}(\text{CO})(\text{NO})(\text{CO}_2)\text{Zr}(\text{SnPh}_3)\text{Cp}_2$ (68)	1336	1275	44
$\text{Cp}^*\text{Ru}(\text{CO})_2(\text{CO}_2)\text{Zr}(\text{Cl})\text{Cp}_2$ (63)	1339	1287	44
$\text{Cp}^*\text{Ru}(\text{CO})_2(\text{CO}_2)\text{Zr}(\text{Me})\text{Cp}_2$ (65)	1341	1285	44
$\text{Cp}^*\text{Ru}(\text{CO})_2(\text{CO}_2)\text{Zr}(\text{SnPh}_3)\text{Cp}_2$ (67)	1339	1265	44
$\text{Cp}^*\text{Re}(\text{CO})(\text{NO})(\text{CO}_2)\text{Mo}(\text{CO})_2\text{Cp}$ (82)	1319	1285	34
$\text{Cp}^*\text{Re}(\text{CO})(\text{NO})(\text{CO}_2)\text{W}(\text{CO})_2\text{Cp}$ (83)	1321	1287	34

reported by Bennett;³⁰ later ones (**39**, **40**) prepared by Strukul *et al.*³¹ have very similar ν_{OCO} bands.

Szalda, Creutz and their co-workers³⁶ reported a polymeric cobalt complex (**49**) which was structurally characterized and showed repeating units with $\mu_2\text{-}\eta^2$ -bonded CO_2 ; the repeating unit is $[\text{Co}(\text{en})_2(\text{CO}_2)]\text{-}(\text{ClO}_4)\cdot\text{H}_2\text{O}$. They suggested that the structure is stabilized by hydrogen bonds between the amine hydrogens and the "free" carboxyl oxygen as well as the one bound to cobalt. The compound showed IR bands at 1645 and 1512 cm^{-1} . The N-deuterated analog showed bands at 1640 and 1521 cm^{-1} . The lower frequency band is analogous to ν_{asym} of the other $\mu_2\text{-}\eta^2$ complexes; it is not clear what is responsible for the other one. No data were given for the 1200–1000 cm^{-1} region.

The ruthenium bipyridyl complex **50** characterized recently by Gibson *et al.*³⁷ shows the ν_{OCO} bands at 1507 and 1176 cm^{-1} . The band positions are in the same region as other compounds of this type and are apparently not greatly affected by the cationic nature of the system bearing the CO_2 ligand.

One of the main group complexes characterized by Gladysz,³⁸ $\text{CpRe}(\text{NO})(\text{PPh}_3)(\text{CO}_2)\text{GePh}_3$ (**51**), is of the $\mu_2\text{-}\eta^2$ type, as evidenced by the ν_{OCO} bands. The spectral data for **42–47** and **52–57** have been reported by Gibson *et al.*^{32–34,40} and have been obtained by the DRIFTS technique⁹³ (diffuse reflectance infrared Fourier transform spectroscopy) from dispersions in KCl. With all these compounds, however, structural data on complexes of this type are sparse and there are at present no clear correlations with spectral data. The ν_{asym} bands vary from 1545 to 1477 cm^{-1} in these acyclic complexes while their ν_{sym} bands appear to vary from 1205 to 1048 cm^{-1} . Band assignments have been made after numerous comparisons with model compounds. However, there are no clear distinctions between the compounds in which the carboxylate oxygen is bound to tin rather than a transition metal as is apparent with the $\mu_2\text{-}\eta^3$ complexes discussed below.

The last five compounds (**33–37**) in Table 11 are metallacyclic compounds which have the CO_2 ligand bridged between two metal centers. Compounds **33–35** have five-membered rings; these show a higher ν_{asym} band than the acyclic compounds of the same bonding type. Bands at 1645 and 1590 cm^{-1} , only,

were reported²⁸ for **36**, which should have a seven-membered ring. Compound **37** shows the highest ν_{asym} because of the strain of the four-membered metallacyclic ring and the short carboxyl C–O bond. These trends parallel the behavior of organic lactones as compared to esters.

Past efforts⁹⁴ to correlate $\Delta\nu$ ($\nu_{\text{asym}} - \nu_{\text{sym}}$) in complexes bearing carboxylate ligands with the η^1 or η^2 bonding mode have met with mixed results, in part because of differences in methodology used to obtain IR data and, in part, because of the limited availability of structural data. With the $\mu_2\text{-}\eta^2$ complexes it is apparent from Table 11 that $\Delta\nu$ is large for these compounds. Differences in $\Delta\nu$ of 300–400 cm^{-1} are typical for the acyclic compounds and can be much larger for those compounds with metallacyclic rings. The magnitude of $\Delta\nu$ and the band positions are sufficient to distinguish these from other types of CO_2 -bridged bimetallic complexes.

4. $\mu_2\text{-}\eta^3$ Complexes

In section IV, two distinct structural types exhibiting $\mu_2\text{-}\eta^3$ bonding were identified. Compounds in class I have the CO_2 ligand bridged between two transition metal atoms. The first of these to be structurally characterized and for which IR band assignments for the CO_2 ligand are also available is $\text{Cp}^*\text{Re}(\text{CO})(\text{NO})(\text{CO}_2)\text{Re}(\text{CO})_3(\text{PPh}_3)$ (**81**),⁴⁷ which shows the ν_{asym} band at 1437 cm^{-1} and the ν_{sym} band at 1282 cm^{-1} . As shown in Table 12, entries 2–5, other compounds derived from iron or rhenium metalcarboxylates and having the carboxylate oxygens bound to an octahedral rhenium center have closely similar spectral properties. The ν_{asym} band varies by only 2 cm^{-1} while the ν_{sym} band position varies slightly with the metalcarboxylate moiety (1282–1247 cm^{-1}).

Compounds **58–68** in Table 12 have been derived from different metalcarboxylate moieties, but all have the carboxylate oxygens bound to a titanocene or zirconocene fragment. With **58–62**, the ν_{OCO} bands have been assigned by the Cutler group⁴¹ with the help of isotopic labeling. Two zirconium compounds (**63**, **64**) were structurally characterized recently by Gibson *et al.*⁴⁴ and show edge-capped tetrahedral geometries at the Zr atom (see discussion

Table 13. IR ν_{OCO} Bands (cm^{-1}) for $\mu_2\text{-}\eta^3$ CO_2 -Bridged Complexes Involving Tin (Class II Compounds)

compound	ν_{asym}	ν_{sym}	ref
CpRe(NO)(PPh ₃)(CO ₂)SnPh ₃ (86)	1395	1188	38
CpRe(NO)(PPh ₃)(CO ₂)SnMe ₃ (85)	1456	1158	38
CpRe(NO)(PPh ₃)(CO ₂)PbPh ₃ (87)	1425	1184	38
Ind Fe(CO)(PPh ₃)(CO ₂)SnPh ₃ (90)	1468	1111	51
CpFe(CO)(PPh ₃)(CO ₂)SnPh ₃ (88)	1431	1161	50
CpFe(CO)(PPh ₃)(CO ₂)SnMe ₃ (91)	1438 or 1433	1134	40
CpFe(CO)(PPh ₃)(CO ₂)Sn(<i>n</i> -Bu) ₃ (92)	1433	1113	40
Cp*Fe(CO) ₂ (CO ₂)SnPh ₃ (93)	1450	1152	40
Cp*Re(CO)(NO)(CO ₂)SnPh ₃ (95)	1429	1188 or 1175	47
Cp*Fe(CO)(PPh ₃)(CO ₂)SnPh ₃ (89)	1418	1140	47
Cp*Ru(CO) ₂ (CO ₂)SnPh ₃ (94)	1464	1171	40
[Cp*Re(CO)(NO)(CO ₂) ₂ SnMe ₂ (96)	1469	1186	52

in section IV). The others can be expected to have similar structures. Note that the ν_{asym} band varies from 1379 to 1336 cm^{-1} and that the ν_{sym} band varies from 1290 to 1265 cm^{-1} . Thus the ν_{asym} band of the titanium and zirconium complexes is much lower than those in the first four entries in Table 12, but the ν_{sym} band is in approximately the same place.

With the characterization of the final two compounds in Table 12, it has become clear that the ν_{asym} band position is dependent upon the coordination geometry at the metal center which anchors the two carboxyl oxygens. The structurally characterized molybdenum complex (**82**)³⁴ has square-based pyramidal geometry at the Mo atom; the analogous tungsten complex (**83**) is expected to have the same geometry at W. These complexes show the lowest ν_{asym} bands of the class I compounds at 1319 and 1321 cm^{-1} , respectively, but the ν_{sym} bands are closely similar to those of the other class I complexes derived from a variety of metallocarboxylates.

Compounds derived from the rhenium metallocarboxylate Cp*Re(CO)(NO)(CO₂) show shortened Re–carboxyl carbon bond lengths (2.0–2.1 Å) which are in the realm for rhenium complexes with oxycarbene ligands.^{95,96} Geoffroy⁴⁶ described the ionic complexes derived from this metallocarboxylate in terms of the carbene formulation shown in Scheme 13. With neutral compounds, however, a similar valence bond description requires a dipolar species as shown below.



However, as noted previously,⁴⁷ IR spectral bands for the terminal carbonyl ligands in these compounds (e.g., entry 1 in Table 12) do not reflect the changes that would be expected for such charge separation.

The values for $\Delta\nu$ for class I compounds range from 34 to 183 cm^{-1} and are much smaller than $\Delta\nu$ for the $\mu_2\text{-}\eta^2$ type. They are smaller, also, than the $\Delta\nu$ values for class II compounds of the $\mu_2\text{-}\eta^3$ type as discussed below.

Compounds in class II include those which have the carboxylate oxygens bound, unsymmetrically, to a tin atom. The IR ν_{OCO} spectra for the 11 known compounds of this type are summarized in Table 13. With the exception of the first three table entries, the data are for compounds reported by Gibson *et al.*^{40,47,50,52} and the spectra were obtained by the DRIFTS technique.⁹³ Band assignments have been made only after extensive comparisons with model

compounds related to each system, including in several cases the decarboxylated compounds. The band positions for **93** are in agreement with those reported by Cutler,³⁹ which were based on isotopic labeling studies. Note that **91** and **92** in this table also appear in the section above on $\mu_2\text{-}\eta^2$ complexes (and in Table 11; **56** and **57**) because two forms of each compound can usually be observed in solid samples.

In general, when a strong donor ligand is bound to the metal that binds the carboxylate carbon and electron-withdrawing groups are bound to the tin atom, the compound exists in the $\mu_2\text{-}\eta^3$ form. If electron donor groups (e.g., alkyl) are bound to the tin atom or if electron donation to the carboxylate carbon is diminished (e.g., by exchanging Cp* for Cp), then the preferred form is $\mu_2\text{-}\eta^2$. Compounds **91** and **92** represent borderline cases where the conditions used to prepare the solid samples can greatly influence the composition of the sample. The structural characterizations of these two compounds were done at low temperatures on samples which had been crystallized at very low temperatures;⁴⁰ under these conditions the $\mu_2\text{-}\eta^3$ form is produced exclusively. The manner in which the IR data is obtained can also have great impact on the distribution of $\mu_2\text{-}\eta^2$ and $\mu_2\text{-}\eta^3$ forms. For example, Figure 20 shows the ν_{asym} region (1600–1300 cm^{-1}) for CpFe(CO)(PPh₃)(CO₂)SnMe₃ (**91**) recorded in several different ways;⁴⁰ all of these data were derived from the same sample of the compound. All compounds having the CpFe(CO)-(PPh₃) fragment show a band near 1480 cm^{-1} and another near 1430 cm^{-1} . Thus, the DRIFTS spectrum (a) shows these bands, but also two others: a shoulder at approximately 1500 cm^{-1} for the ν_{asym} band of the $\mu_2\text{-}\eta^2$ form and an additional band near 1430 cm^{-1} for the ν_{asym} band of the $\mu_2\text{-}\eta^3$ form. The two higher frequency bands are partially resolved in the Nujol spectrum (b). Spectra c and d were obtained in solution; in both cases, the ν_{asym} band for the $\mu_2\text{-}\eta^3$ form is absent and the ν_{asym} band for the $\mu_2\text{-}\eta^2$ form has broadened and also moved to slightly higher frequency. In the case of THF, dechelation of one carboxylate oxygen may be assisted by this donor solvent. An additional main group complex, CpRe(NO)(PPh₃)(CO₂)PbPh₃ (**87**), appears to be of the $\mu_2\text{-}\eta^3$ type also; it shows ν_{OCO} bands at 1425 and 1184 cm^{-1} .

The recently characterized⁵² compound **96** with two bridging CO₂ ligands to a central tin atom is the only carbon dioxide complex with a six-coordinate tin

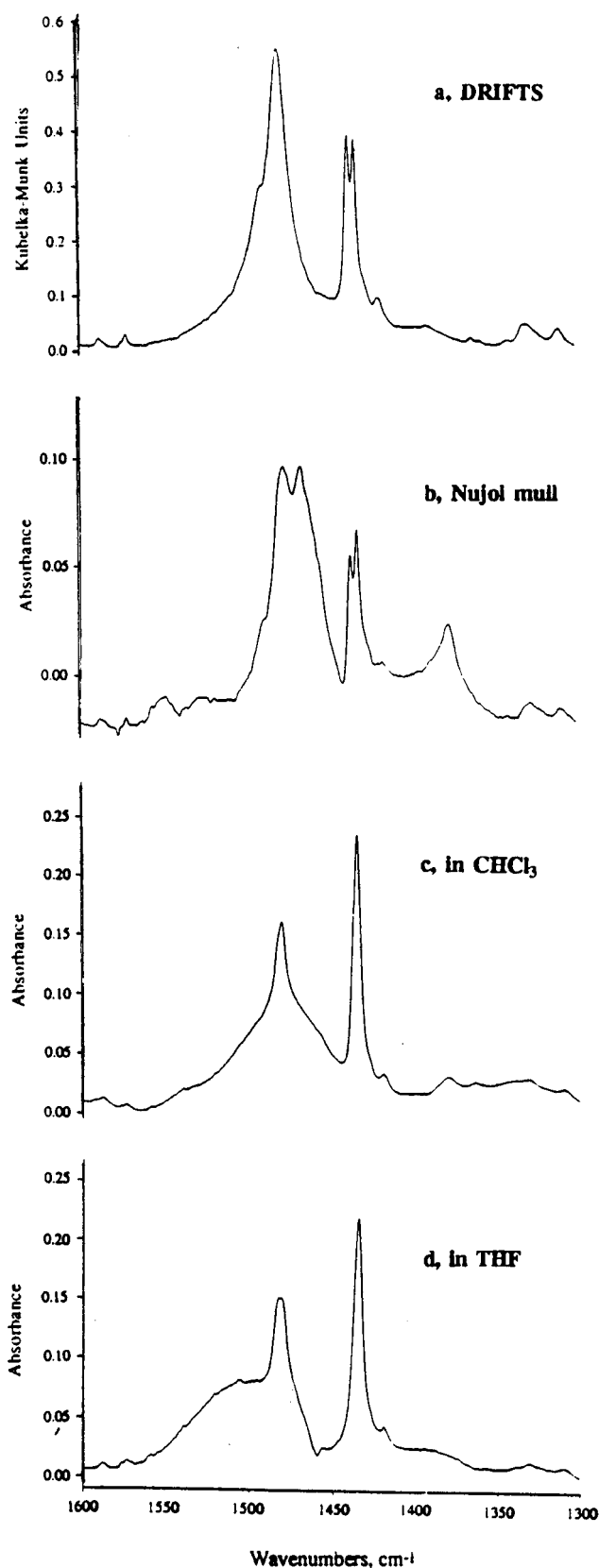


Figure 20. Infrared spectra (1600–1300 cm^{-1} region) of $\text{CpFe(CO)(PPh}_3\text{)(CO}_2\text{)SnMe}_3$ (**91**) recorded by different methods.

atom. Like the others in Table 13 that have been structurally characterized, however, it has unequal C–O bond lengths. Thus, its ν_{OCO} bands are quite similar to the others in this class.

The values for $\Delta\nu$ in class II compounds shown in Table 13 range from 210 to 350 cm^{-1} and are thus

greater than those for class I compounds. However, most of these are tin complexes of similar structure where the geometry at the tin atom is that of a distorted trigonal bipyramid. In comparing class I and class II compounds derived from the same metalcarboxylate, it is apparent that the ν_{asym} bands are at about the same frequency but the ν_{sym} bands for class II compounds are lowered by approximately 100 cm^{-1} . Whether this is a characteristic of unsymmetrical $\mu_2\text{-}\eta^3$ complexes or is simply characteristic of this particular group cannot be determined at present.

5. $\mu_3\text{-}\eta^3$ Complexes

The number of $\mu_3\text{-}\eta^3$ CO_2 -bridged compounds that have been characterized are very few. The first was reported by Lewis, Johnson *et al.*⁵³ and involved an osmium cluster anion, $\text{PPN}^+\text{HOS}_3(\text{CO})_{10}(\text{CO}_2)\text{Os}_6(\text{CO})_{17}^-$ (**97**), which was structurally characterized; it showed a C–O stretching band at 1270 cm^{-1} . Later, three additional related anionic complexes were reported:⁵⁴ $\text{HOS}_3(\text{CO})_{10}(\mu\text{-CO}_2)\text{Os}_5(\text{CO})_{15}^-$, $\text{HOS}_3(\text{CO})_{10}(\mu\text{-CO}_2)\text{Os}_7(\text{CO})_{20}^-$, and $\text{HOS}_3(\text{CO})_{10}(\mu\text{-CO}_2)\text{Ru}_6\text{C}(\text{CO})_{16}^-$. Although not fully characterized, these complexes also showed absorption in the 1240–1260 cm^{-1} region which was attributed to a carboxyl C–O stretching band.

In 1982, Beck *et al.*⁵⁶ reported and structurally characterized the tetranuclear rhenium cluster $[\text{Re}(\text{CO})_5(\text{CO}_2)\text{Re}(\text{CO})_4]$ (**98**), which had two bridging $\mu_3\text{-}\eta^3$ CO_2 ligands. The compound showed ν_{OCO} bands at 1380, 1295, and 1260 cm^{-1} . No IR ν_{OCO} bands were reported by Ziegler⁵⁵ for the related rhenium compound **99**.

Caulton *et al.*⁵⁷ reported the trinuclear compound $[(\text{COD})\text{Rh}]_2(\text{CO}_2)\text{OsH}_2(\text{PMe}_3\text{Ph})_3$ (**100**), which exhibited $\mu_3\text{-}\eta^3$ bonding of the bridging CO_2 ligand. The compound showed ν_{OCO} bands at 1365 and 1260 cm^{-1} which were identified with the help of isotopic labeling studies. The carboxylate carbon is bound to osmium, and the rhodium atoms are symmetrically bound to the carboxyl oxygens; the geometry and spectra are thus similar to the cesium metal complex Cs_2CO_2 type with C_{2v} symmetry identified in Table 9. The IR spectrum of the ZnBr_2 derivative of this compound differs and is discussed in section 7 below.

6. $\mu_4\text{-}\eta^4$ Complexes

Only one compound of this type has been identified and that is *cis*- $\text{Ru}(\text{bpy})_2(\text{CO})(\text{CO}_2)\cdot 3\text{H}_2\text{O}$ (**101**) reported by Tanaka and co-workers.⁵⁹ The compound shows ν_{OCO} bands at 1428 and 1242 cm^{-1} ; thus the band positions are very similar to some of the class I $\mu_2\text{-}\eta^3$ complexes shown in Table 12.

7. $\mu_4\text{-}\eta^5$ Complexes

Only one compound of this type has been reported, $[(\text{COD})\text{Rh}]_2(\text{CO}_2)\text{H}_2\text{Os}(\text{PMe}_2\text{Ph})_3\text{ZnBr}_2\cdot\text{THF}$ (**102**), which was structurally characterized by Caulton^{57b} and prepared by reaction between ZnBr_2 and the $\mu_3\text{-}\eta^3$ rhodium–osmium complex described above. A major change in the ν_{asym} band position occurs upon formation of the ZnBr_2 adduct: it shifts from 1365 cm^{-1} in the $\mu_3\text{-}\eta^3$ complex to 1280 cm^{-1} in the adduct; the O–C–O angle is compressed by about 4° in the

Table 14. ^{13}C Data for Representatives from Several Structural Types of CO_2 Complexes

structural type	compound	δCO_2 (ppm)	ref
η^2	$[(\text{Cy})_3\text{P}]_2\text{Ni}(\text{CO}_2)$ (4)	159.28	89
	$(\text{Ph}_2\text{MeP})_2\text{Pd}(\text{CO}_2)$ (10)	166.2	16
	$\text{Cp}'_2\text{Nb}(\text{CO}_2)(\text{CH}_2\text{SiMe}_3)$ (11)	200.5	17
	$\text{Cp}'_2\text{Ti}(\text{PMe}_3)(\text{CO}_2)$ (13)	212.3	19
	<i>trans</i> - $\text{Mo}(\text{CO}_2)_2(\text{PMe}_3)_4$ (20)	206.1	25
	<i>trans</i> - $[\text{Mo}(\text{CO}_2)_2(\text{PMe}_3)_3(\text{CN-}i\text{-Pr})]$ (22)	201.4	25
$\mu_2\text{-}\eta^2$	$[\text{Pt}(\text{Ph})(\text{PEt}_3)_2](\text{CO}_2)$ (38)	201.0	30
	$\text{CpRe}(\text{NO})(\text{PPh}_3)(\text{CO}_2)\text{GePh}_3$ (51)	198.8	38
	<i>cis</i> - $\text{CpFe}(\text{CO})(\text{PPh}_3)(\text{CO}_2)\text{Re}(\text{CO})_4(\text{PPh}_3)$ (42)	211.91	32
	<i>cis</i> - $\text{CpFe}(\text{CO})(\text{PPh}_3)(\text{CO}_2)\text{Re}(\text{CO})_4[\text{P}(\text{OEt})_3]$ (44)	211.61	33
	$\text{Cp}^*\text{Fe}(\text{CO})_2(\text{CO}_2)\text{SnMe}_3$ (52)	209.57	40
	$(\text{PPh}_3)_2(\text{Cl})(t\text{-Bupy})\text{Ir}(\mu\text{-O})(\text{CO}_2)\text{Os}(\text{O})_2(t\text{-Bupy})_2$ (33)	187.2	26
	$\text{Cp}^*\text{Mn}(\text{CO})(\text{NO})(\text{CO}_2)\text{WCp}_2^+\text{BF}_4^-$ (72)	271.9	46
	$\text{Cp}^*\text{Re}(\text{CO})(\text{NO})(\text{CO}_2)\text{WCp}_2^+\text{BF}_4^-$ (70)	247.4	46
$\mu_2\text{-}\eta^3$, class I	$\text{Cp}^*\text{Re}(\text{CO})(\text{NO})(\text{CO}_2)\text{Re}(\text{CO})_3(\text{PPh}_3)$ (81)	219.17	47
	$\text{Cp}^*\text{Re}(\text{CO})(\text{NO})(\text{CO}_2)\text{Ti}(\text{tmtaa})^+\text{BF}_4^-$ (69)	226.2	45
	$\text{Cp}^*\text{Re}(\text{CO})(\text{NO})(\text{CO}_2)\text{Zr}(\text{Cl})\text{Cp}_2$ (64)	217.91	44
	$\text{CpFe}(\text{CO})(\text{PPh}_3)(\text{CO}_2)\text{Re}(\text{CO})_3[\text{P}(\text{OEt})_3]$ (80)	245.94	33
	$\text{CpFe}(\text{CO})(\text{PPh}_3)(\text{CO}_2)\text{Re}(\text{CO})_3(\text{PPh}_3)$ (81)	245.88	32
	$\text{Cp}^*\text{Ru}(\text{CO})_2(\text{CO}_2)\text{Zr}(\text{Cl})\text{Cp}_2$ (63)	220.41	44
	$\text{Cp}^*\text{Ru}(\text{CO})_2(\text{CO}_2)\text{SnPh}_3$ (94)	204.79	40
	$\text{Cp}^*\text{Re}(\text{CO})(\text{NO})(\text{CO}_2)\text{SnPh}_3$ (95)	201.13	47
	$\text{CpRe}(\text{NO})(\text{PPh}_3)(\text{CO}_2)\text{SnPh}_3$ (86)	207.6	38
	$\text{Cp}^*\text{Fe}(\text{CO})_2(\text{CO}_2)\text{SnPh}_3$ (93)	217.74	40
$\mu_3\text{-}\eta^3$	$[(\text{COD})\text{Rh}]_2(\text{CO}_2)\text{H}_2\text{Os}(\text{PMe}_2\text{Ph})_3$ (100)	193	57
	$[(\text{COD})\text{Rh}]_2(\text{CO}_2)\text{H}_2\text{Os}(\text{PMe}_2\text{Ph})_3\text{ZnBr}_2\cdot\text{THF}$ (102)	201	57
$\mu_4\text{-}\eta^5$ metallocarboxylate anions	$[\text{W}(\text{CO})_5\text{CO}_2]\text{Li}_2$ (108)	223.4	66
	$\text{CpFe}(\text{CO})_2(\text{CO}_2)^-\text{Li}^+$ (103)	217.0	62b
	$\text{CpFe}(\text{CO})(\text{PPh}_3)(\text{CO}_2)^-\text{K}^+$ (118)	220.34	50
	$\text{Cp}^*\text{Fe}(\text{CO})(\text{PPh}_3)(\text{CO}_2)^-\text{K}^+$ (119)	220.26	50

derivative (see section IV.E,H). The ν_{sym} band changes only slightly from 1260 to 1250 cm^{-1} . This appears to represent a further example in which the coordination geometry around the carboxylate oxygen atoms greatly influences the position of the ν_{asym} band.

8. Metallo-carboxylate Anions

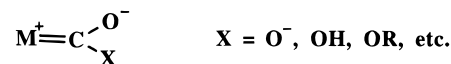
The only complex of this type to be structurally characterized is the potassium salt of the cobalt *n*-Pr-salen complex **116** reported by Floriani *et al.*⁵⁸ This compound has a polymeric structure with repeating $\mu_3\text{-}\eta^4$ CO_2 -bridging units in which one carboxylate oxygen is bound to two potassium ions as shown in Figure 14. The IR spectrum showed bands at approximately 1650, 1280, and 1215 cm^{-1} which were confirmed as CO_2 bands through isotopic labeling. The $\mu_3\text{-}\eta^4$ -type structure and the ν_{OCO} bands for the compound are unique among CO_2 -bridged compounds. IR ν_{OCO} bands were also reported for the sodium analog; the two lower frequency bands were in about the same place as those in the potassium salt, but the upper band was at approximately 1720 cm^{-1} . Spectral data for the lithium salt were not reported.

With the other metallo-carboxylate salts that have been characterized with the help of IR spectroscopy, the degree of coordination of the CO_2 ligand to the metal ions is not known. However, several of these exhibit ν_{OCO} bands closely similar to the symmetrical $\mu_2\text{-}\eta^3$ complexes described above. The lithium and potassium salts of $\text{CpRe}(\text{NO})(\text{PPh}_3)\text{CO}_2^-$ showed ν_{asym} bands at 1435 and 1405 cm^{-1} and ν_{sym} bands at 1248 and 1239 cm^{-1} , respectively.³⁸ DRIFTS data for hydrated and anhydrous salts of $\text{CpFe}(\text{CO})(\text{PPh}_3)\text{CO}_2^-$ have been reported by Gibson *et al.*⁵⁰ The ν_{asym} band

appears at 1452–1434 cm^{-1} , and the ν_{sym} band appears at 1243–1204 cm^{-1} . In general, the separation of these two bands appears to be greater for the anhydrous salts. The bands for the $\text{Cp}^*\text{Fe}(\text{CO})(\text{PPh}_3)\text{CO}_2^-\text{K}^+\cdot\text{XH}_2\text{O}$ appeared at 1395 and 1203 cm^{-1} in spectra obtained in a KBr disk.⁵⁰ The band positions for these compounds are quite similar to those of the $\mu_2\text{-}\eta^3$ bimetallic complexes having the $\text{CpFe}(\text{CO})(\text{PPh}_3)\text{CO}_2$ group bound to an octahedral rhenium center (see Table 12).

B. ^{13}C NMR Spectral Data

All metallo-carboxylates (anions, acids, esters, CO_2 complexes, etc.) show a low-field resonance for the carboxyl carbon as expected (because of their relationship to organic analogs in the case of the first three). Also, acyl–metal complexes are considered to have some carbene character because of the resonance form shown below;



this factor contributes to lowered ^{13}C resonance positions. Table 14 shows the ^{13}C chemical shift position for the CO_2 ligand in representative compounds from each structural type. The ^{13}C data for all such compounds are relatively sparse, making correlations with structural data difficult at this time. No ^{13}C data are available on the $\eta^1\text{-CO}_2$ complexes characterized by Herskovitz.^{7,8} The $\eta^2\text{-CO}_2$ complexes **4** and **10** show much higher chemical shifts than those of the metallocene derivatives (**11**, **13**) of the same type. Whether this is due to the differences in geometry or simply to the types of metal centers involved is not clear. There is little difference

between the ^{13}C shifts of the nickel and palladium complexes (**4**, **10**), which both bear phosphine ligands.

Where compounds derived from the same metal-carboxylate can be compared, it is apparent that the carboxylate carbon resonance in $\mu_2\text{-}\eta^2$ complexes appears at higher field than a terminal carbonyl on the same metal center. With compounds **42** and **81**, the carboxylate carbon can be identified easily since it is coupled to phosphorus ligands on both metal centers in both the $\mu_2\text{-}\eta^2$ and $\mu_2\text{-}\eta^3$ complex. In both compounds, the terminal carbonyl on iron appears at $\delta 220.5 \pm 1.0$, but the carboxylate carbon shifts from $\delta 211.91$ in the $\mu_2\text{-}\eta^2$ complex (**42**) to $\delta 245.88$ in the $\mu_2\text{-}\eta^3$ complex **81**. The same trend is apparent with the $\mu_2\text{-}\eta^2$ and $\mu_2\text{-}\eta^3$ tin complexes, although the magnitude of the effect is much less. For example, **52** and **93** in Table 14 exhibit the terminal carbonyl resonance at $\delta 215.4 \pm 0.3$, but the carboxyl carbon resonances differ by 6 ppm.

The cationic $\mu_2\text{-}\eta^3$ rhenium–tungsten complex, **70**, has the lowest chemical shift position for a carboxylate carbon and also the shortest rhenium–carboxylate carbon bond of any of the compounds derived from this metalcarboxylate. The lowest field carboxylate carbon resonance yet observed for a bridged complex of this type is for the manganese analog, **72**, which appears at $\delta 271.9$. Thus, the nature of the metal center plays a large role in determining the carboxylate carbon chemical shift positions.

Gibson and Ong⁶⁸ used ion-selective crown ethers to assist in distinguishing the chemical shifts of the carbonyl and carboxylate carbon atoms in the anions $\text{CpFe}(\text{CO})(\text{PPh}_3)(\text{CO}_2)^-\text{M}^+\text{X}\text{H}_2\text{O}$ ($\text{M} = \text{K}, \text{Li}$). With both compounds, the higher of the two low-field resonances moved to higher field in the presence of the crown ether, allowing its identification as the carboxyl carbon.

C. Electronic Spectra

The electronic spectral properties of CO_2 complexes, particularly those that have been generated by addition of $\cdot\text{CO}_2^-$ to cationic metal complexes, have been discussed recently by Creutz.^{3e} The variability of the band positions makes this data less useful than IR and ^{13}C NMR data for characterization purposes.

VII. Characteristic Reactions

A. Thermolysis Reactions

1. Dissociation of CO_2

The thermal lability of the CO_2 complexes influences their handling characteristics and may dictate what further chemical reactions can be studied. As indicated in section III, the η^1 and η^2 complexes and some of the metalcarboxylate anion complexes are very prone to dissociate the CO_2 ligand. With the anions the lability is directly related to the stability of the corresponding metal anion; if the anion is known to be stable, dissociative loss of CO_2 from the metalcarboxylate can be expected. The differing behavior of two iron metalcarboxylate anions will serve to illustrate the magnitude of this problem. Following the report of Evans,⁶¹ the research groups

Table 15. Summary of Thermolysis Results for Compounds of Type $\text{Cp}'\text{M}(\text{CO})(\text{L})(\text{CO}_2)\text{SnR}_3$ ($\text{L} = \text{CO}, \text{NO}$)⁴⁰

$\text{Cp}'\text{M}(\text{CO})(\text{L})(\text{CO}_2)\text{SnR}_3 \xrightarrow{\Delta} \text{Cp}'\text{M}(\text{CO})(\text{L})\text{SnR}_3$						
Cp'	M	L	R	time (h)	temp (°C)	yield (%)
Cp	Fe	CO	Ph	2	70	89
Cp*	Fe	CO	Me	1	70	73
Cp*	Fe	CO	<i>n</i> -Bu	1.5	90	78
Cp*	Fe	CO	Ph	3	120	71
Cp*	Re	NO	Me	20.5	90	73
Cp*	Re	NO	Ph	2	185	small

of Cutler⁶² and Cooper⁶⁴ sought to study the properties of alkali metal salts of $\text{CpFe}(\text{CO})_2\text{CO}_2^-$. Since the iron anion readily dissociates CO_2 , full characterization of the salts was rendered impossible and studies of the reaction characteristics were made very difficult and limited to those occurring readily at low temperatures. By contrast, salts of $\text{CpFe}(\text{CO})(\text{PPh}_3)\text{CO}_2^-$ can be isolated and characterized and their reactions can be studied at higher temperatures;^{50,68} salts of the corresponding metal anion, $\text{CpFe}(\text{CO})(\text{PPh}_3)^-$, are not known and cannot be made by the usual synthetic methods for such compounds. Floriani *et al.*⁵⁸ observed that the nature of the alkali metal exerted some control over the reversibility of CO_2 binding with cobalt(salen)(CO_2) $^-\text{M}^+$ (**110–113**; $\text{M} = \text{Li}, \text{Na}, \text{K}$). Although the sodium and potassium salts would lose CO_2 under vacuum, the lithium salt did not. Also, solutions of the sodium salt lost CO_2 upon addition of dicyclohexano-18-crown-6.

The η^1 complexes reported by Herskovitz^{7,8} suffer very easy loss of CO_2 . Clearly, the only such compounds that can be formed are those in which a low-valent metal is further enriched in electron density by good σ -donor/poor π -acceptor ligands. As the η^2 coordination would suggest, the stability of compounds of this type toward CO_2 loss appears to parallel the stability of ethylene–metal complexes toward loss of the alkene.⁹⁷ Thus strong electron donor groups on the metal are required (see compounds listed in Table 1) for the thermal stability of these compounds, probably to enhance the back-bonding to the CO_2 ligand.

Among the compounds having a CO_2 ligand bound between two metal centers, the ones that appear to lose CO_2 most readily are the $\mu_2\text{-}\eta^2$ and $\mu_2\text{-}\eta^3$ complexes in which the carboxylate oxygen (one or both) is bound to a main group atom such as tin. These systems have been studied by Gladysz,³⁸ Cutler,³⁹ and Gibson⁴⁰ and their co-workers. Electron donor groups (e.g., alkyl) on the tin atom discourage binding of the second oxygen to tin whereas electron-attracting groups, such as phenyl, promote the formation of the $\mu_2\text{-}\eta^3$ type of complex. Strong electron donor groups on the metal that binds the carboxylate carbon also promote the formation of a $\mu_2\text{-}\eta^3$ -type complex. In addition to these factors, there are two distinct types of reactions resulting in dissociative loss of CO_2 . Those systems for which the corresponding transition metal anion is known undergo simple loss of CO_2 and formation of a heterobimetallic compound, usually in high yield. A series of these compounds studied by Gibson *et al.*⁴⁰ and the conditions for their thermolysis are shown in Table 15. The

Scheme 22

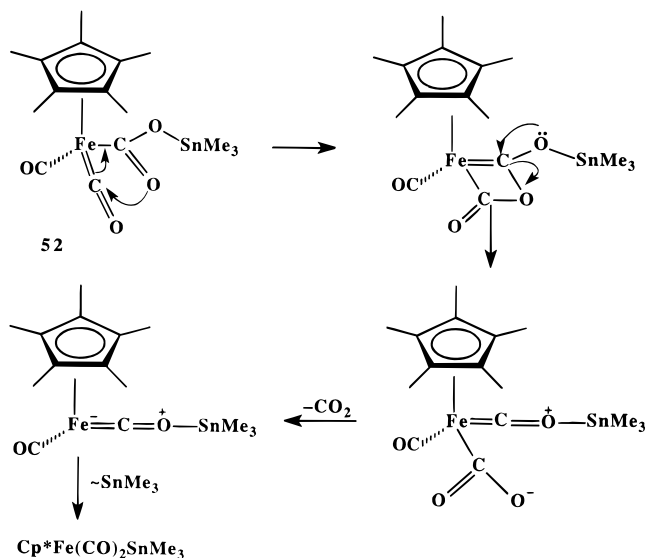


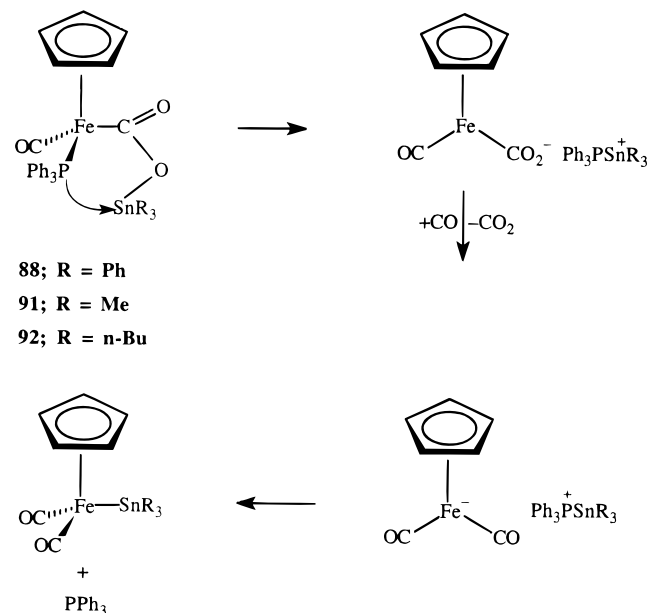
Table 16. Summary of Thermolysis Results for Compounds of Type $\text{Cp}'\text{Fe}(\text{CO})(\text{PPh}_3)(\text{CO}_2)\text{SnR}_3$ ⁴⁰
 $\text{Cp}'\text{Fe}(\text{CO})(\text{PPh}_3)(\text{CO}_2)\text{SnR}_3 \xrightarrow{\Delta}$

				$\text{Cp}'\text{Fe}(\text{CO})_2\text{SnR}_3 + \text{PPh}_3$ (A)	
Cp'	R	time (h)	temp (°C)	yield (%)	
				A	PPh ₃
Cp	Me	8	100	26	79
Cp	<i>n</i> -Bu	10	100	44	44
Cp	Ph	10	130	22	75
Cp*	Ph	8	120		77

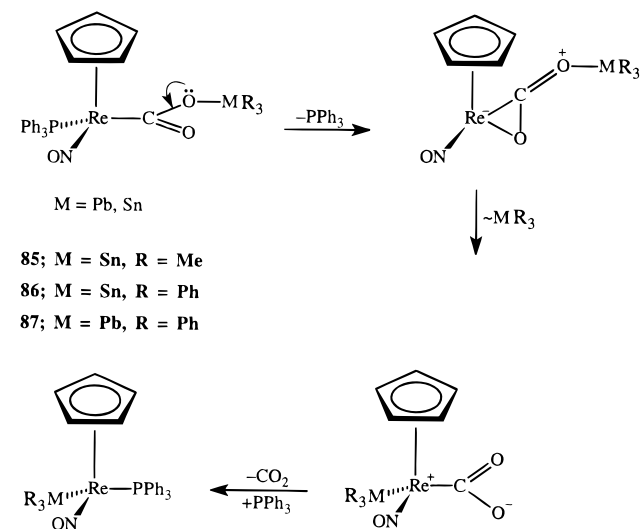
mechanism shown in Scheme 22 has been suggested to rationalize the behavior of these compounds. The mechanism is consistent with the observations of Pinkes and Cutler³⁹ regarding the label scrambling that attends the thermolysis of $\text{Cp}^*\text{Fe}(\text{CO})_2(^{13}\text{CO}_2)\text{SnMe}_3$ and also involves intermediate species similar to isocarbonyls that have been observed with other systems.⁹⁸ The second type of reaction involves both dissociative loss of CO_2 and disproportionation. This appears to be a characteristic of the compounds derived from metallocarboxylate systems that do not bind CO_2 reversibly (i.e., those for which the carbonyl metalate is not known). The systems of this type that have been studied to the present time are shown in Table 16. The mechanism proposed⁴⁰ for these reactions is shown in Scheme 23; it is consistent with the low yields observed in each case for the heterobimetallic product (a 50% yield of this product is the most possible).

The lead and tin derivatives **85–87** derived from the rhenium metallocarboxylate $\text{CpRe}(\text{NO})(\text{PPh}_3)\text{CO}_2^-$, studied by Gladysz *et al.*,³⁸ decarboxylate readily and give the corresponding heterobimetallic compounds in high yield. However, each final product contains the phosphine ligand; the related metal anion is known in this case also. Clearly, an intermediate metalloanhydride, such as shown in Scheme 22, cannot be involved here. The decarboxylation pathway suggested⁴⁰ for these systems is shown in Scheme 24.

Scheme 23



Scheme 24

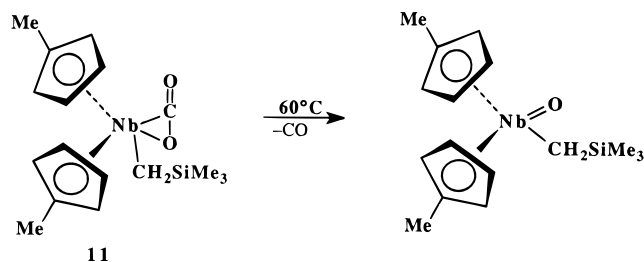


2. Cleavage of a Carboxyl C–O Bond

Thermolysis (83 °C) of $\text{Ni}(\text{PCy}_3)_2(\text{CO}_2)$ (**4**) was reported by Aresta and Nobile⁹ and afforded $\text{Ni}(\text{CO})_2(\text{PCy}_3)_2$ as a major product. The phosphine oxide was not detected but carbonate-containing species were found. By contrast, the palladium complex, $\text{Pd}(\text{PMePh}_2)_2(\text{CO}_2)$ (**10**), recently reported by Yamamoto¹⁶ gives CO and $\text{O}=\text{PMePh}_2$ as thermolysis products. Allowing $\text{Fe}(\text{CO}_2)(\text{PMe}_3)_4$ (**8**) to stand in pentane with CO_2 converts it to $\text{Fe}(\text{CO})(\text{CO}_3)(\text{PMe}_3)_3$.¹⁴ Thermolysis of the CO_2 complex, or this carbonate derivative, afforded $\text{Fe}(\text{CO})_2(\text{PMe}_3)_3$, $\text{Fe}(\text{CO})(\text{PMe}_3)_4$, and Me_3PO ; the same product composition was found in both cases. The molybdenum complexes $\text{Cp}_2\text{Mo}(\text{CO}_2)$ (**12**)¹⁸ and *trans*- $\text{Mo}(\text{CO}_2)_2(\text{PMe}_3)_4$ (**20**)²⁵ (and isonitrile complexes derived from it) are relatively stable but do decompose upon heating at elevated temperatures; the decomposition products have not been identified.

A reaction that may be characteristic of η^2 complexes formed from early transition metals is thermolysis with cleavage of the O–metal bond and one

Scheme 25



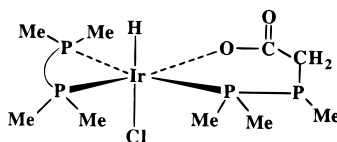
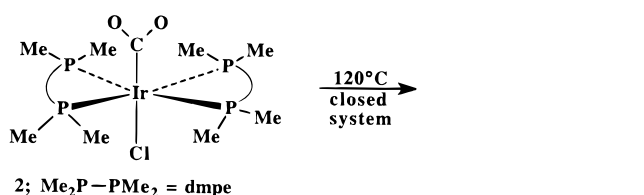
C–O bond, resulting in loss of carbon monoxide and formation of a complex with an oxo ligand. The reaction has been clearly demonstrated with the niobium complexes studied by Nicholas *et al.*²¹ and is illustrated in Scheme 25. A similar reaction may be involved in the reaction of $\text{WCl}_2(\text{PMePh}_2)_4$ with CO_2 , which yields $\text{W}(\text{O})\text{Cl}_2(\text{CO})(\text{PMePh}_2)_2$ with cis oxo and carbonyl ligands.⁹⁹ Whereas $\text{Cp}_2\text{Ti}(\text{PMe}_3)_2$ reacts with CO_2 to give the $\eta^2\text{-CO}_2$ complex **13**, $\text{Cp}_2\text{Zr}(\text{PMe}_3)_2$ gives CO and a polymer containing the $\text{Cp}_2\text{-ZrO}$ fragment; the greater oxophilicity of Zr may be responsible for the different results.¹⁸ $\text{CpFe}(\text{CO})_2\text{-(CO)}_2\text{Zr}(\text{Cl})\text{Cp}_2$ and its congeners degrade cleanly upon thermolysis⁴² with formation of $[\text{Cp}_2\text{Zr}(\text{Cl})]_2\text{O}$, again demonstrating the effects of an oxophilic zirconium center.

3. Thermolysis with Loss of an Ancillary Ligand and/or with Rearrangement

Thermolysis⁷ of $\text{Ir}(\text{dmpe})_2(\text{Cl})(\text{CO}_2)$ (**2**) at 120 °C afforded an isomeric compound which was formulated as a metallacycle as shown in Scheme 26. This type of thermal reorganization appears unique among CO_2 complexes but may also be responsible for the results obtained by Karsch¹⁴ in efforts to synthesize **8** in THF solution. Compounds having a $\mu_2\text{-}\eta^2$ -bridged carbon dioxide ligand can sometimes be converted to the related $\mu_2\text{-}\eta^3$ complexes by dissociation of a ligand from the metal center bound to the carboxylate oxygen. This has been demonstrated for several systems by Gibson *et al.*^{32–34} and implied as an intermediate step in other cases.⁴⁷ An example is shown in Scheme 16. These reactions have been observed with relatively oxophilic metal centers such as rhenium, molybdenum, and tungsten.

In addition to the conversion of $\mu_2\text{-}\eta^2$ to $\mu_2\text{-}\eta^3$ complexes, Gibson *et al.*³³ observed a series of ligand reorganization reactions resulting from thermolysis of CO_2 -bridged compounds derived from *cis*- $\text{CpFe}(\text{CO})(\text{PPh}_3)(\text{CO}_2)\text{Re}(\text{CO})_4[\text{P}(\text{OEt})_3]$ (**44**). With the $\mu_2\text{-}\eta^3$ complexes derived from this compound, only those

Scheme 26



having a facial arrangement of the CO ligands on Re are observed. However, isomers having a syn or anti arrangement of the phosphorus ligands on the two metal centers are possible. The anti isomer, $\text{CpFe}(\text{CO})(\text{PPh}_3)(\text{CO}_2)\text{Re}(\text{CO})_3[\text{P}(\text{OEt})_3]$ (**80**) was structurally characterized (see section IV.D). Thermolysis of the $\mu_2\text{-}\eta^2$ complex was monitored by ³¹P spectral data that showed distinct resonances for each phosphorus ligand on the starting material, three intermediate compounds, and the final product, $\text{CpFe}(\text{CO})[\text{P}(\text{OEt})_3]\text{-(CO)}_2\text{Re}(\text{CO})_3(\text{PPh}_3)$, which is believed to have the anti configuration. The transformations are profiled in Scheme 27. The phosphorus ligand exchange is believed to result from O–Re bond breaking in **C**, followed by migration of the PPh_3 ligand to the vacant site on rhenium, followed by rotation and then migration of $\text{P}(\text{OEt})_3$ to the vacant site on iron, and then closure to give **D** as shown in Scheme 28. The ligand exchange would be followed by facial to facial isomerization to give **E** (Scheme 27). Decarboxylation is not a competing reaction with these compounds. As noted in section A, above, the tin complexes derived from $\text{CpFe}(\text{CO})(\text{PPh}_3)\text{CO}_2^-$ also do not lose CO_2 readily under thermolysis conditions, but disproportionate, with loss of PPh_3 and CO_2 , in reactions that appear to be related to the ligand rearrangements profiled in Scheme 27.

B. Photolysis Reactions

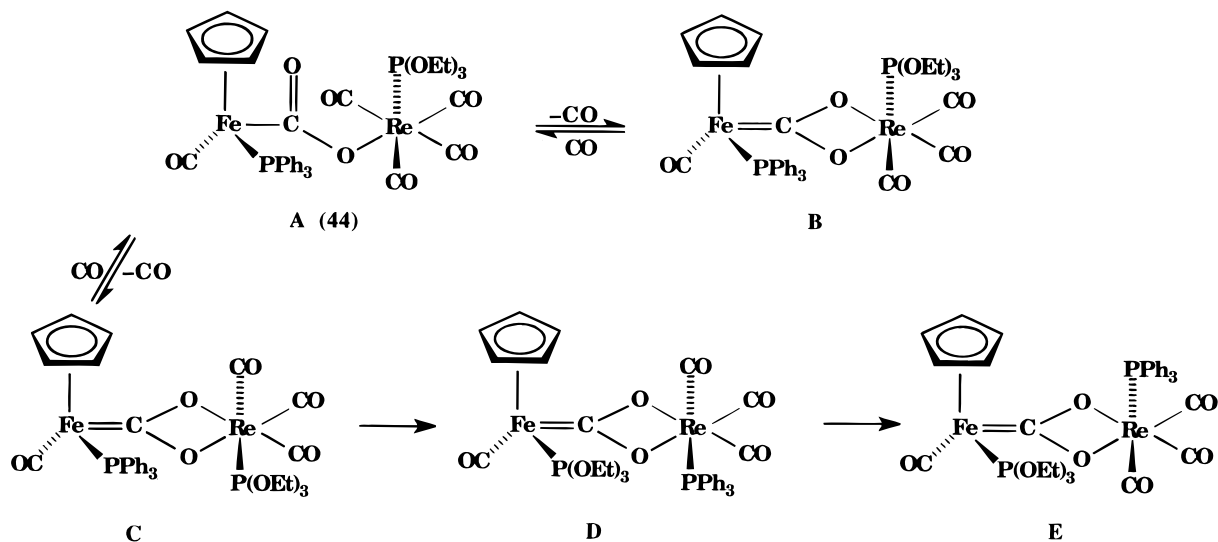
There has been very little work reported on reactions of CO_2 complexes under photochemical conditions. Nicholas *et al.*¹⁰⁰ reported that photolysis of $\text{Cp}_2\text{Mo}(\text{CO}_2)$ (**12**) in the presence of carbon dioxide resulted in the η^2 -carbonato complex, $\text{Cp}_2\text{Mo}(\text{O}_3\text{C})$, $\text{Cp}_2\text{Mo}(\text{CO})$, and free CO. The reaction pathway is not known, but it was shown that thermal or photochemical reaction of $\text{Cp}_2\text{Mo}(\text{O})$ with CO_2 to give the carbonato complex was much slower than the reaction involving the carbon dioxide complex. Later,²¹ however, this group showed that both thermolysis (section A.2 above) and photolysis of $\text{Cp}'_2\text{Nb}(\text{CO}_2)(\text{CH}_2\text{-SiMe}_3)$ afforded the oxo complex $\text{Cp}'_2\text{Nb}(\text{O})(\text{CH}_2\text{-SiMe}_3)$. The photolytic cleavage occurred within minutes at -20 °C.

Photolysis of *trans*- $\text{Mo}(\text{CO})_2(\text{PMe}_3)_4$ (**20**) through quartz in toluene solution at -20 °C yields *cis*- $\text{Mo}(\text{CO})_2(\text{PMe}_3)_4$ and Me_3PO (29% and 35%, respectively) as major products together with free Me_3P ; smaller amounts of *mer*- $\text{Mo}(\text{CO})_3(\text{PMe}_3)$, *fac*- $\text{Mo}(\text{CO})_3(\text{PMe}_3)_3$, and $\text{Mo}(\text{CO})(\text{PMe}_3)_5$ were also generated. When the photolysis was conducted in pyrex, an intermediate was generated which was formulated as the unstable *trans* isomer of the final dicarbonyl product.¹⁰¹

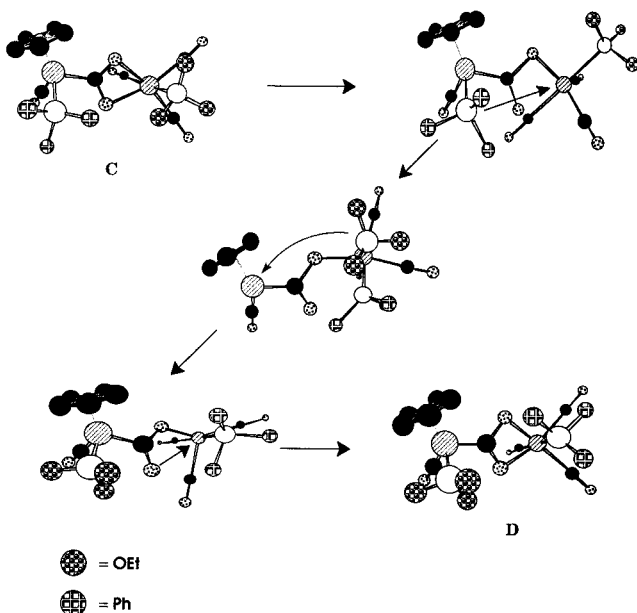
C. Reactions with Electrophiles

Herskovitz *et al.*⁷² alkylated the iridium complex $\text{Ir}(\text{dmpe})_2(\text{Cl})(\text{CO}_2)$ (**2**) with MeFSO_3 and structurally characterized the product, a methyl ester. This work reinforced the structural assignment of the carbon dioxide adduct as an η^1 -type complex and provided the first demonstration that the carboxylate oxygens can behave as nucleophiles. Subsequent work by others has provided further examples of the additions of electrophiles to a carboxylate oxygen but also show

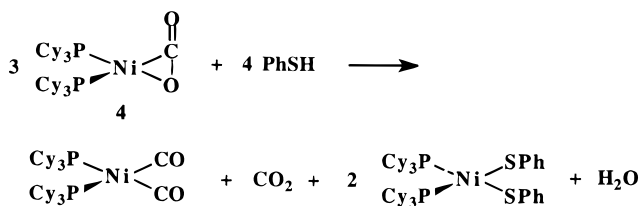
Scheme 27



Scheme 28



Scheme 29



that O–M or C–O cleavage reactions can be dominant.^{15,42,50a}

Aresta *et al.*¹⁰² reported that $\text{Ni}(\text{PCy}_3)_2(\text{CO}_2)$ (**4**) would disproportionate when treated with thiols, as illustrated in Scheme 29; initial protonation is followed by reduction. Reactions of other η^2 complexes with simple electrophiles are more straightforward. Nicholas *et al.*¹⁰³ studied the behavior of $\text{Cp}_2\text{Mo}(\text{CO}_2)$ (**12**) toward a variety of electrophiles as shown in Scheme 30. Although it is clear from the nature of the products that both O–Mo and C–O bond-breaking reactions occur, it has not been possible to determine which occurs first or even which carboxy-

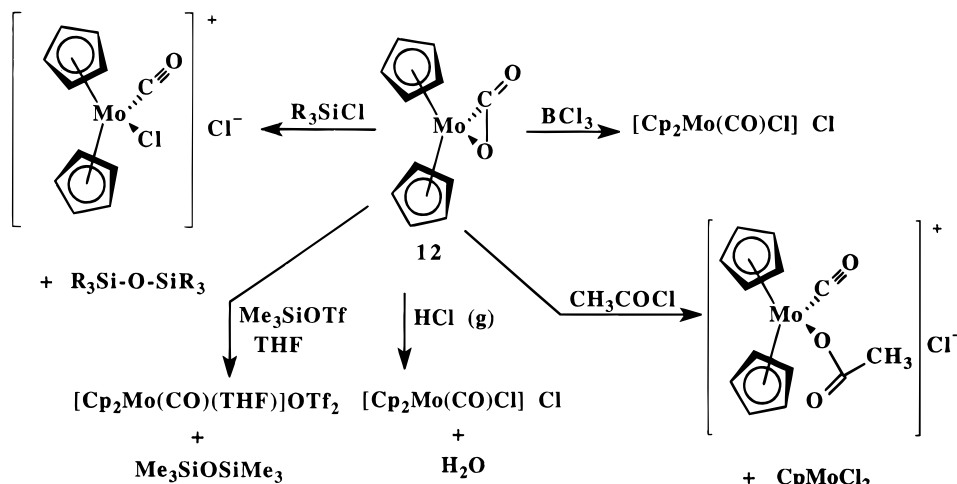
late oxygen reacts first; either of two proposed pathways would give rise to the same compounds. Nicholas *et al.*¹⁰⁴ also studied the reactions of $\text{Cp}'_2\text{Nb}(\text{CO}_2)\text{CH}_2\text{SiMe}_3$ (**11**) with several electrophiles. In direct contrast to the molybdenum complex, reaction of Me_3SiCl with the niobium complex yields $\text{Cp}'_2\text{Nb}(\text{O})\text{Cl}$, the product of both decarbonylation and dealkylation. Deoxygenation results from treating the iron compound **9** with excess methyl iodide or methyl triflate.¹⁵

Nicholas *et al.*¹⁰⁵ studied the reactions of $\text{Cp}_2\text{Mo}(\text{CO}_2)$ (**12**) with two acidic metal hydrides, $\text{HCo}(\text{CO})_4$ and $\text{H}_2\text{Fe}(\text{CO})_4$. With either hydride (in excess), the initial reactions result in hydride transfer to molybdenum and deoxygenation of the CO_2 ligand as illustrated with $\text{HCo}(\text{CO})_4$ in Scheme 31. Labeling studies showed that the CO_2 ligand was the source of the carbonyl ligand bound to Mo in the product.

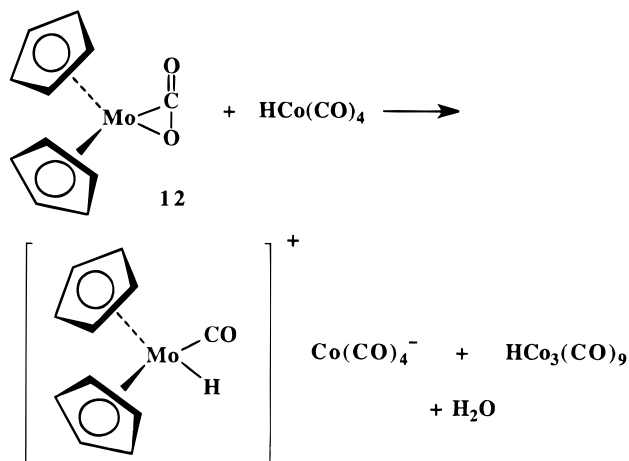
In contrast, the palladium complex $\text{Pd}(\text{CO}_2)(\text{PMePh}_2)_2$ (**10**) reacts with various electrophiles with total loss of the CO_2 ligand.¹⁶ Thus, reaction with excess Me_3SiCl afforded a 1:1 mixture of *cis*- and *trans*- $\text{PdCl}_2(\text{PMePh}_2)_2$ whereas reaction with PhSH yields *trans*- $\text{Pd}(\text{SPh})_2(\text{PMePh}_2)_2$, H_2 , and CO_2 .

Because of the increased nucleophilicity of the metallocarboxylate anions, the reactions of these compounds with electrophiles have been the subject of several studies. Initially such reactions were employed in efforts to obtain stable derivatives which might be more readily characterized than the labile anions (as Herskovitz had done with the η^1 complex **2**). Cutler^{62a} reported that efforts to alkylate $\text{CpFe}(\text{CO})_2(\text{CO}_2)^-\text{Na}^+$ (**104**) with MeI or MeOTf resulted only in $\text{CpFe}(\text{CO})_2\text{CH}_3$; however, the magnesium salt **106** was alkylated by MeOTf and afforded the desired methyl ester.⁶³ Later, Cutler^{62b} found that hard, oxophilic trialkylsilyl chlorides were effective in generating the corresponding esters with the sodium or lithium salts of this metallocarboxylate. However, with the lithium salt of $\text{W}(\text{CO})_5(\text{CO}_2)^{2-}$, Cooper *et al.*^{65,66} obtained only $\text{W}(\text{CO})_6$ from reactions with a variety of electrophiles, including Me_3SiOTf . The behavior of these metallocarboxylate anions toward alkylating or silylating agents contrasts somewhat with that of the salts of $\text{CpFe}(\text{CO})-$

Scheme 30



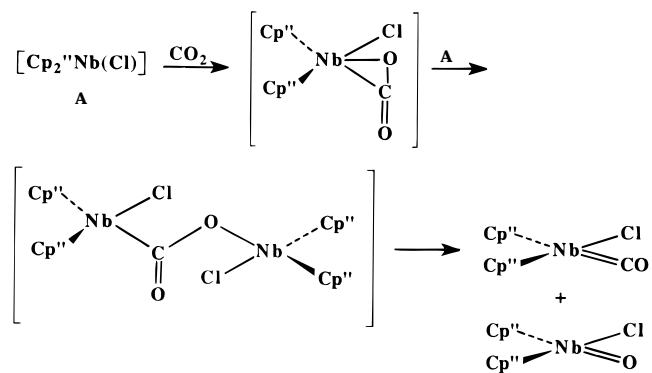
Scheme 31



(PPh_3) CO_2^- and $\text{Cp}^*\text{Fe}(\text{CO})(\text{PPh}_3)\text{CO}_2^-$ studied by Gibson *et al.*^{50a} Reactions of the potassium salts of these anions provide the corresponding esters in reactions with CH_3I and $\text{Et}_3\text{O}^+\text{BF}_4^-$ as the result of O–M bond cleavage. But, with the lithium and sodium salts, carboxylate C–O bond cleavage is dominant and the metal carbonyl cation is the main product. These comparisons suggest that the more oxophilic metal centers promote C–O bond cleavage. Reactions of these iron salts with protonic acids result in either the metalcarboxylic acid (O–M bond cleavage), the metal carbonyl cation (C–O bond cleavage), or mixtures of these products; product distribution is highly dependent on the solvent medium.^{50a}

Reaction of $\text{Cp}_2'\text{Nb}(\text{CO}_2)\text{CH}_2\text{SiMe}_3$ (**11**) with LiPF_6 afforded $\text{Cp}_2'\text{Nb}(\text{F})\text{CH}_2\text{SiMe}_3$.¹⁰⁴ Furthermore, it was shown that $\text{Cp}_2'\text{Nb}(\text{O})\text{CH}_2\text{SiMe}_3$ afforded the same product in reaction with the lithium salt. Reaction of the CO_2 complex with ZnCl_2 gave an unstable product that decomposed, with loss of CO, to the zinc adduct of the oxo complex which was structurally characterized.¹⁰⁵ Thus, this early transition metal complex showed a clear preference for decarbonylation rather than deoxygenation. Bruno *et al.*¹⁰⁶ recently reported that reactions of $[\text{Cp}''_2\text{Nb}(\text{Cl})]_x$ with CO_2 affords both $\text{Cp}_2''\text{Nb}(\text{Cl})(\text{CO})$ and $\text{Cp}_2''\text{Nb}(\text{O})(\text{Cl})$. These results were rationalized as shown in Scheme 32 and are proposed to involve electrophilic attack

Scheme 32

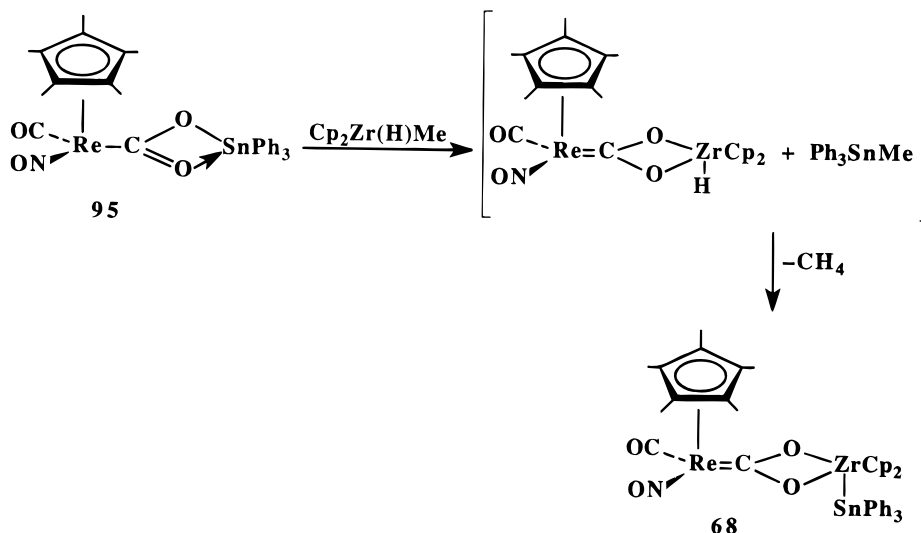


by the niobium reagent on an intermediate η^2 complex followed by thermolysis of the resulting μ_2 - η^2 complex.

Perhaps the greatest success in reactions of the metalcarboxylate anions with electrophiles has been in the synthesis of carbon dioxide-bridged bimetallic compounds. These reactions have already been discussed in section III. A further type of metal electrophile that is reactive toward metalcarboxylate anions, and at least one metalcarboxylic acid, is the one with a coordinated ethylene ligand. Where the ethylene cation is bound strongly, addition occurs with formation of a bridging carboxyethylene ligand.⁴⁸ In cases where the ethylene is less strongly bound, displacement occurs and a CO_2 -bridged complex results,³⁴ as shown in Scheme 7. Other reactions of metalcarboxylates with metal carbonyls are treated in section D, below.

Reports of the reactions of electrophiles with compounds having bridging CO_2 ligands are relatively few in number. The μ_3 - η^3 CO_2 -bridged complex **100** studied by Caulton *et al.*⁵⁷ binds ZnBr_2 at the carboxylate oxygens and forms a stable adduct (**102**) which was structurally characterized. The same CO_2 complex reacted with NaBPh_4 , but the product was not characterized. The μ_2 - η^3 CO_2 -bridged complex, $\text{CpRe}(\text{CO})(\text{NO})(\text{CO}_2)\text{Zr}(\text{Cl})\text{Cp}_2$, prepared by Cutler⁴¹ was cleaved by strong electrophiles, HBF_4 etherate, and $\text{Et}_3\text{O}^+\text{PF}_6^-$, with formation of $\text{CpRe}(\text{CO})_2(\text{NO})^+$ (the zirconium product was not identified). More recently, Gibson *et al.*³³ reported similar cleavage of the μ_2 - η^3 complex, $\text{CpFe}(\text{CO})[\text{P}(\text{OEt})_3](\text{CO}_2)\text{Re}(\text{CO})_3$ -

Scheme 33



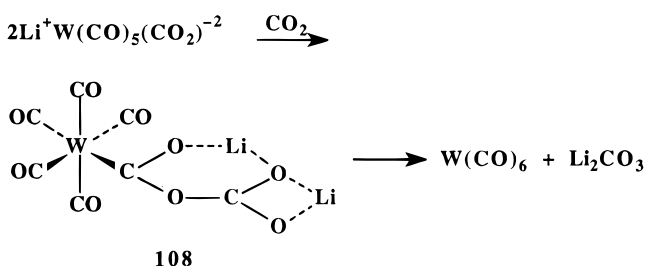
(PPh₃), with formation of the iron cation CpFe(CO)₂-[P(OEt)₃]⁺ (the rhenium product could not be identified). Gibson *et al.*³² also reported the cleavage of the $\mu_2\text{-}\eta^2$ complex CpFe(CO)(PPh₃)(CO₂)Re(CO)₄(PPh₃) by Me₃SiOTf which afforded the iron cation and (Me₃-SiO)Re(CO)₄(PPh₃) as a result of C–O bond cleavage.

Reactions of zirconium reagents with several CO₂-bridged complexes involving tin have been reported recently by Gibson *et al.*⁴⁴ With Cp₂Zr(Cl)(Me) there is exchange of the SnPh₃ group for Cp₂Zr(Cl) as illustrated in Scheme 13. With the same tin complex, or with a rhenium/tin analog as shown in Scheme 33, reaction with Cp₂Zr(H)(Me) yields a trimetallic complex in which zirconium again binds both carboxylate oxygens in the product. All of these transmetalation reactions are believed to be initiated by dechelation of one oxygen in the initial $\mu_2\text{-}\eta^3$ complex followed by binding to the highly oxophilic 16e zirconium center. Such reactions are very useful for the synthesis of compounds derived from very labile metallocarboxylate anions or acids since the bimetallic tin compounds can be prepared in aqueous media after generating the metallocarboxylate anion *in situ*. The scope of the transmetalation reactions is being examined.

D. Intra- or Intermolecular Oxygen Transfer Reactions

One of the first reactions reported for the metallocarboxylate anions was oxide transfer.⁶⁴ Reaction of Li₂W(CO)₅(CO₂) with additional CO₂ results in formation of W(CO)₆ and Li₂CO₃ as shown in Scheme 34, a reaction described as reductive disproportionation.

Scheme 34

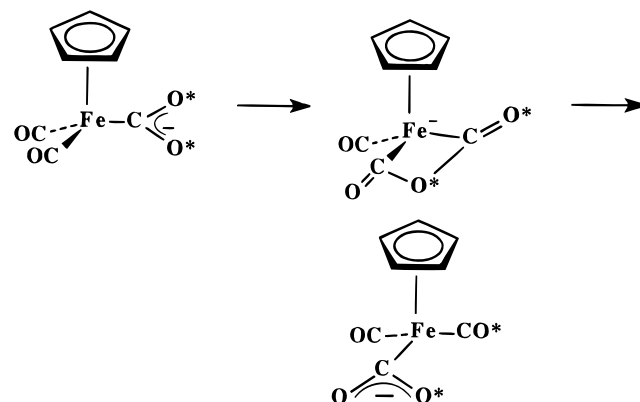


108

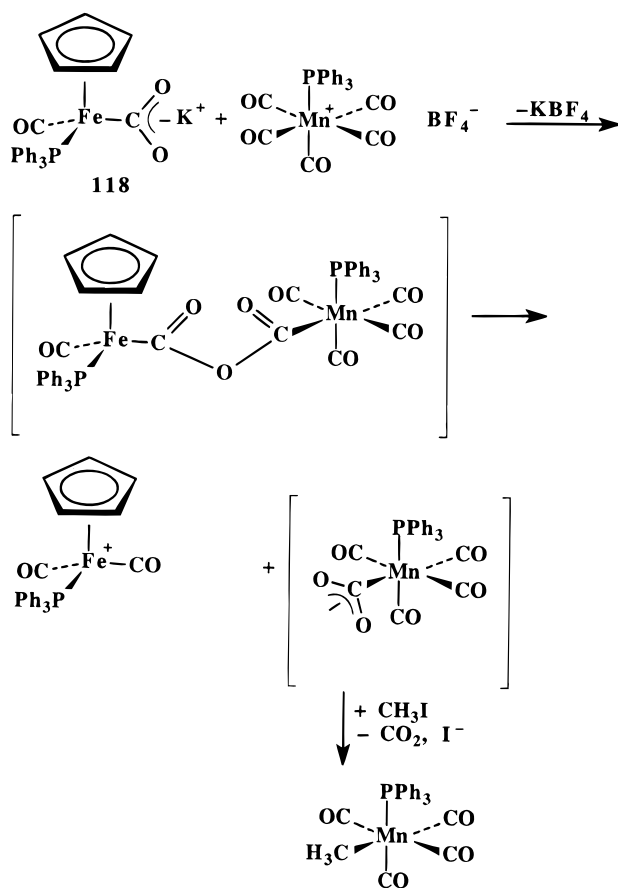
ation. Spectral evidence for the intermediate was obtained by Cooper *et al.*,^{65,66} and labeling studies showed the oxide transfer to be a facile process. Lee and Cooper^{64b} also showed that this dianion would transfer oxide to CpFe(CO)₃⁺BF₄⁻; labeling studies showed that oxygen, but not carbon, of the CO₂ ligand was incorporated into the iron product [CpFe(CO)₂]₂. Two possible mechanisms were considered to explain the formation of the iron dimer (following oxide transfer from the tungsten complex): (a) electron transfer from the iron metallocarboxylate to the iron cation followed by degradation to the iron dimer or (b) initial metalloanhydride formation followed by degradation to the dimer. In a separate study, Lee and Cooper^{64a} observed intramolecular oxide transfer from coordinated CO₂ to coordinated CO in the iron complex CpFe(CO)₂(CO₂)⁻Li⁺. Again, labeling studies were used to support conclusions that the reaction mechanism involves intramolecular oxide transfer as indicated in Scheme 35. Oxide transfer from this metallocarboxylate to CO₂ (reductive disproportionation) is a minor competing path.

Further results of work on the tungsten metallocarboxylate and its chromium and molybdenum analogs was later provided by Cooper *et al.*⁶⁶ together with studies of the reactions of group 8 carbonylmetalates Na₂M(CO)₄ [M = Fe, Ru, Os] and Na₂[CpV(CO)₃] with CO₂. The latter compounds also yield the metal carbonyl together with alkali-metal carbonate

Scheme 35



Scheme 36

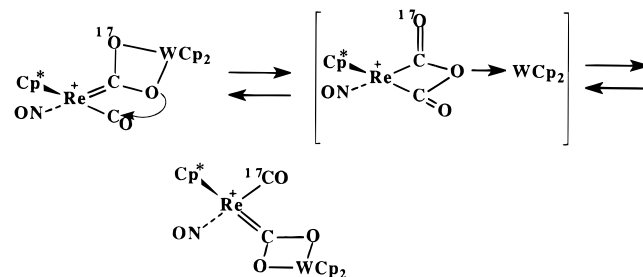


as products of reductive disproportionation. Thus the behavior of the metallocarboxylate dianions toward CO_2 is distinct from that of salts of $\text{CpFe}(\text{CO})_2\text{CO}_2^-$ for which reductive disproportionation is not a characteristic reaction. However, oxide transfer from coordinated CO_2 to coordinated CO was observed with the group 6 metallocarboxylate anions; thus, this reaction is characteristic of both groups of metallocarboxylate anions.

Reactions of $\text{CpFe}(\text{CO})(\text{PPh}_3)\text{CO}_2^-\text{M}^+$ ($\text{M} = \text{Na}, \text{Li}, \text{K}$) with $\text{Mn}(\text{CO})_5(\text{PPh}_3)^+\text{BF}_4^-$ have been studied by Gibson *et al.*^{50a} Examination of IR spectral data of the product mixtures showed ν_{CO} bands for the cation $\text{CpFe}(\text{CO})_2(\text{PPh}_3)^+$ together with several at lower frequencies that are more characteristic of metal carbonyl anions. Addition of CH_3I to the product mixture resulted in disappearance of the latter bands and formation of $\text{CH}_3\text{Mn}(\text{CO})_4(\text{PPh}_3)$, in high yield, in all cases. The results are consistent with a path involving oxide transfer to a CO ligand on manganese followed by loss of CO_2 as illustrated in Scheme 36.

Geoffroy *et al.*^{46b} reported that label scrambling occurred in the preparation of $\mu_2\text{-}\eta^3$ CO_2 -bridged complexes from $\text{Cp}_2\text{W}=\text{}^{17}\text{O}$ and $\text{Cp}^*\text{Re}(\text{CO})_2(\text{NO})^+\text{BF}_4^-$ or $\text{Cp}^*\text{Fe}(\text{CO})_3^+\text{BF}_4^-$. In both product mixtures, approximately equal amounts of the ^{17}O were contained in the carboxylate and terminal carbonyl ligands. To test possible alternative mechanisms for this, the authors attempted to intercept dissociated $\text{Cp}_2\text{W}=\text{}^{17}\text{O}$ by adding a different metal carbonyl cation to solutions of the CO_2 -bridged compounds; no cross products resulted. Furthermore, although $\text{PhN}=\text{C}=\text{O}$ and Me_3SiCl react readily with the oxo

Scheme 37



complex, neither of them intercepted this species from solutions of the CO_2 -bridged complexes. These results led this group to propose intermediate metalloanhydride-like species to account for the label scrambling as shown in Scheme 37. Recently, Pinkes and Cutler³⁹ presented evidence of oxygen transfer from carboxylate to CO within the $\mu_2\text{-}\eta^2$ CO_2 -bridged complex $\text{Cp}^*\text{Fe}(\text{CO})_2(^{13}\text{CO}_2)\text{SnMe}_3$. Studies of this system are complicated by the competing, and apparently faster, decarboxylation of the CO_2 -bridged complex.

E. Reactions with Nucleophiles

Very few reactions of CO_2 complexes with nucleophiles have been reported. Aresta and Nobile¹² noted that CO_2 could be displaced from $\text{Ni}(\text{CO})_2(\text{PCy}_3)_2$ (**4**) by the action of triphenyl phosphite at room temperature. However, these investigators noted that solutions of $\text{RhCl}(\text{CO})_2[\text{P}(n\text{-Bu})_3]_2$ (**7**) in CH_2Cl_2 developed the phosphine oxide complex, $\text{Rh}(\text{Cl})(\text{CO})[\text{O}=\text{P}(n\text{-Bu})_3][\text{P}(n\text{-Bu})_3]$ upon standing at room temperature.¹³

Gibson and Ye³³ have reported that either CO or $\text{P}(\text{OEt})_3$ will react with $\text{CpFe}(\text{CO})(\text{PPh}_3)(\text{CO}_2)\text{Re}(\text{CO})_3[\text{P}(\text{OEt})_3]$ (**80**) to convert this $\mu_2\text{-}\eta^3$ complex to the corresponding $\mu_2\text{-}\eta^2$ complex by addition of this ligand at the rhenium center and displacement of one carboxyl oxygen. Reaction of a tin derivative of this metallocarboxylate, $\text{CpFe}(\text{CO})(\text{PPh}_3)(\text{CO}_2)\text{SnPh}_3$ (**88**), with $\text{KBH}(\text{sec-Bu})_3$ afforded $\text{CpFe}(\text{CO})(\text{PPh}_3)\text{CO}_2^-\text{K}^+$ and HSnPh_3 (in addition to the borane).¹⁰⁷ It is not known whether this may be a general reaction of the tin derivatives.

Caulton *et al.*⁵⁷ reported efforts to reduce the CO_2 ligand in $[(\text{COD})\text{Rh}]_2(\text{CO}_2)\text{OsH}_2\text{P}(\text{Me}_2\text{Ph})_3$ (**100**) with LiBET_3H , LiBH_4 and $\text{Cp}_2\text{Zr}(\text{H})(\text{Cl})$; all were unsuccessful. Reaction with LiAlH_4 resulted in intractable products.

Geoffroy *et al.*⁴⁵ reported that $\text{Cp}^*\text{Re}(\text{CO})(\text{NO})(\text{CO}_2)\text{Ti}(\text{tmtaa})$ (**69**) reacted with 2 equiv of $\text{Ph}_3\text{P}=\text{NPh}$ with displacement of $(\text{tmtaa})\text{Ti}=\text{O}$, formation of 2 equiv of $\text{Ph}_3\text{P}=\text{O}$, and formation of the cationic complex $\text{Cp}^*\text{Re}(\text{NO})(\text{CNPh})_2^+\text{BF}_4^-$. The same cation could also be formed from reaction of $\text{Cp}^*\text{Re}(\text{CO})_2(\text{NO})^+\text{BF}_4^-$ with $\text{Ph}_3\text{P}=\text{NPh}$; thus the reaction with the CO_2 -bridged complex is thought to be initiated by attack of the imine nitrogen on the electrophilic carboxyl carbon atom.

Tso and Cutler⁴¹ showed that the reaction of $\text{CpRe}(\text{CO})(\text{NO})(\text{CO}_2)\text{Zr}(\text{Cl})\text{Cp}_2$ (**58**) with 2 equiv of $\text{Cp}_2\text{Zr}(\text{H})(\text{Cl})$ afforded the formaldehyde-bridged complex $\text{CpRe}(\text{CO})(\text{NO})(\text{CH}_2\text{O})\text{Zr}(\text{Cl})\text{Cp}_2$ and the oxo complex $[\text{Cp}_2\text{Zr}(\text{Cl})]_2\text{O}$. However, the reaction apparently does not involve direct reduction of the bridging

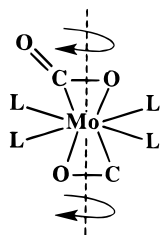
carboxyl group. Reduction of $\text{CpRu}(\text{CO})_2(\text{CO}_2)\text{Zr}(\text{Cl})\text{Cp}_2$ by the same reagent also affords the formaldehyde-bridged complex.¹⁰⁸ However, labeling studies showed that the terminal carbonyl on ruthenium is reduced by the zirconium reagent. It is nonetheless an interesting reaction and provides a unique method of synthesis for the formaldehyde-bridged complexes.

F. Fluxional Behavior

In the process of characterizing $\text{Mo}(\text{CO})_2(\text{PMe}_3)_4$ (**20**) and $\text{Mo}(\text{CO})_2(\text{PMe}_3)(\text{CN}-t\text{-Bu})$ (**23**), Carmona *et al.*^{25c} observed temperature-dependent NMR spectra of the complexes which was attributed to fluxional behavior. For the complex *trans*- $\text{Mo}(\text{CO})_2(\text{PMe}_3)_4$, an AA'BB' pattern was observed at low temperature in the $^{31}\text{P}\{^1\text{H}\}$ NMR spectrum which became a singlet upon warming to 50 °C. Also, spectra of $\text{Mo}(\text{CO})_2(\text{PMe}_3)_3(\text{CN}-t\text{-Bu})$ showed a mixture of two species in dynamic equilibrium; crystallographic data had shown that the two metallacyclic rings are orthogonal in this compound. Five different pathways were considered to account for the observed behavior: (a) CO_2 dissociation/reassociation, (b) independent rotation of the CO_2 ligands about the bond axis to Mo, (c) interchange of the coordinated and free oxygens of the CO_2 ligands, (d) concerted rotation of the CO_2 ligands in the same direction (conrotatory), and (e) concerted rotation of the CO_2 ligands in opposite directions (disrotatory). The first mechanistic pathway was discarded because $^{31}\text{P}-^{13}\text{CO}_2$ coupling is maintained in the fast exchange limit; also $^{13}\text{CO}_2-^{12}\text{CO}_2$ exchange could not be detected. Several new complexes, with one or two chelating phosphine ligands, were prepared which had better thermal stability than the ones first observed. Studies of these systems allowed a distinction to be made among the three remaining possible pathways.^{24d} The results are consistent with the path involving concerted rotation of the CO_2 ligands in the same direction as shown in Scheme 38. Later studies^{24e} with additional related compounds reinforced the conclusions reached with this first group of compounds. The experimental conclusions are in agreement with the results of earlier theoretical calculations on such systems by Sanchez-Marcos *et al.*⁷⁷

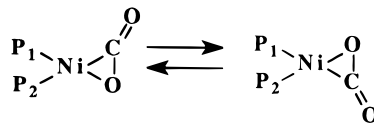
Mason and Ibers¹¹ were first to observe that the single ^{31}P resonance for $\text{Ni}(\text{PCy}_3)_2(\text{CO}_2)$ (**4**) in room-temperature NMR spectra could be resolved into a pair of doublets at low temperature (185 K); ΔG^\ddagger for the exchange process was calculated as 9.8 ± 0.2 kcal/mol. Aresta *et al.*⁸⁹ recently re-examined the spectra of the complex, including considerations of solid state (CPMAS) ^{31}P and ^{13}C spectra. For the dynamic process, this group found a ΔG^\ddagger of 39.3 kJ mol⁻¹ (9.4 kcal mol⁻¹) in agreement with the earlier report. Also,

Scheme 38

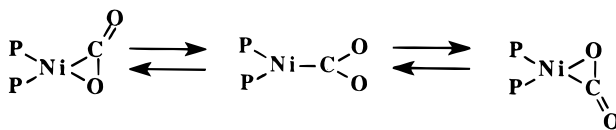


Scheme 39

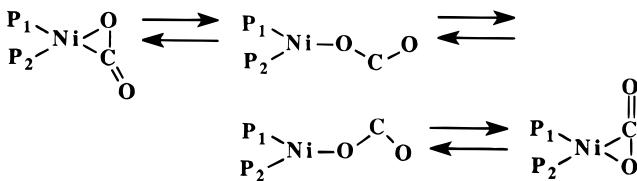
Mechanism a:



Mechanism b:



Mechanism c:



a low-temperature limiting spectrum was found (^{13}C) at 173 K for a $^{13}\text{CO}_2$ -enriched sample which showed a doublet of doublets at δ 159.88 with $J_{\text{PC}} = 41$ and 10 Hz. In the fast-exchange mode, at 253 K, a triplet appeared for the coordinated CO_2 , thus ruling out a rapid dissociation/recoordination process. The other mechanisms considered for the observed equilibration of the phosphorus ligands are (shown in Scheme 39) (a) rapid rotation of the CO_2 ligand about the Ni-CO bond axis, (b) equilibration as a result of formation of an $\eta^1\text{-C}$ intermediate, and (c) equilibration as a result of formation of an $\eta^1\text{-O}$ intermediate. Although the authors favor mechanism c, a clear distinction among the three possibilities is not yet available. Path c bears close resemblance to the σ/π ($\eta^1\text{-O}/\eta^2\text{-C,O}$) rearrangements which have been documented experimentally by Gladysz *et al.*¹⁰⁹ for aldehyde and ketone complexes of rhenium with the metal fragment $\text{CpRe}(\text{NO})(\text{PPh}_3)$. There has been a theoretical treatment of this general subject also.¹¹⁰ In general, ketones are primarily σ complexes (in part for steric reasons) whereas aldehydes, including formaldehyde, prefer π bonding. Indeed, there appears to be no evidence for equilibria in solutions of the formaldehyde complex with this rhenium fragment.¹¹¹ For the dynamic behavior of the nickel complex, this reviewer prefers path b (involving an intermediate $\eta^1\text{-C}$ complex). The $\text{Ni}(\text{PCy}_3)_2$ fragment should be a strong donor (which favors C coordination), and nickel is not an oxophilic metal; thus, a path that includes O coordination only should not be favored.

VIII. Concluding Remarks

Particularly in the past decade, there has been much information gained about the structures, bonding, and spectral characteristics of soluble metal- CO_2 complexes. All of the structurally characterized complexes have bent CO_2 ligands, but the wealth of structural types is quite surprising for a molecule once thought to be inert toward reactions with

metals. Reaction characteristics for coordinated CO₂ such as thermolysis behavior and reactivity toward electrophiles have been studied and are becoming predictable. However, the precise relationships between these model compounds and their catalytically active relatives are not yet clear, and the structural and/or electronic properties of metal-carbon dioxide adducts that may be required for catalytic activity are not yet understood. It is hoped that this article will stimulate further interest in research that may lead to the development of carbon dioxide as a new source for fuels and fine chemicals.

IX. Acknowledgments

It is with pleasure that I acknowledge the contributions of my co-workers whose names appear in the references. Particular thanks are due to John F. Richardson and Mark S. Mashuta for their extensive help in the structural characterizations of our CO₂-bridged compounds. Generous financial support has been provided by the United States Department of Energy, Division of Chemical Sciences, Office of Basic Energy Sciences throughout our investigations. Finally, I wish to thank the reviewers for many helpful comments.

X. References

- Halmann, M. M. *Chemical Fixation of Carbon Dioxide. Methods for Recycling CO₂ into Useful Products*; CRC Press: Boca Raton, FL, 1993.
- (a) Behr, A. In *Catalysis in C₁ Chemistry*; Keim, W., Ed.; D. Reidel Publ. Co.: Dordrecht, Holland, 1983; p 169. (b) Walther, D. *Coord. Chem. Rev.* **1987**, *79*, 135. (c) Braunstein, P.; Matt, D.; Nobel, D. *Chem. Rev.* **1988**, *88*, 747. (d) Cutler, A. R.; Hanna, P. K.; Vites, J. C. *Chem. Rev.* **1988**, *88*, 1363. (e) Behr, A. *Angew. Chem., Int. Ed. Engl.* **1988**, *27*, 661. (f) Miller, J. D. In *Reactions of Coordinated Ligands*; Braterman, P. S., Ed.; Plenum Press: New York, 1989; Vol. 2, p 1.
- (a) Vol'pin, M. E.; Kolominkov, I. S. *Pure Appl. Chem.* **1973**, *33*, 567. (b) Eisenberg, R.; Hendriksen, D. E. *Adv. Catal.* **1979**, *28*, 79. (c) Ibers, J. A. *Chem. Soc. Rev.* **1982**, *11*, 57. (d) Inoue, S.; Yamazaki, N. In *Organic and Bioorganic Chemistry of Carbon Dioxide*; Kodansha, L. T. D., Ed.; Wiley and Sons: New York, 1982; p 199. (e) Creutz, C. In *Electrochemical and Electrocatalytic Reactions of Carbon Dioxide*; Sullivan, B. P., Krist, K., Guard, H. E., Eds.; Elsevier: Amsterdam, 1993; Chapter 2. (f) Aresta, M.; Quaranta, E.; Tommasi, I. *New J. Chem.* **1994**, *18*, 133.
- Ford, P. C.; Rokicki, A. *Adv. Organomet. Chem.* **1988**, *28*, 139.
- (a) Darenbourg, D. J.; Kudoroski, R. A. *Adv. Organomet. Chem.* **1983**, *22*, 129. (b) Jessop, P. G.; Ikariya, T.; Noyori, R. *Chem. Rev.* **1995**, *95*, 259.
- See ref 3d, p 35.
- Herskovitz, T. *J. Am. Chem. Soc.* **1977**, *99*, 2391.
- Calabrese, J. C.; Herskovitz, T.; Kinney, J. B. *J. Am. Chem. Soc.* **1983**, *105*, 5914.
- Aresta, M.; Nobile, C. F. *J. Chem. Soc., Chem. Commun.* **1975**, 636.
- Dohring, A.; Jolly, P. W.; Krüger, C.; Romao, M. J. *Z. Naturforsch.* **1985**, *40B*, 484.
- Mason, M. G.; Ibers, J. A. *J. Am. Chem. Soc.* **1982**, *104*, 5153.
- Aresta, M.; Nobile, C. F. *J. Chem. Soc., Dalton Trans.* **1977**, 708.
- Aresta, M.; Nobile, C. F. *Inorg. Chim. Acta* **1977**, *24*, L49.
- Karsch, H. H. *Chem. Ber.* **1977**, *110*, 2213.
- Komiya, S.; Akita, M.; Kasuga, N.; Hirano, M.; Fukuoka, A. *J. Chem. Soc., Chem. Commun.* **1994**, 1115.
- Sakamoto, M.; Shimizu, I.; Yamamoto, A. *Organometallics* **1994**, *13*, 407.
- Bristow, G. S.; Hitchcock, P. B.; Lappert, M. F. *J. Chem. Soc., Chem. Commun.* **1981**, 1145.
- Gambarotta, S.; Floriani, C.; Chiesi-Villa, A.; Guastini, C. *J. Am. Chem. Soc.* **1985**, *107*, 2985.
- Alt, H. G.; Schwind, K.-H.; Rausch, M. D. *J. Organomet. Chem.* **1987**, *321*, C9.
- Iwashita, Y.; Hayata, A. *J. Am. Chem. Soc.* **1969**, *91*, 2525.
- (a) Fu, P.-F.; Khan, M. A.; Nicholas, K. M. *J. Am. Chem. Soc.* **1992**, *114*, 6579. (b) Fu, P.-F.; Khan, M. A.; Nicholas, K. M. *J. Organomet. Chem.* **1996**, 506, 49.
- Fu, P. F.; Fazlur-Rahman, A. K.; Nicholas, K. M. *Organometallics* **1994**, *13*, 413.
- Ishida, T.; Hayashi, T.; Mizobe, Y.; Hidai, M. *Inorg. Chem.* **1992**, *31*, 4481.
- Chatt, J.; Kubota, M.; Leigh, G. J.; March, F. C.; Mason, R.; Yarrow, D. J. *J. Chem. Soc., Chem. Commun.* **1974**, 1033.
- (a) Alvarez, R.; Carmona, E.; Gutierrez-Puebla, E.; Marin, J. M.; Monge, A.; Poveda, M. L. *J. Chem. Soc., Chem. Commun.* **1984**, 1326. (b) Alvarez, R.; Carmona, E.; Poveda, M. L.; Sanchez-Delgado, J. *Am. Chem. Soc.* **1984**, *106*, 2731. (c) Alvarez, R.; Carmona, E.; Morin, J. M.; Poveda, M. L.; Gutierrez-Puebla, E.; Monge, A. *J. Am. Chem. Soc.* **1986**, *108*, 2286. (d) Carmona, E.; Munoz, M. A.; Perez, P. J.; Poveda, M. L. *Organometallics* **1990**, *9*, 1337. (e) Carmona, E.; Hughes, A. K.; Munoz, M. Z.; O'Hare, D. M.; Perez, P. J.; Poveda, M. L. *J. Am. Chem. Soc.* **1991**, *113*, 9210.
- Audett, J. D.; Collins, T. J.; Santarsiero, B. D.; Spies, G. H. *J. Am. Chem. Soc.* **1982**, *104*, 7352.
- Hanna, T. A.; Baranger, A. M.; Bergman, R. G. *J. Am. Chem. Soc.* **1995**, *117*, 11363.
- Kubiak, C. P.; Woodcock, C.; Eisenberg, R. *Inorg. Chem.* **1982**, *21*, 2119.
- (a) Field, J. S.; Haines, R. J.; Sundermeyer, J.; Woollam, S. F. *J. Chem. Soc., Chem. Commun.* **1990**, 985. (b) Field, J. S.; Haines, R. J.; Sundermeyer, J.; Woollam, S. F. *J. Chem. Soc., Dalton Trans.* **1993**, 2735.
- Bennett, M. A.; Robertson, G. B.; Rokicki, A.; Wickramasinghe, W. A. *J. Am. Chem. Soc.* **1988**, *110*, 7098.
- Torresan, I.; Michelin, R. A.; Marsella, A.; Zanardo, A.; Pinna, F.; Strukul, G. *Organometallics* **1991**, *10*, 623.
- Gibson, D. H.; Ye, M.; Richardson, J. F. *J. Am. Chem. Soc.* **1992**, *114*, 9716.
- Gibson, D. H.; Ye, M.; Richardson, J. F.; Mashuta, M. S. *Organometallics* **1994**, *13*, 4559.
- Gibson, D. H.; Franco, J. O.; Mehta, J. M.; Mashuta, M. S.; Richardson, J. F. *Organometallics* **1995**, *14*, 5068.
- Yang, Y.-L.; Chen, J.-D.; Lin, Y.-C.; Cheng, M.-C.; Wang, Y. J. *Organomet. Chem.* **1994**, *467*, C6.
- Szalda, D. J.; Chou, M. H.; Fujita, E.; Creutz, C. *Inorg. Chem.* **1992**, *31*, 4712.
- Gibson, D. H.; Ding, Y.; Sleadd, B. A.; Franco, J. O.; Richardson, J. F.; Mashuta, M. S., submitted to *J. Am. Chem. Soc.*
- Senn, D. R.; Gladysz, J. A.; Emerson, K.; Larsen, R. D. *Inorg. Chem.* **1987**, *26*, 2737.
- Pinkes, J. R.; Cutler, A. R. *Inorg. Chem.* **1994**, *33*, 759.
- Gibson, D. H.; Ye, M.; Sleadd, B. A.; Mehta, J. M.; Mbadike, O. P.; Richardson, J. F.; Mashuta, M. S. *Organometallics* **1995**, *14*, 1242.
- Tso, C. T.; Cutler, A. R. *J. Am. Chem. Soc.* **1986**, *108*, 6069.
- Vites, J. C.; Steffey, B. D.; Giuseppetti-Dery, M. E.; Cutler, A. R. *Organometallics* **1991**, *10*, 2827.
- Pinkes, J. R.; Steffey, B. D.; Vites, J. C.; Cutler, A. R. *Organometallics* **1994**, *13*, 21.
- Gibson, D. H.; Mehta, J. M.; Sleadd, B. A.; Mashuta, M. S.; Richardson, J. F. *Organometallics* **1995**, *14*, 4886.
- Housmekerides, C. E.; Ramage, D. L.; Kretz, C. M.; Shontz, J. T.; Pilato, R. S.; Geoffroy, G. L.; Rheingold, A. L.; Haggerty, B. S. *Inorg. Chem.* **1992**, *31*, 4453.
- (a) Pilato, R. S.; Geoffroy, G. L.; Rheingold, A. L. *J. Chem. Soc., Chem. Commun.* **1989**, 1287. (b) Pilato, R. S.; Housmekerides, C. E.; Jernakoff, P.; Rubin, D.; Geoffroy, G. L.; Rheingold, A. L. *Organometallics* **1990**, *9*, 2333.
- Gibson, D. H.; Mehta, J. M.; Ye, M.; Richardson, J. F.; Mashuta, M. S. *Organometallics* **1994**, *13*, 1070.
- Gibson, D. H.; Franco, J. O.; Mehta, J. M.; Harris, M. T.; Ding, Y.; Mashuta, M. S.; Richardson, J. F. *Organometallics* **1995**, *14*, 5073.
- Mandal, S. K.; Krause, J. A.; Orchin, M. *Polyhedron* **1993**, *12*, 1423.
- (a) Gibson, D. H.; Ong, T.-S.; Ye, M. *Organometallics* **1991**, *10*, 1811. (b) Gibson, D. H.; Richardson, J. F.; Ong, T.-S. *Acta Crystallogr.* **1991**, *C47*, 259.
- Gibson, D. H.; Richardson, J. F.; Mbadike, O. P. *Acta Crystallogr.* **1993**, *B49*, 784.
- Gibson, D. H.; Mehta, J. M.; Mashuta, M. S.; Richardson, J. F., unpublished results.
- Eady, C. R.; Guy, J. J.; Johnson, B. F. G.; Lewis, J.; Malatesta, M. C.; Sheldrick, G. M. *J. Chem. Soc., Chem. Commun.* **1976**, 602.
- John, G. R.; Johnson, B. F. G.; Lewis, J.; Wong, K. C. *J. Organomet. Chem.* **1979**, *169*, C23.
- Balbach, B. K.; Helus, F.; Oberdorfer, F.; Ziegler, M. L. *Angew. Chem., Int. Ed. Engl.* **1981**, *20*, 470.
- Beck, W.; Raab, K.; Nagel, U.; Steimann, M. *Angew. Chem., Int. Ed. Engl.* **1982**, *21*, 526.
- (a) Lundquist, E.; Huffman, J. C.; Caulton, K. G. *J. Am. Chem. Soc.* **1986**, *108*, 8309. (b) Lundquist, E. G.; Huffman, J. C.; Foltling, K.; Mann, B. E.; Caulton, K. G. *Inorg. Chem.* **1990**, *29*, 128.

- (58) (a) Floriani, C.; Fachinetti, G. *J. Chem. Soc., Chem. Commun.* **1974**, 615. (b) Fachinetti, G.; Floriani, C.; Zanazzi, P. F. *J. Am. Chem. Soc.* **1978**, *100*, 7405. (c) Gambarotta, S.; Arena, F.; Floriani, C.; Zanazzi, P. F. *J. Am. Chem. Soc.* **1982**, *104*, 5082.
- (59) (a) Tanaka, H.; Nagao, H.; Peng, S.-M.; Tanaka, K. *Organometallics* **1992**, *11*, 1450. (b) Tanaka, H.; Tzeng, B.-C.; Nagao, H.; Peng, S.-M.; Tanaka, K. *Inorg. Chem.* **1993**, *32*, 1512.
- (60) Gibson, D. H.; Sleadd, B. A.; Mashuta, M. S.; Richardson, J. F., unpublished observations.
- (61) Evans, G. O.; Walter, W. F.; Mills, D. R.; Streit, C. A. *J. Organomet. Chem.* **1978**, *144*, C-34.
- (62) (a) Bodnar, T.; Conan, E.; Menard, K.; Cutler, A. R. *Inorg. Chem.* **1982**, *21*, 1275. (b) Giuseppetti, M. E.; Cutler, A. R. *Organometallics* **1987**, *6*, 970.
- (63) Forschner, T.; Menard, K.; Cutler, A. R. *J. Chem. Soc., Chem. Commun.* **1984**, 121.
- (64) (a) Lee, G. R.; Cooper, N. J. *Organometallics* **1985**, *4*, 794. (b) Lee, G. R.; Cooper, N. J. *Organometallics* **1985**, *4*, 1467.
- (65) (a) Maher, J. M.; Cooper, N. J. *J. Am. Chem. Soc.* **1980**, *102*, 7606. (b) Maher, J. M.; Lee, G. R.; Cooper, N. J. *J. Am. Chem. Soc.* **1982**, *104*, 6797.
- (66) Lee, G. R.; Maher, J. M.; Cooper, N. J. *J. Am. Chem. Soc.* **1987**, *109*, 2956.
- (67) Grice, M. C.; Kao, S. C.; Pettit, R. *J. Am. Chem. Soc.* **1979**, *101*, 1627.
- (68) Gibson, D. H.; Ong, T. S. *J. Am. Chem. Soc.* **1987**, *109*, 7191.
- (69) Gibson, D. H.; Ong, T.-S.; Ye, M.; Franco, J. O.; Owens, K. *Organometallics* **1988**, *7*, 2569.
- (70) Simon, A.; Peters, K. *Acta Crystallogr.* **1980**, *B36*, 2750.
- (71) Gibson, D. H.; Bardon, R. F.; Mehta, J. M.; Richardson, J. F.; Mashuta, M. S. *Acta Crystallogr.* **1996**, *C52*, 852.
- (72) Harlow, R. L.; Kinney, J. B.; Herskovitz, T. *J. Chem. Soc., Chem. Commun.* **1980**, 813.
- (73) Guy, J. J.; Sheldrick, G. M. *Acta Crystallogr.* **1978**, *334*, 1718.
- (74) Dedieu, A.; Bo, C.; Ingold, F. In *Metal Ligand Interactions from Atoms to Clusters to Surfaces*; Salahub, D. R., Russo, N., Eds.; NATO ASI Series, Ser. C, 378; Kluwer Academic Publishers: Dordrecht, The Netherlands, 1992; p 175.
- (75) Sirois, S.; Castro, M.; Salahub, D. *Int. J. Quant. Chem.; Quant. Chem. Symp.* **1994**, *28*, 645.
- (76) Sodupe, M.; Branchadell, V.; Oliva, A. *J. Phys. Chem.* **1995**, *99*, 8567.
- (77) Sanchez-Marcos, E.; Caballol, R.; Tringuier, G.; Barthelat, J. C. *J. Chem. Soc., Dalton Trans.* **1987**, 2373.
- (78) Nakamoto, K. *Infrared Spectra of Inorganic and Coordination Compounds*, 2nd ed.; Wiley-Interscience: New York, 1970.
- (79) Shao, Y.; Paul, J.; Axelsson, O.; Hoffmann, F. M. *J. Phys. Chem.* **1993**, *97*, 7652.
- (80) Yoshioka, Y.; Jordan, K. D. *Chem. Phys. Lett.* **1981**, *84*, 370.
- (81) Kafafi, Z. H.; Hauge, R. H.; Billups, W. E.; Margrave, J. L. *J. Am. Chem. Soc.* **1983**, *105*, 3886.
- (82) Kafafi, Z. H.; Hauge, R. H.; Billups, W. E.; Margrave, J. L. *Inorg. Chem.* **1984**, *23*, 177.
- (83) Mascetti, J.; Tranquille, M. *J. Phys. Chem.* **1988**, *92*, 2177.
- (84) Le Quere, A. M.; Xu, C.; Manceron, L. *J. Phys. Chem.* **1991**, *95*, 3031.
- (85) Bartos, B.; Freund, H. J.; Kuhlenbeck, H.; Neumann, M.; Lindner, H.; Miller, K. *Surf. Sci.* **1987**, *179*, 59.
- (86) Asscher, M.; Kao, C.-T.; Somorjai, G. *J. Phys. Chem.* **1988**, *92*, 2711.
- (87) Brousseau, R.; Ellis, T. H.; Wang, H. *Chem. Phys. Lett.* **1991**, *177*, 118.
- (88) Xu, C.; Goodman, D. W. *J. Am. Chem. Soc.* **1995**, *117*, 12354.
- (89) (a) Aresta, M.; Gobetto, R.; Quaranta, E.; Tommasi, I. *Inorg. Chem.* **1992**, *31*, 4286. (b) Jegat, C.; Fouassier, M.; Tranquille, M.; Mascetti, J.; Tommasi, I.; Aresta, M.; Ingold, F.; Dedieu, A. *Inorg. Chem.* **1993**, *32*, 1279.
- (90) Jegat, C.; Fouassier, M.; Mascetti, J. *Inorg. Chem.* **1991**, *30*, 1521.
- (91) Nakamoto, K. *Infrared and Raman Spectra of Inorganic and Coordination Compounds*; Wiley: New York, 1978; p 231.
- (92) Jegat, C.; Fouassier, M.; Tranquille, M.; Mascetti, J. *Inorg. Chem.* **1991**, *30*, 1529.
- (93) Griffiths, P. W.; deHaseth, J. A. *Fourier Transform Infrared Spectroscopy*; Wiley: New York, 1986; Chapter 5.
- (94) (a) Deacon, G. B.; Phillips, R. J. *Coord. Chem. Rev.* **1980**, *33*, 227. (b) Deacon, G. B.; Huber, F.; Phillips, R. J. *Inorg. Chim. Acta* **1985**, *104*, 41.
- (95) Casey, C. P.; Cyr, C. R.; Anderson, R. L.; Marten, D. F. *J. Am. Chem. Soc.* **1975**, *97*, 3053.
- (96) Miessler, G. L.; Kim, S.; Jacobson, R. A.; Angelici, R. J. *Inorg. Chem.* **1987**, *26*, 1690.
- (97) See: Collman, J. P.; Hegedus, L. S.; Norton, J. R.; Finke, R. G. *Principles and Applications of Organotransition Metal Chemistry*; University Science Books: Mill Valley, CA, 1987; Chapter 3.
- (98) (a) Longato, B.; Martin, B. D.; Norton, J. R.; Anderson, O. P. *Inorg. Chem.* **1985**, *24*, 1389. (b) Kovacs, J. A.; Bergman, R. G. *J. Am. Chem. Soc.* **1989**, *111*, 2378.
- (99) Bryan, J. C.; Mayer, J. M. *J. Am. Chem. Soc.* **1990**, *112*, 2298.
- (100) Belmore, K. A.; Vanderpool, R. A.; Tsai, J.-C.; Khan, M. A.; Nicholas, K. M. *J. Am. Chem. Soc.* **1988**, *110*, 2004.
- (101) Ziegler, W.; Nicholas, K. M. *J. Organomet. Chem.* **1992**, *423*, C35.
- (102) Aresta, M.; Quaranta, E.; Tommasi, I. *J. Chem. Soc., Chem. Commun.* **1988**, 450.
- (103) Tsai, J.-C.; Khan, M.; Nicholas, K. M. *Organometallics* **1989**, *8*, 2967.
- (104) Fu, P.-F.; Khan, M. A.; Nicholas, K. M. *Organometallics* **1992**, *11*, 2607.
- (105) Tsai, J.-C.; Khan, M. A.; Nicholas, K. M. *Organometallics* **1991**, *10*, 29.
- (106) Thiyagorajan, B.; Kerr, M. E.; Bruno, J. W. *Inorg. Chem.* **1995**, *34*, 3444.
- (107) Gibson, D. H.; Ong, T.-S., unpublished results.
- (108) Steffey, B. D.; Vites, J. C.; Cutler, A. R. *Organometallics* **1991**, *10*, 3432.
- (109) See, for example: (a) Huang, Y.-H.; Gladysz, J. A.; *J. Chem. Educ.* **1988**, *65*, 298. (b) Dalton, D. M.; Fernandez, J. M.; Emerson, K.; Larsen, R. D.; Arif, A. M.; Gladysz, J. A. *J. Am. Chem. Soc.* **1990**, *112*, 9198. (c) Mendez, N. Q.; Seyler, J. W.; Arif, A. M.; Gladysz, J. A. *J. Am. Chem. Soc.* **1993**, *115*, 2323.
- (110) Delbecq, F.; Sautet, P. *J. Am. Chem. Soc.* **1992**, *114*, 2446.
- (111) Buhro, W. E.; Georgiou, S.; Fernandez, J. M.; Patton, A. T.; Strouse, C. E.; Gladysz, J. A. *Organometallics* **1986**, *5*, 956.

CR940212C

